SAND2015-4635C

Exceptional service in the national interest

Sandia National Laboratories

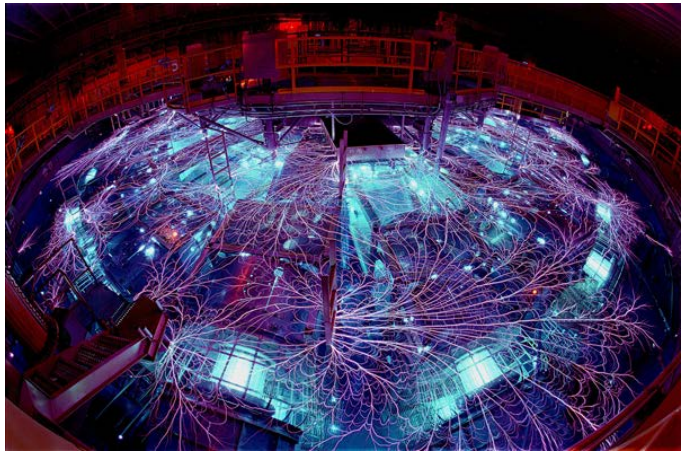

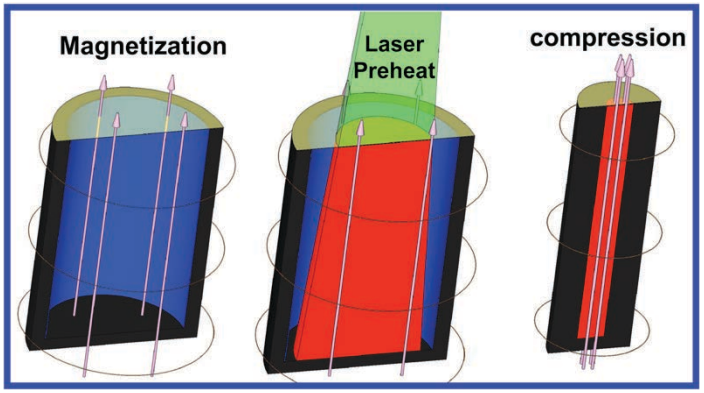

Magnetized Liner Inertial Fusion on the Z Pulsed-Power Accelerator

R.D. McBride, D.B. Sinars, S.A. Slutz, M.R. Gomez, A.B. Sefkow, S.B. Hansen, T.J. Awe, K.J. Peterson, P.F. Knapp, P.F. Schmit, D.C. Rovang, M. Geissel, R.A. Vesey, A.J. Harvey-Thompson, C.A. Jennings, M.R. Martin, R.W. Lemke, K.D. Hahn, E.C. Harding, M.E. Cuneo, J.L. Porter, G.A. Rochau, W.A. Stygar, and many more!

Sandia National Laboratories

Radiation from High Energy Density Plasmas Workshop
South Lake Tahoe, Nevada, June 9–12, 2015

U.S. DEPARTMENT OF ENERGY | NNSA National Nuclear Security Administration

Sandia National Laboratories is a multi-program laboratory managed and operated by Sandia Corporation, a wholly owned subsidiary of Lockheed Martin Corporation, for the U.S. Department of Energy's National Nuclear Security Administration under contract DE-AC04-94AL85000.

The United States ICF program is pursuing three main approaches to ignition

Sandia National Laboratories

Radiation-drive	Laser-drive	Magnetic-drive

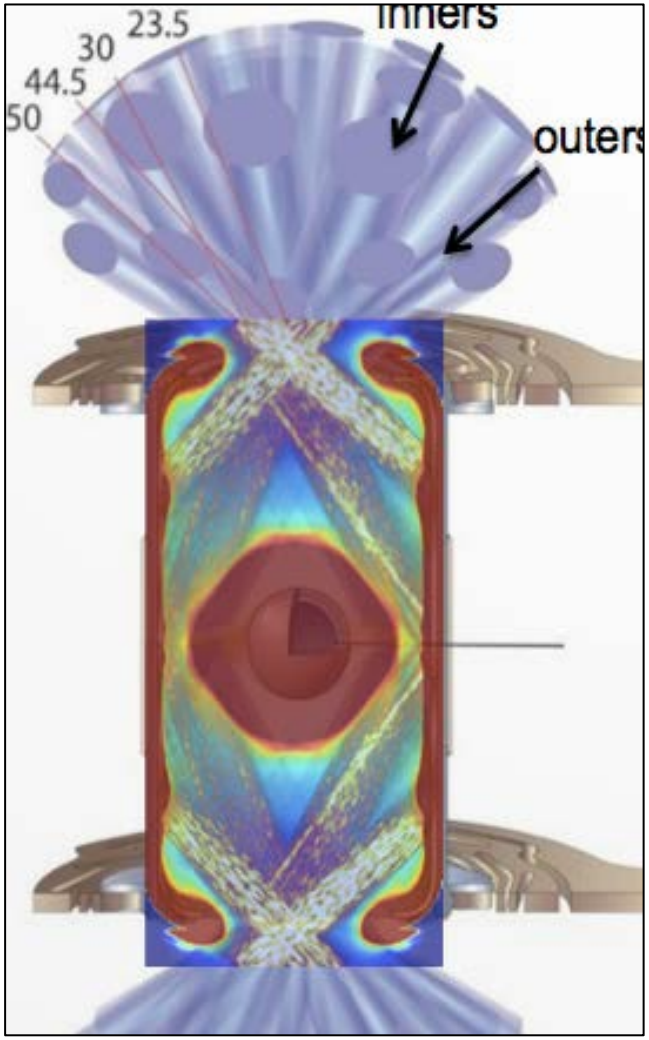

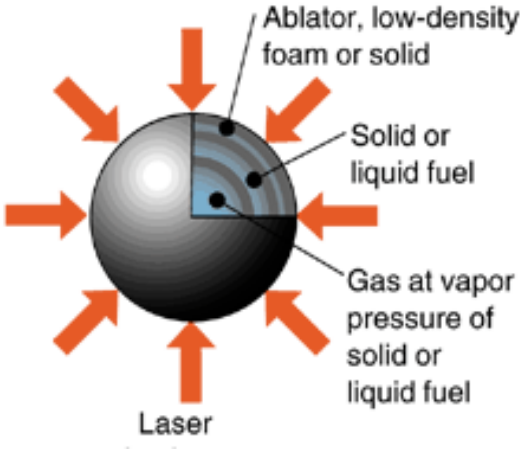

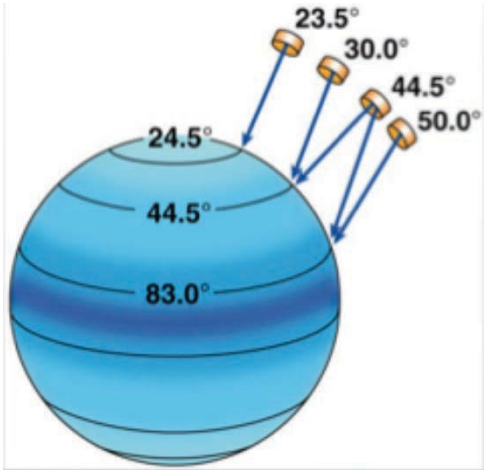

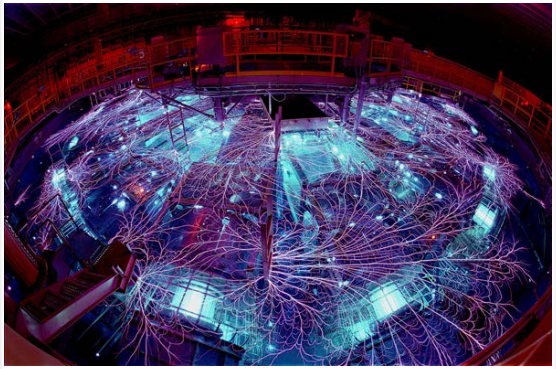

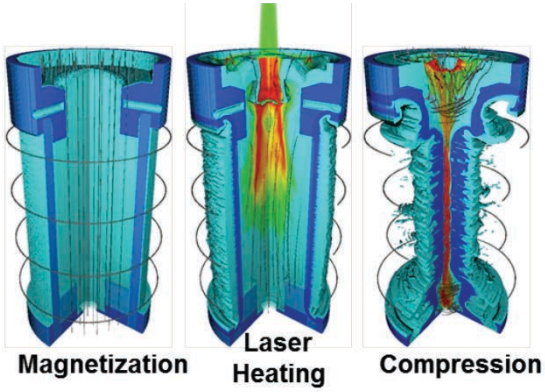

Focus of today's talk

The Z pulsed-power facility combines a compact MJ-class target physics platform (the Z accelerator) with a TW-class laser (ZBL)

Sandia National Laboratories

2–4 kJ Z Beamlet Laser (ZBL) for radiography and MagLIF fuel preheating

10,000 ft^2

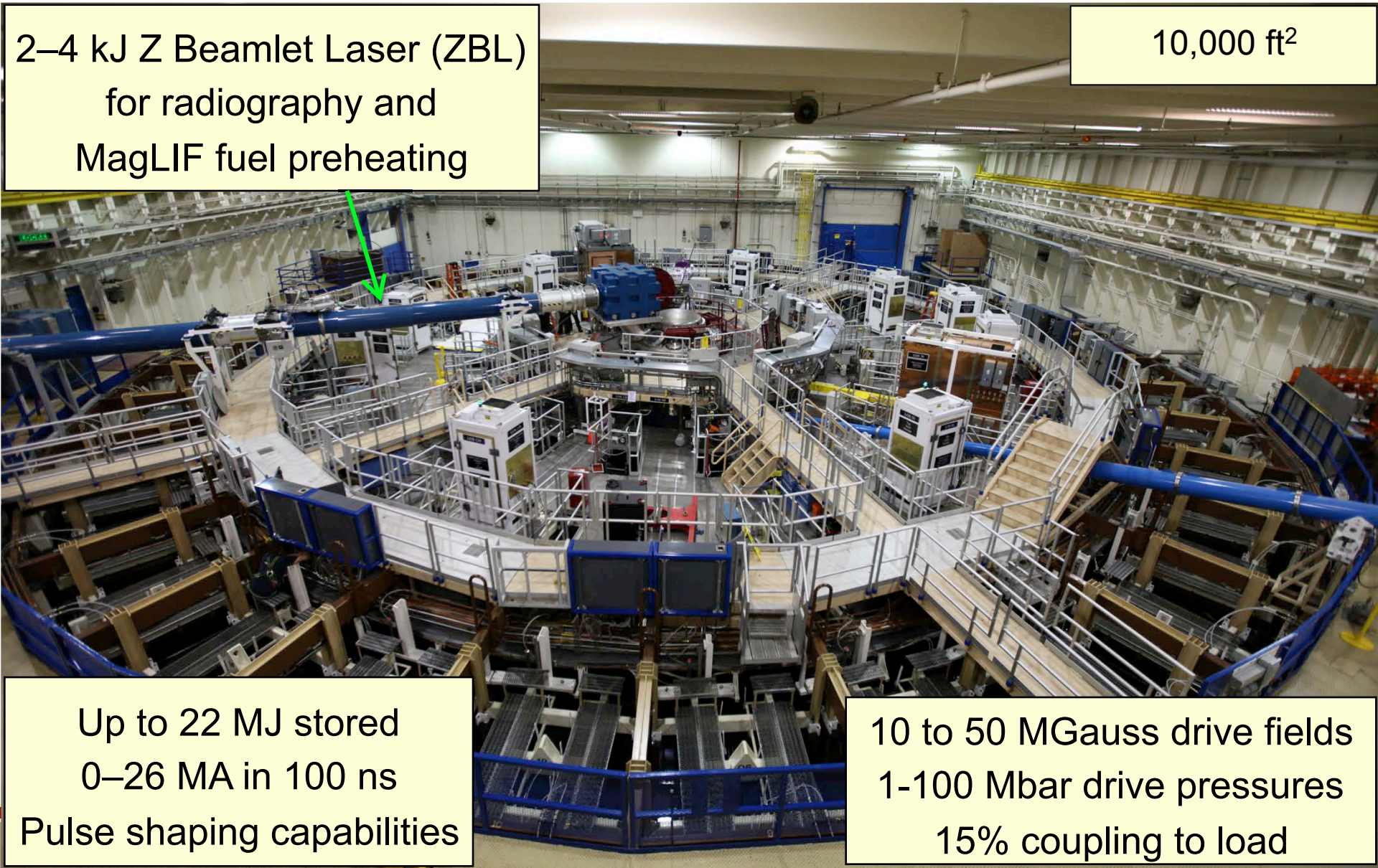

Up to 22 MJ stored
0–26 MA in 100 ns
Pulse shaping capabilities

10 to 50 MGauss drive fields
1-100 Mbar drive pressures
15% coupling to load

MagLIF is a Magnetically-driven implosion concept that we are pursuing on the Z facility

Sandia National Laboratories

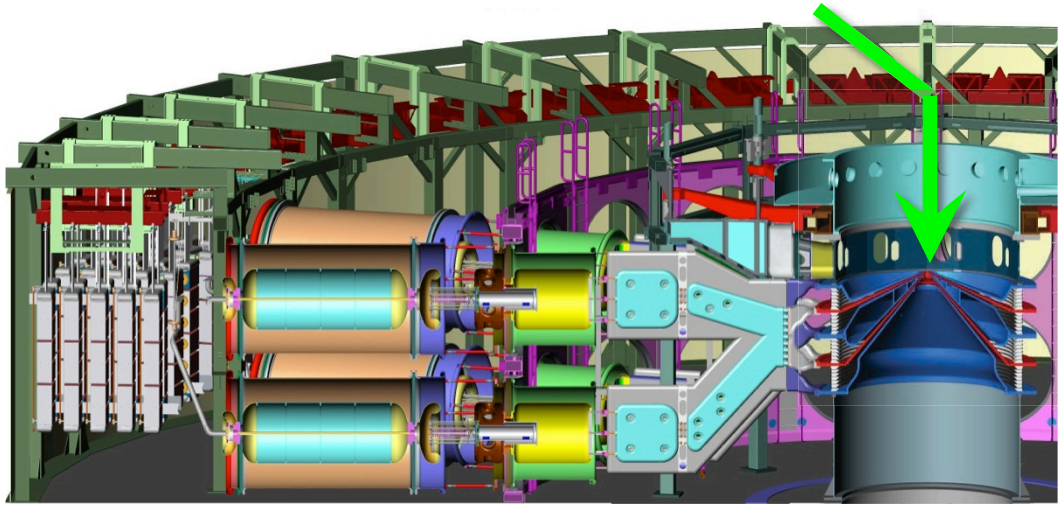

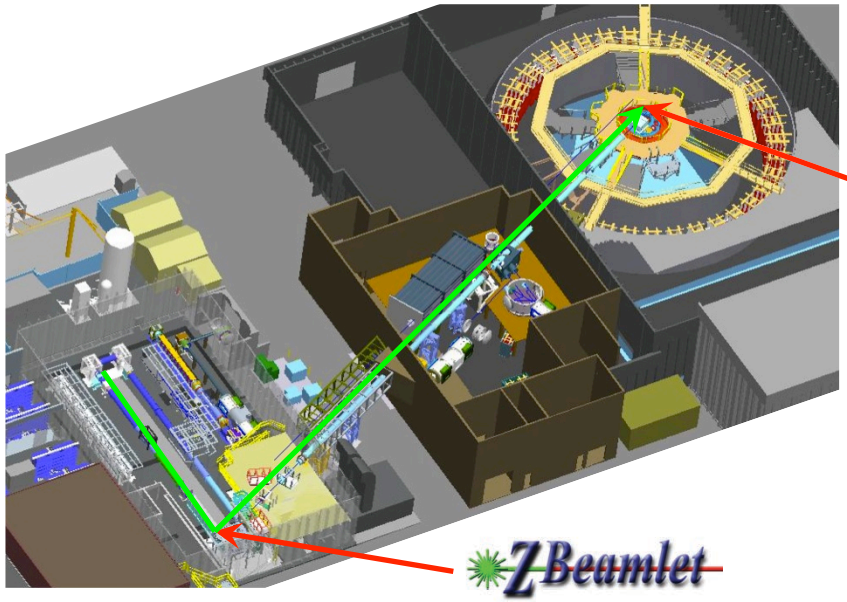

Z Machine

22 MJ stored energy
3 MJ delivered to target
Up to 26 MA peak current
100 ns risetime
50 MG B-field
100 Mbar pressure

Z Beamlet

2ω Nd:glass (527 nm)
1 TW, up to 4 kJ,
up to 6 ns pulse length

We are presently using the Z facility to study the Magnetized Liner Inertial Fusion (MagLIF)* concept

Sandia National Laboratories

1. A 10–50 T axial magnetic field (B_z) is applied to inhibit thermal conduction losses and to enhance alpha particle deposition

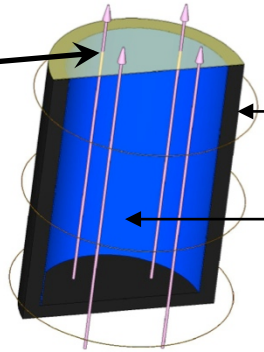

Liner (Li, Be, or Al)

Cold DD or DT gas (fuel)

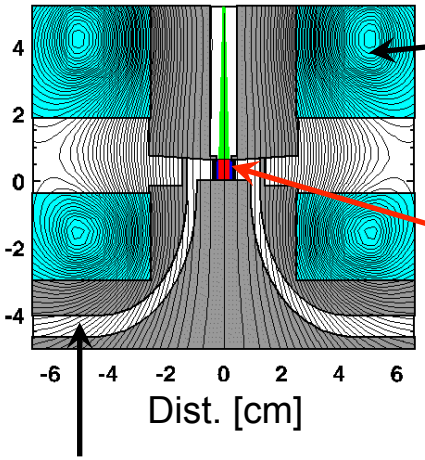

B_z coils

Z power flow (A-K gap)

2. ZBL preheats the fuel to ~100–250 eV to reduce the required compression to CR≈20–30

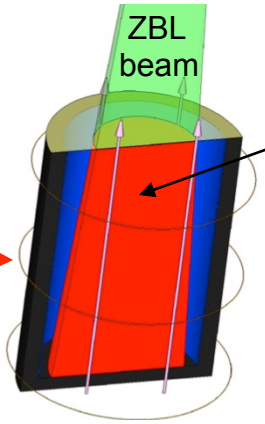

ZBL preheated fuel

Compressed B_z field

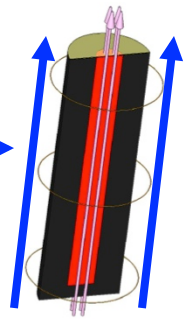

3. Z drive current and B_θ field implode the liner (via z-pinch) at 50–100 km/s, compressing the fuel and B_z field by factors of 1000

With DT fuel, simulations indicate scientific breakeven may be possible on Z (fusion energy out = energy deposited in fusion fuel)

* S. A. Slutz *et al.*, PoP **17**, 056303 (2010). S. A. Slutz and R. A. Vesey, PRL **108**, 025003 (2012).

MagLIF has three stages: Stage 1 is Magnetization

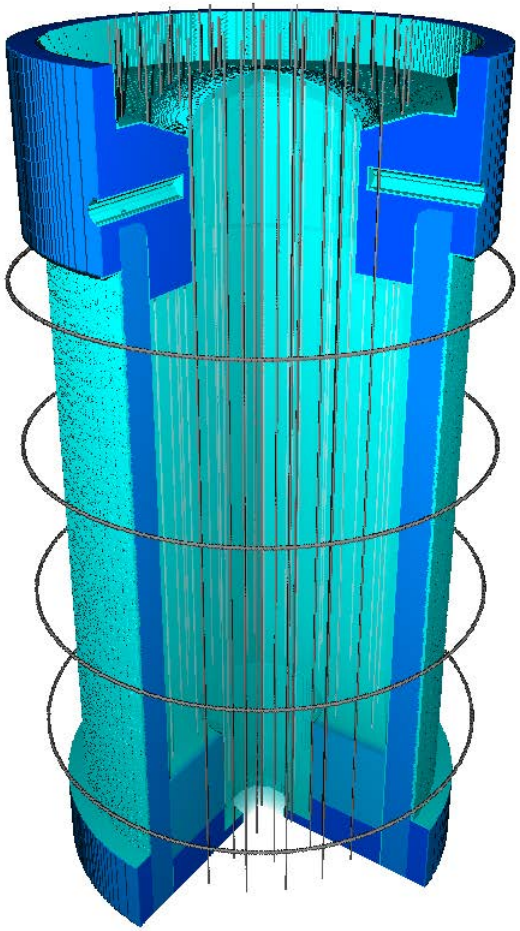

- **Start with a thick metal liner containing gaseous fusion fuel**
- **An axial magnetic field is applied slowly so the field can diffuse through conductors**

S. A. Slutz et al., Phys. Plasmas, 17 056303 (2010).

MagLIF has three stages: Stage 2 is Laser heating

Sandia National Laboratories

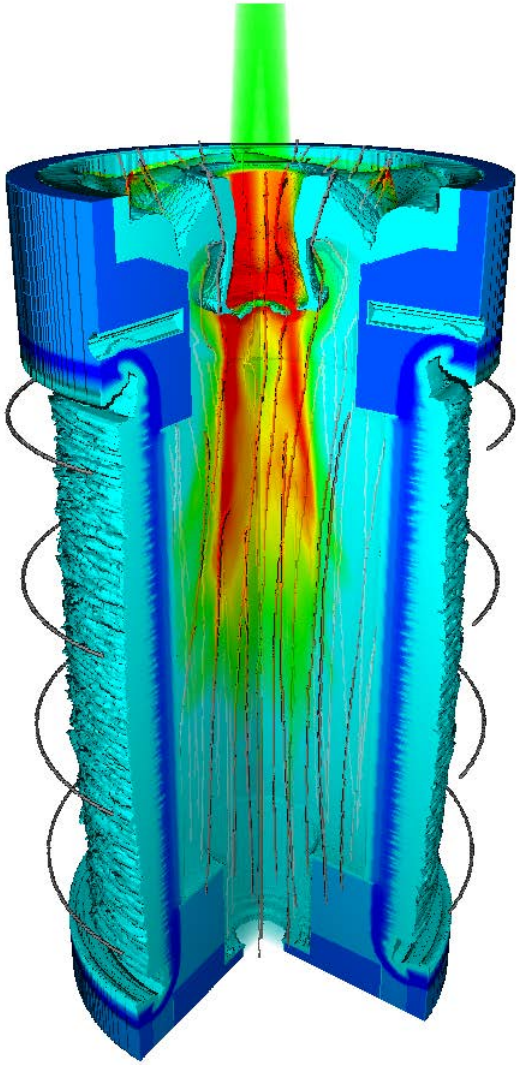

- A laser enters the target axially and heats the fuel through inverse bremsstrahlung absorption
- The magnetic field insulates the warm gas from the cool liner
- The low fuel density limits radiative losses

S. A. Slutz et al., Phys. Plasmas, 17 056303 (2010).

MagLIF has three stages: Stage 3 is Compression

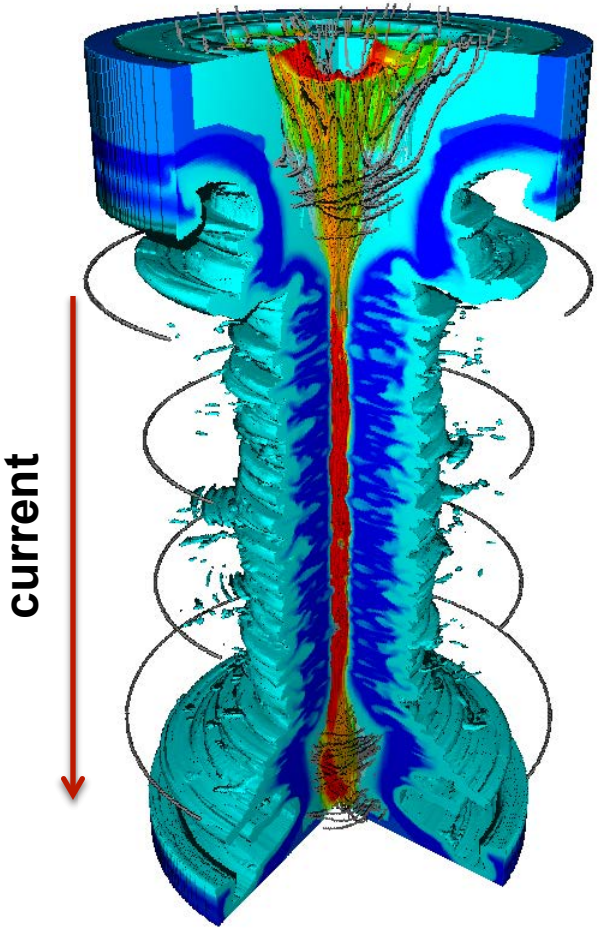

- Current flowing on the outside of the target squeezes the liner which compresses the fuel and magnetic field
- The fuel heats through near adiabatic compression to fusion relevant temperatures

S. A. Slutz et al., Phys. Plasmas, 17 056303 (2010).

MagLIF Timing Overview

~ 60–100-ns implosion times
~ adiabatic fuel compression (thus preheating the fuel is necessary)
~ 5-keV fuel stagnation temperatures
~ 1-g/cc fuel stagnation densities
~ 5-Gbar fuel stagnation pressures

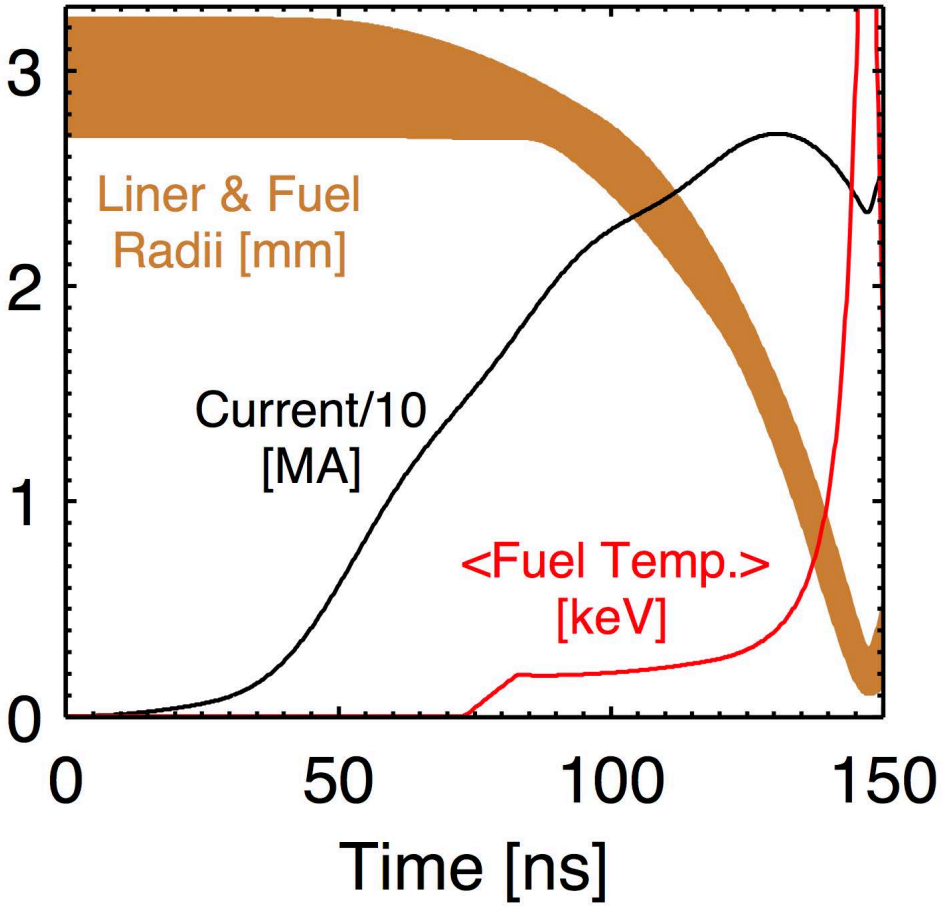

Semi-analytic simulation results from R. D. McBride and S. A. Slutz, PoP **22**, 052708 (2015).

MagLIF employs a slow implosion (70-100 km/s) so preheat and magnetization are required to achieve thermonuclear conditions

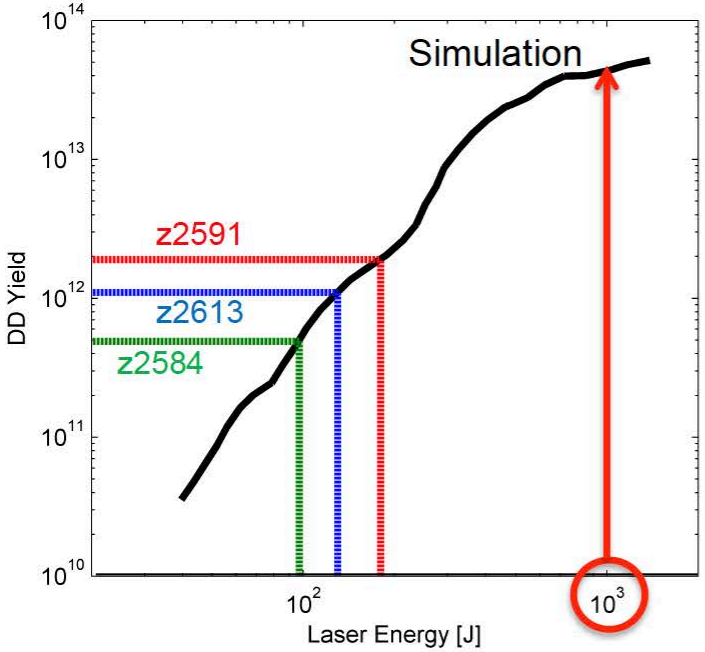

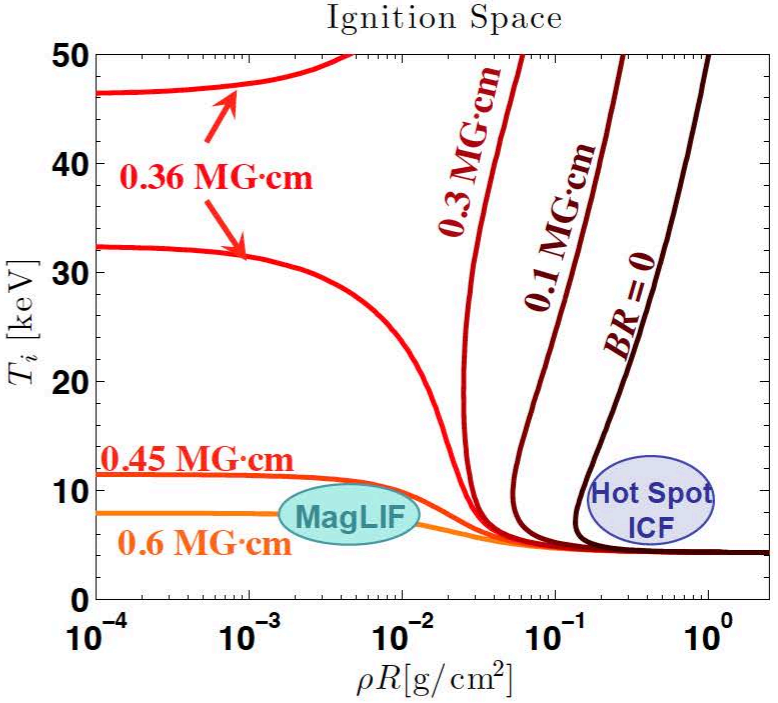

- Laser energy coupling is the single biggest lever on target performance
- Long dwell time between preheat and stagnation requires B-field to insulate electrons during implosion
- Flux compression allows charged burn products to be confined at low ρR
- All this conspires to allow self-heating at much reduced driver power

Anatomy of a MagLIF Experiment

Sandia National Laboratories

- **Field Coils**: Helmholtz-like pair produce a 10-30T axial field w/ ~10 ms rise time
- **ZBL**: 1-4 kJ green laser, 1-4 ns square pulse w/ adjustable prepulse
- **Final Feed**: Raised ~1" compared to standard feed to accommodate coils. Increases feed inductance by ~1.25 nH
- **Convolute**: Combines the 4 levels of the MITL's to a single A-K gap. Posts sit at 15 cm diameter, likely source of current loss

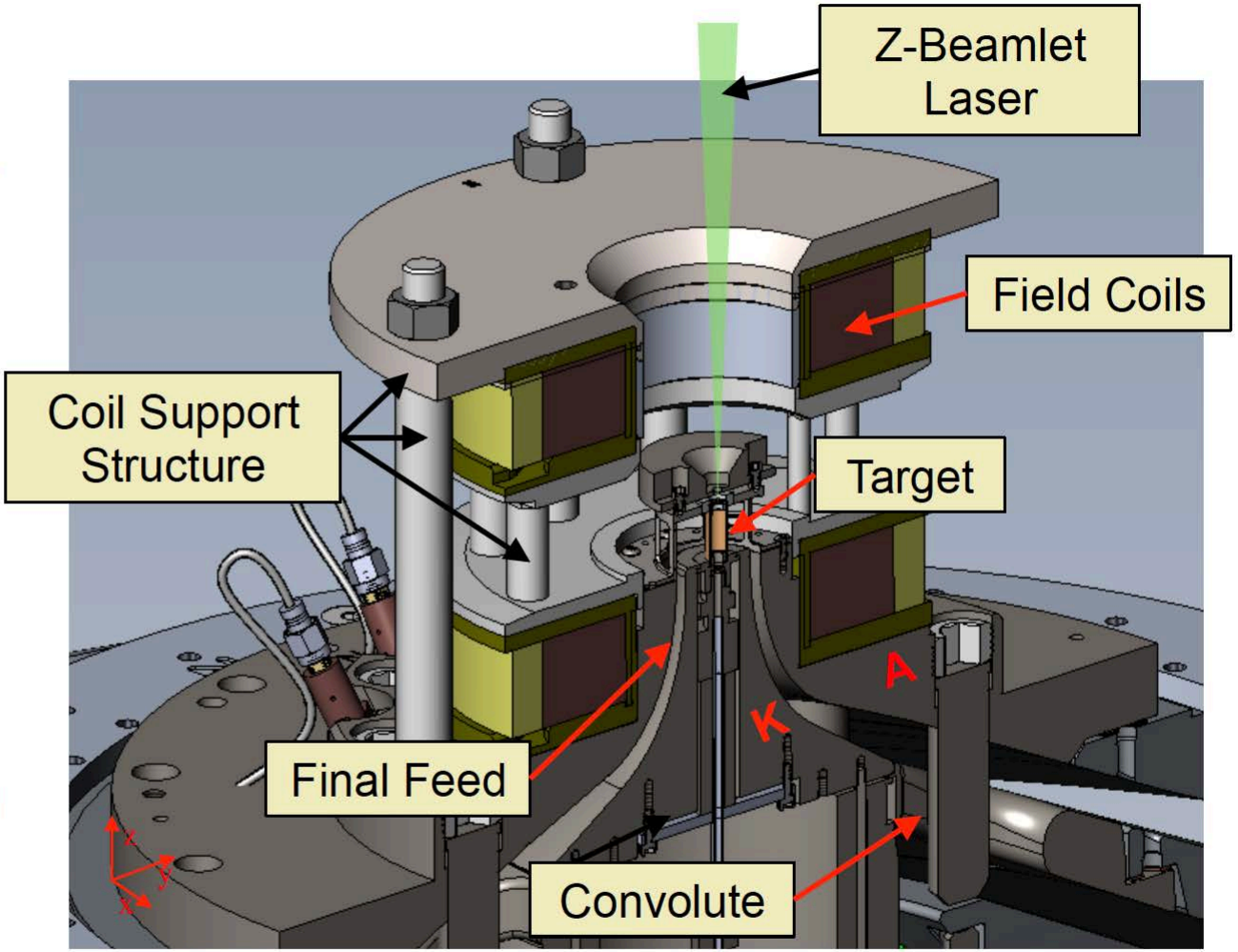

Anatomy of a MagLIF target

- **Liner**: Be, OD = 5.63 mm, ID = 4.65 mm
- **LEH Window**: 1-3 μm thick plastic window. Supports 60 PSI pure D2 gas fill.
- **Washer**: Metal (Al) washer supporting LEH window
- **Channel**: Al structure used to mitigate the wall instability (also referred to as a "cushion"). Also reduces LEH window diameter to allow thinner windows

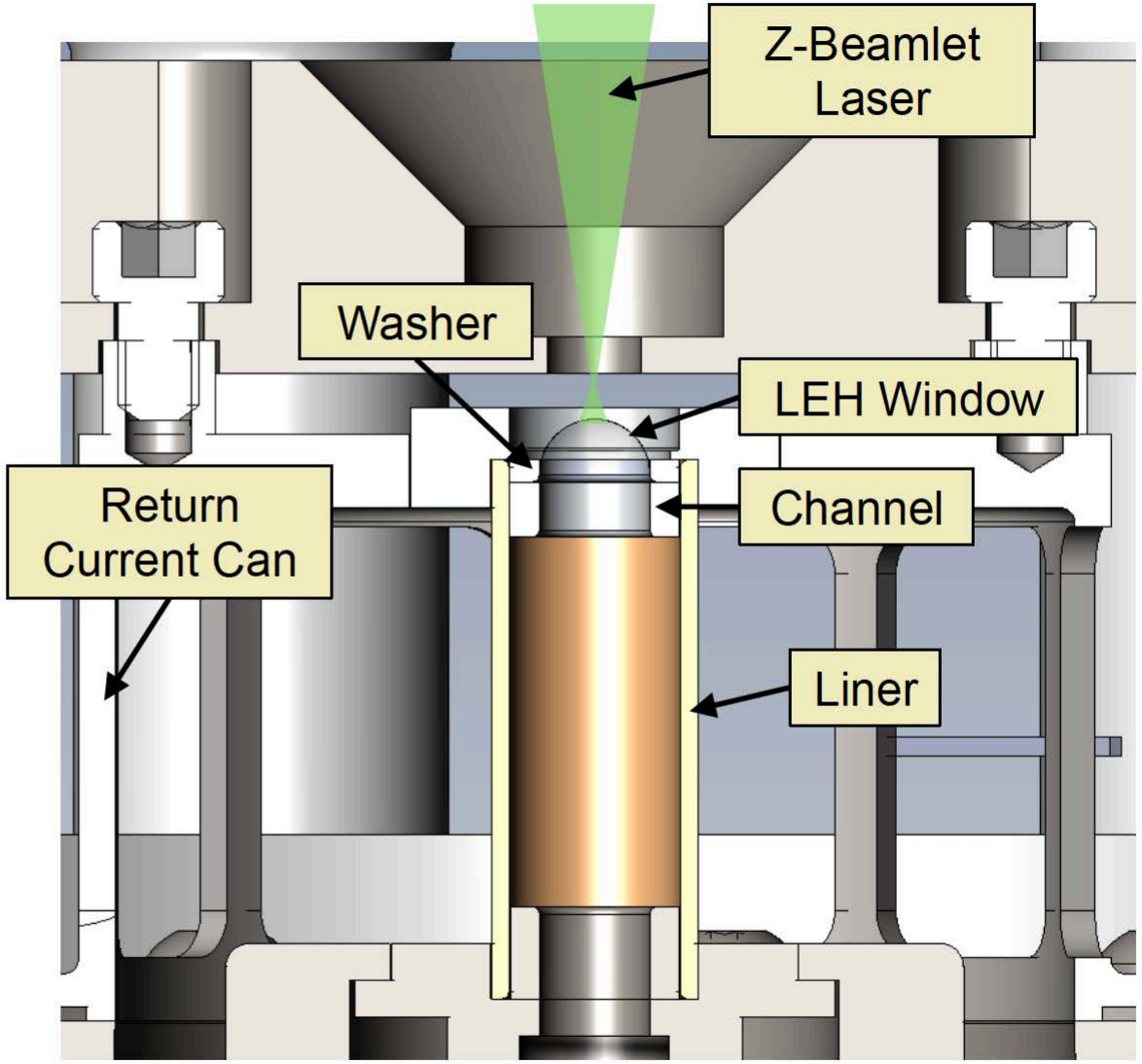

MagLIF has successfully demonstrated key aspects of magneto-inertial fusion

Sandia National Laboratories

Thermonuclear neutron generation

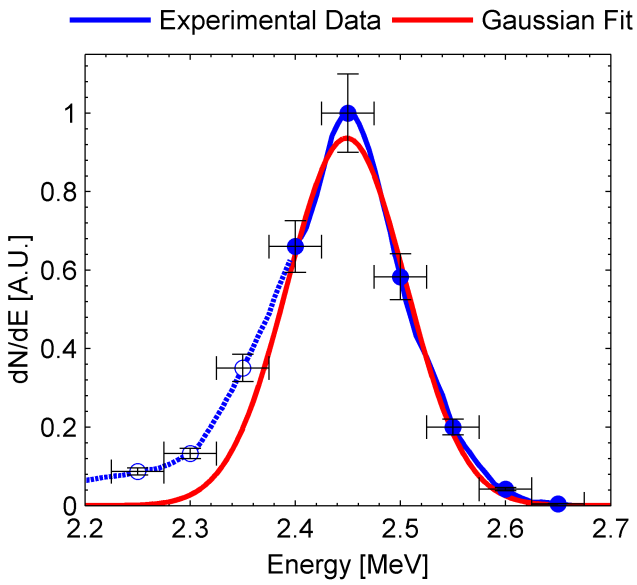

Isotropic, Gaussian DD neutron spectra

High yields and temperatures

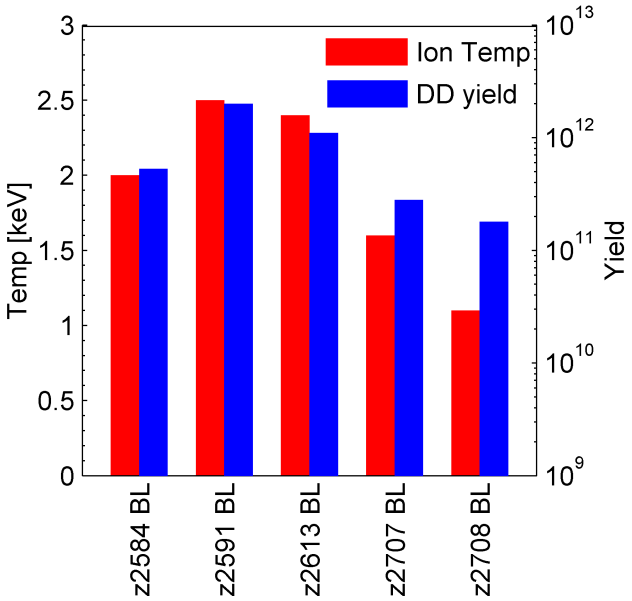

Max yield = 2e12
Max ion temp = 2.5 keV

Magnetic flux compression

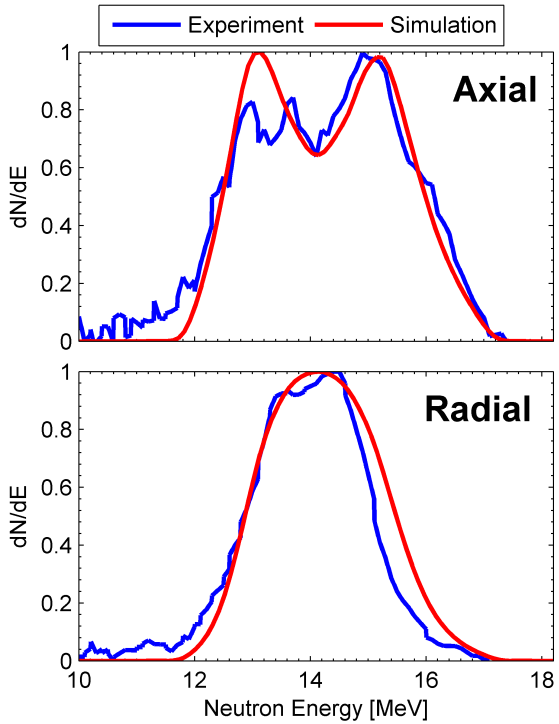

BR = 40 T-cm

M. R. Gomez et al., Phys. Rev. Lett. 113, 155003 (2014). P. F. Schmit et al., Phys. Rev. Lett. 113, 155004 (2014).

Emission-averaged ion and electron temperatures at stagnation are 2.5-3 keV

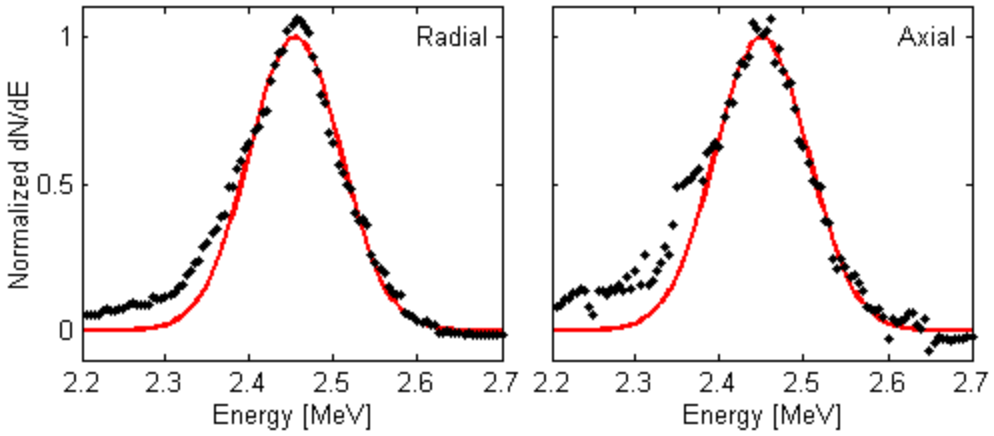

Axial and radial NTOF signals are both consistent with 2.5 keV burn-averaged ion temperature

Emissivity weighted electron temperature is approximately 3.1 keV in experiment with B-field, laser, and implosion

Temperature is < 1 keV for experiments that do not include all three components of MagLIF

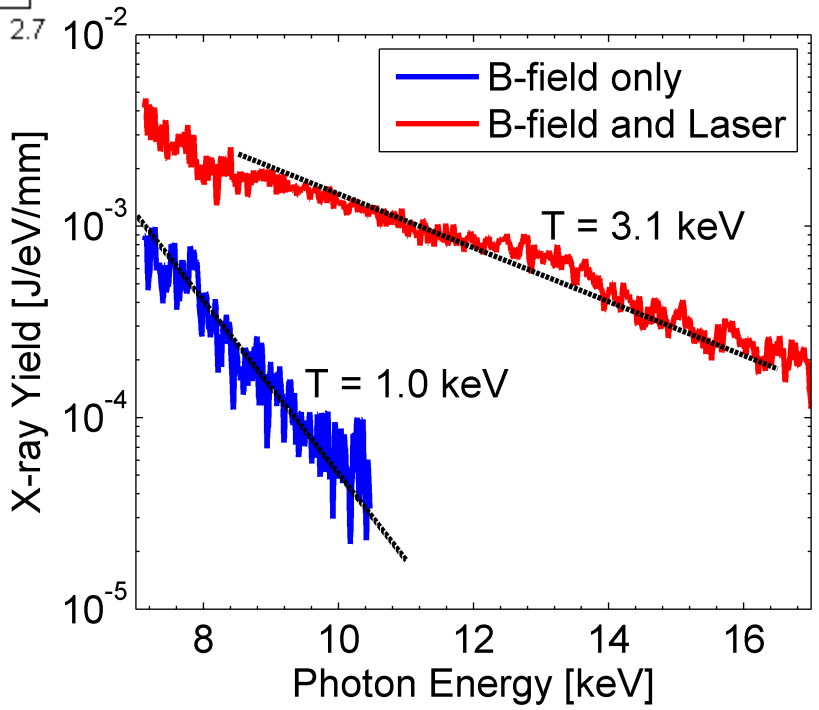

High temperatures and yields were only observed in fully integrated experiments

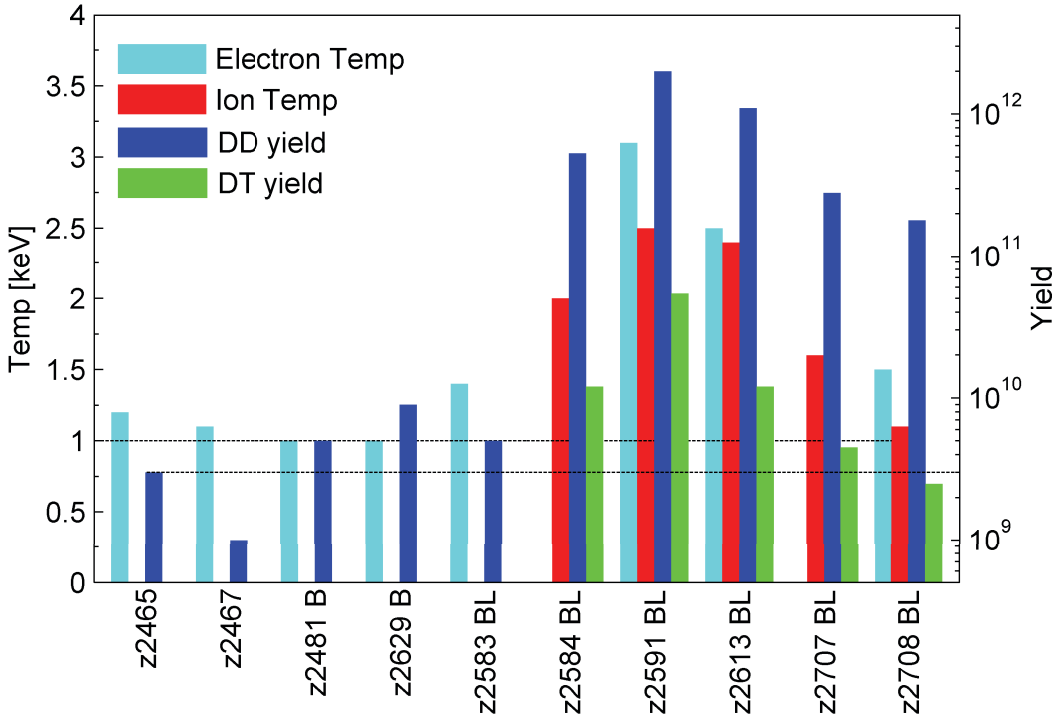

Some fully-integrated experiments did not produce high yields or temperatures

No experiments without laser or B-field have produced high yields or temperatures

These implosions are SLOW – 70 km/s peak
Without the preheating the fuel, the required convergence is >100
Without the magnetic field, the fuel cannot maintain the preheat

Experiments require laser heating and insulating magnetic field to be successful

M. R. Gomez et al., Phys. Rev. Lett. 113, 155003 (2014).

X ray emission timing is consistent with neutron bang time

Sandia National Laboratories

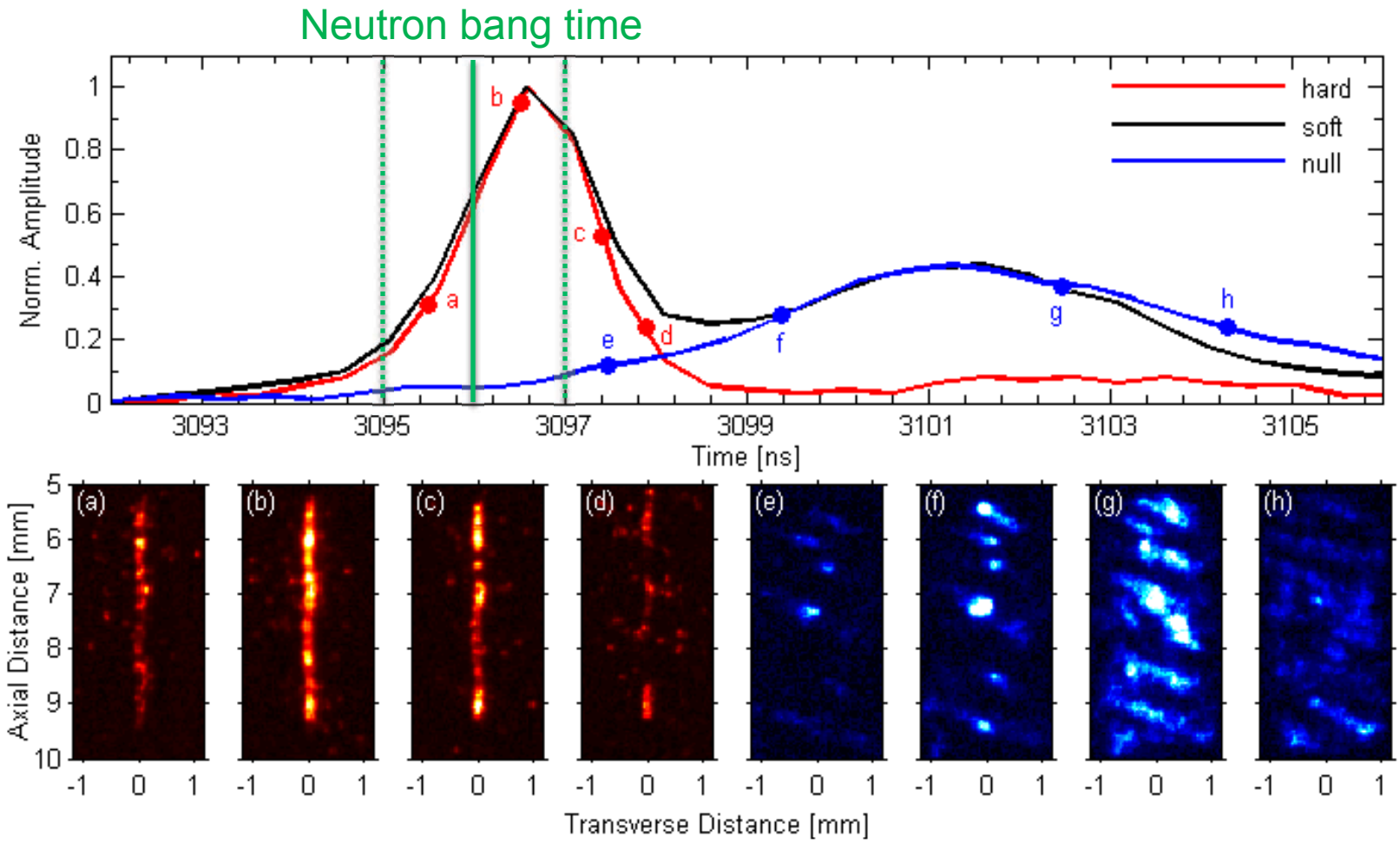

Narrow x-ray emission column observed at neutron bang time

M. R. Gomez et al., Phys. Rev. Lett. 113, 155003 (2014). M. R. Gomez et al., Phys. Plasmas 22, 056306 (2015).

X ray emission from the fuel shows a high aspect ratio stagnation column

- **Emission region does not define the fuel-liner boundary, but defines the hottest region of the fuel**
- **Emission FWHM is 50-110 µm**
- **Emission height is > 6mm (approximately 80% of target height)**
- **Axial intensity variations indicate variations in both the fuel conditions (temperature and density) and the liner opacity**
- **Stagnation column is weakly helical**

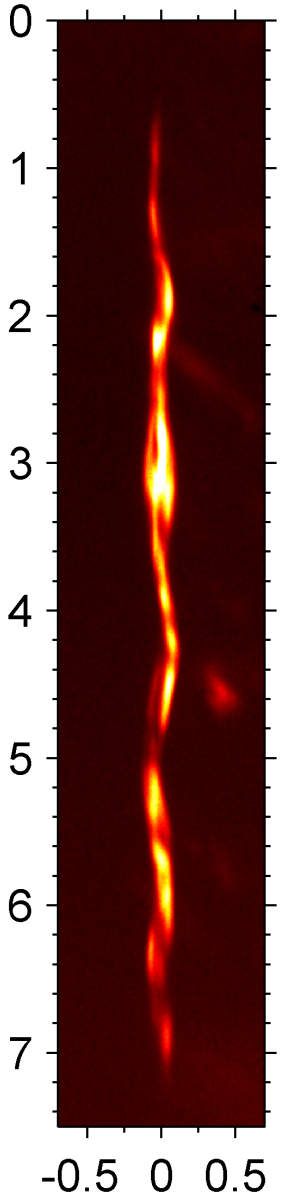

M. R. Gomez et al., Phys. Rev. Lett. 113, 155003 (2014).

These experiments utilize deuterium gas as the fusion fuel

Sandia National Laboratories

- Primary reactions

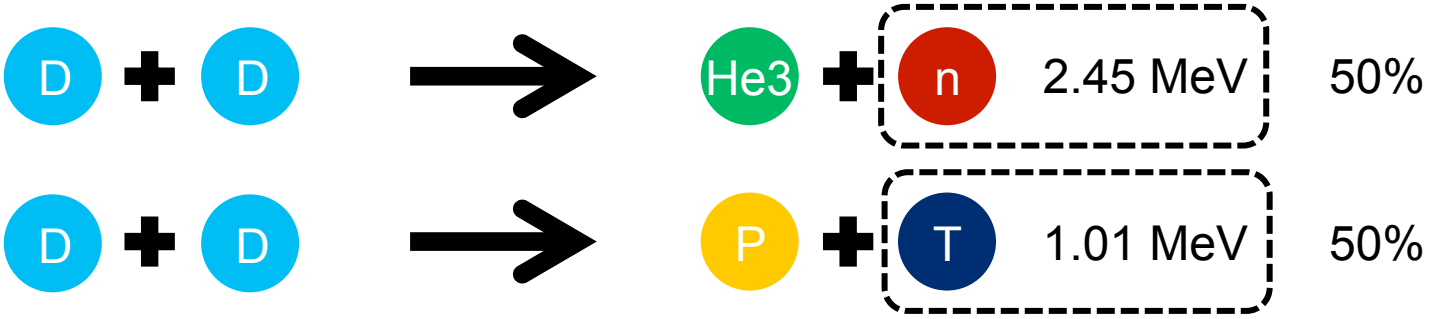

- Secondary reactions

- Triton may still retain fraction of birth energy when reacting

In our fully integrated MagLIF experiments[1], DT/DD yield ratios and neutron time-of-flight data are consistent with the fusing particles being magnetized[2,3]

Sandia National Laboratories

Magnetized tritons implies magnetized electrons:

$$\omega_{ci}\tau_{ie} \approx \omega_{ce}\tau_{ee}$$

Magnetized tritons implies magnetized alpha particles:

$$r_t \approx 1.1 r_\alpha$$

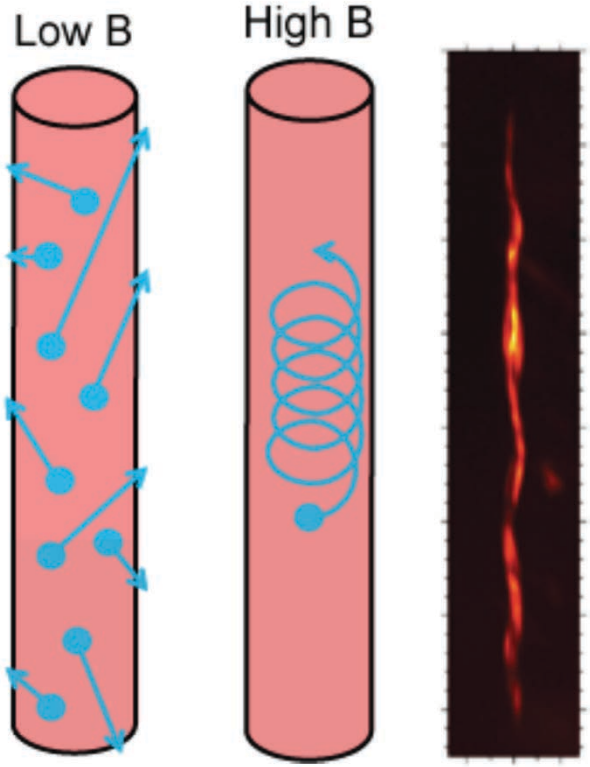

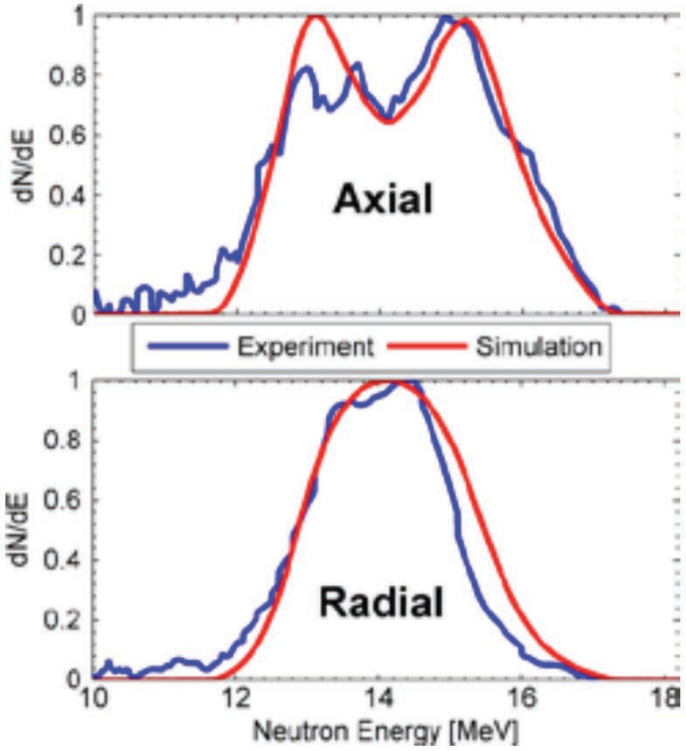

[1]M. R. Gomez *et al*., PRL **113**, 155003 (2014).
[2]P. F. Schmit *et al.,* PRL **113**, 155004 (2014).
[3]P. F. Knapp *et al*. PoP **22**, 056312 (2015).

See invited talks by
P. F. Knapp, SO19-3
M. R. Gomez, PPC-O-14-2

2D HYDRA simulations predict yields in excess of 1e13 for these targets

Sandia National Laboratories

- Simulations use a smooth beam and do not include laser plasma instabilities
- Predict > 1 kJ of laser energy deposited in fuel
- All measured parameters are well matched if laser energy is limited to a few 100 J

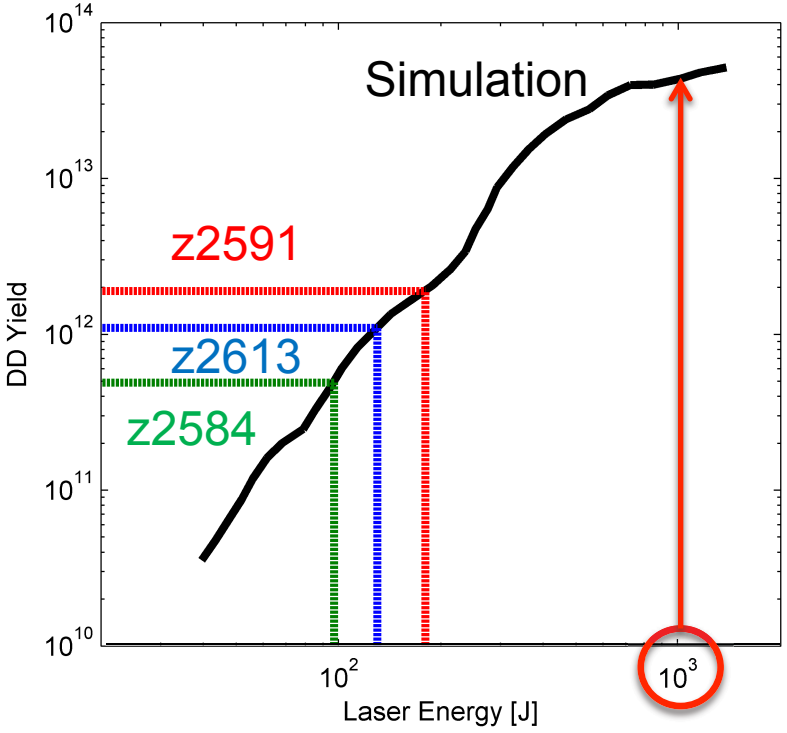

How realistic is it to assume poor laser energy coupling?

A. B. Sefkow et al., Phys. Plasmas 21, 072711 (2014).

Energy coupled to fuel was less than expected in laser heating experiments

Sandia National Laboratories

1.5 micron LEH window

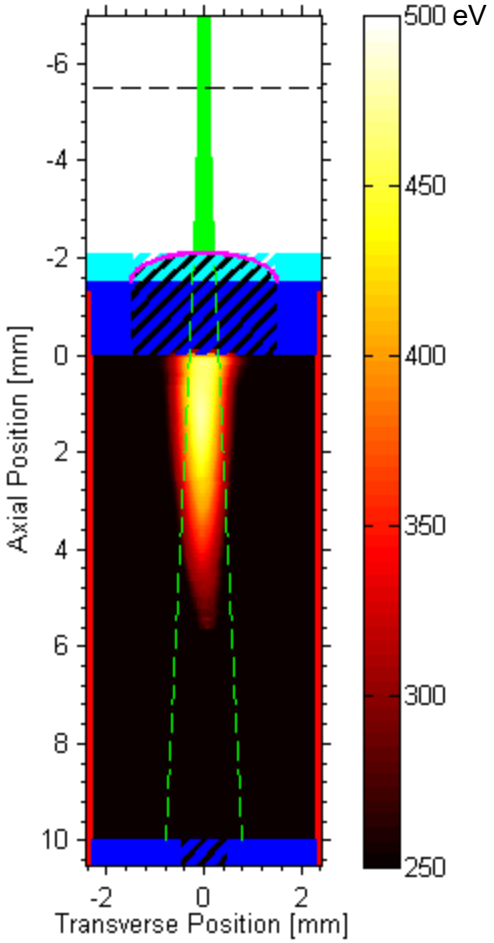

- Measured energy is not 50% of delivered laser energy as expected
  - Measured energy is only 100 J
- Diagnostic is not sensitive to regions below 250 eV
  - There could be 100s of J hidden
  - New target and diagnostic designs to access lower temperature regions
- Energy deposition linearly increases towards the top of the target
  - There is unmeasured energy in the laser entrance channel
- Beam is unconditioned which can substantially affect energy deposition
  - Phase plates are on order and should make deposition more uniform

Data with >3 micron LEH window not collected yet

All targets to date have utilized Al endcaps

- Simulations assuming uniform mix of a material at the time of laser heating indicate small levels of high Z mix can be catastrophic

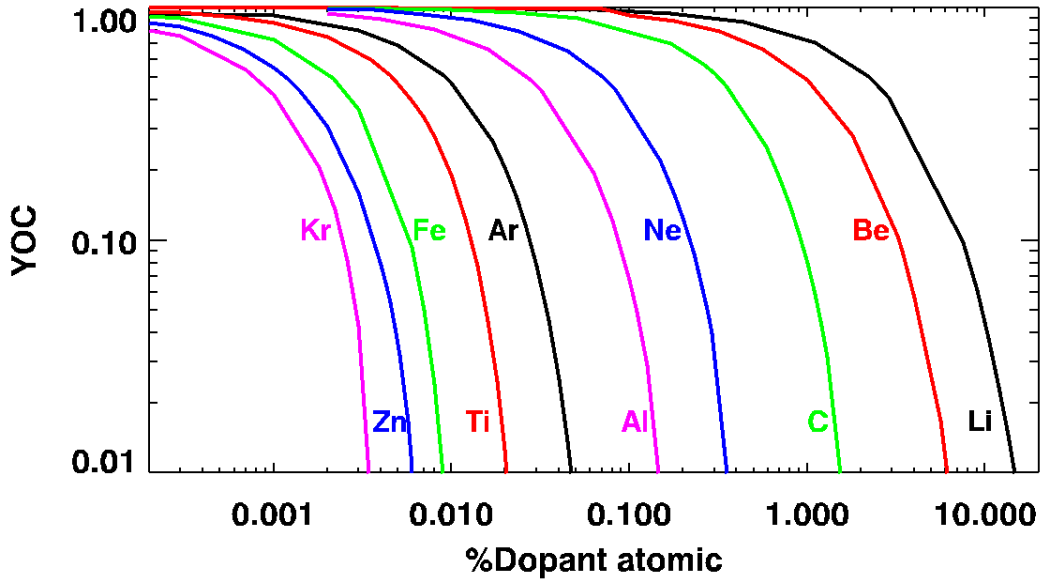

- The fuel can tolerate over 10x more Be mix than Al and produce the same yield
- Assuming 0.1% mix, a target with Be out performs one with Al by a factor of 10 in yield

Attempts to improve performance above our baseline design have proven difficult

Sandia National Laboratories

- Poor laser coupling to fuel (~10%) suspected as a major factor contributing to lower than expected yield
  - Increased laser energy from 2-4 kJ: Expected dramatic improvement
    - Actually degraded yield below detectable limits
    - Suspect mix induced by LEH interaction
  - Reduced window thickness from 3μm to 1.5 μm: Expected to improve laser coupling and yield
    - Yield was reduced
    - Mix is again suspected
- Laser interactions are potentially deleterious
  - X-rays generated can ablate Al walls
  - Laser ablation of window can push plastic into fuel
  - Scattered light can cause ablation of walls
  - Mix in the channel can cause further absorption, preventing penetration of beam into imploding region

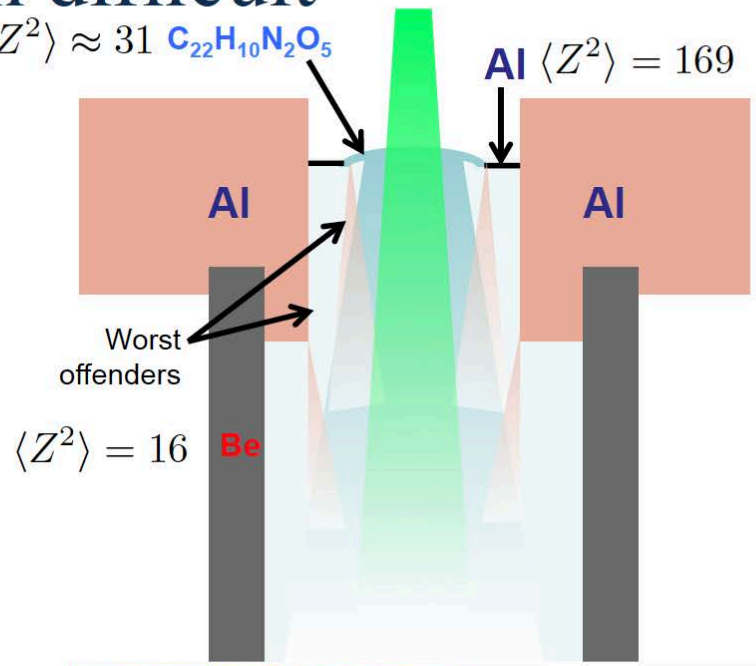

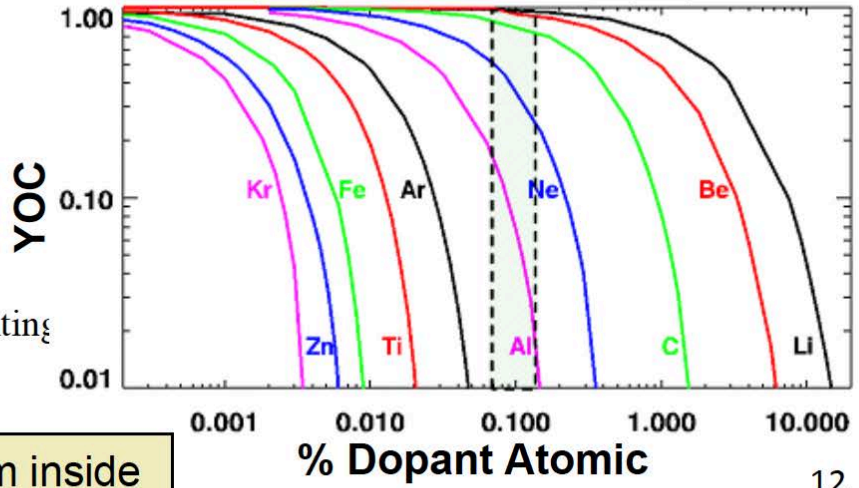

Removing ALL Al from inside of target in future designs

Upcoming experiments will test the mix hypothesis and reduce the impact of mix

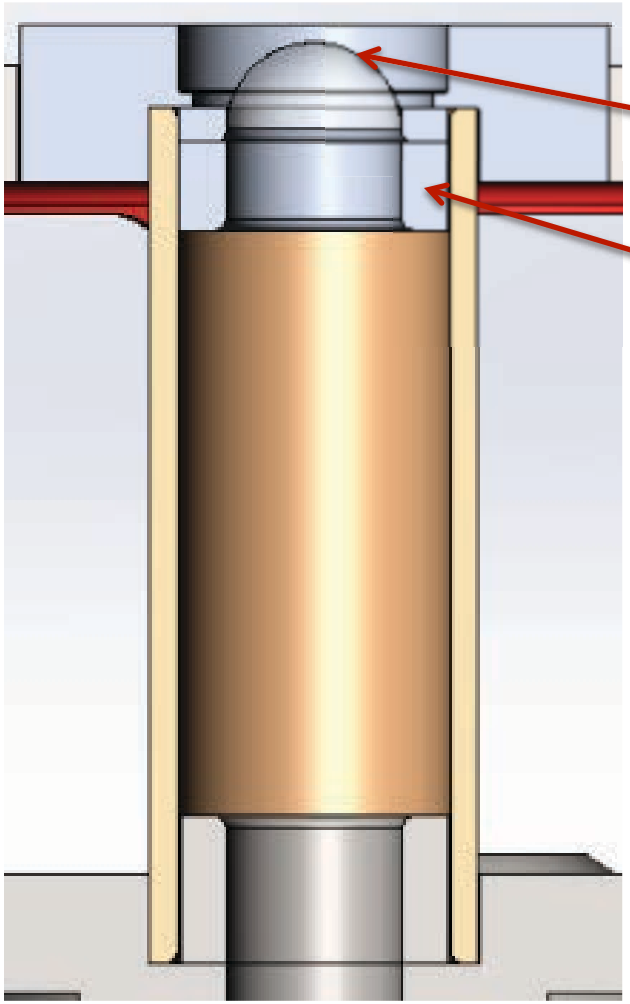

- New targets are modular
  - LEH window thickness can be 1.5 or >3 microns
  - Top endcap can be Al or Be

- Upcoming experiments
  - >3 micron window + Al
  - >3 micron window + Be
  - 1.5 micron window + Al
  - 1.5 micron window + Be

Laser heating experiments with >3 micron LEH windows will be conducted

We are also developing cryogenic capabilities and investing in phase plates

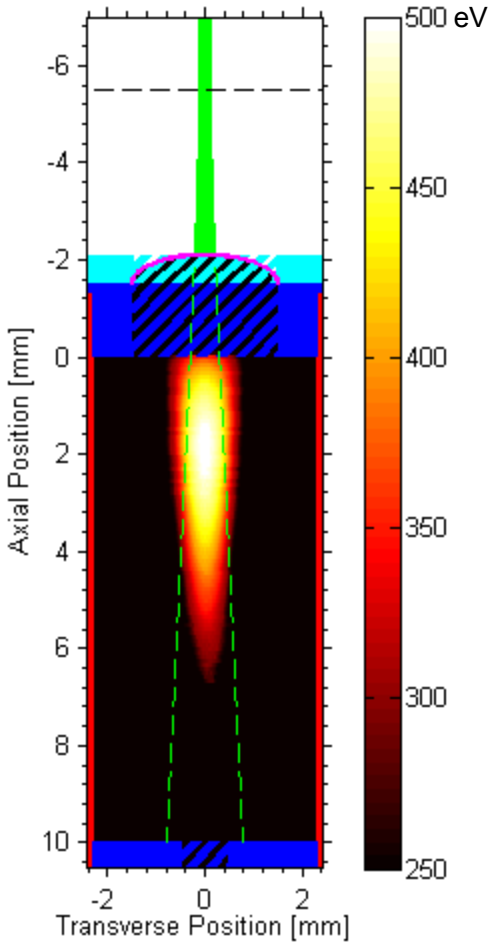

- These efforts are expected to improve laser heating in MagLIF experiments
- Cryogenics will allow much thinner windows for the same fill density
  - 0.25-0.40 µm compared to 1.5 µm at room temperature
  - Improved laser transmission
  - Larger LEH diameter reduces concerns about endcap mix
- Phase plates on loan from LLE have demonstrated improved energy deposition in laser heating experiments
  - ~40% increase in coupled energy

A cryogenic target has been designed to help mitigate the laser interaction issues

Sandia National Laboratories

- Why cryogenic?
  - Cooling allows us to get the same gas density (~0.7 mg/cm^3) at much lower pressure (15 PSI @ 70 K)
  - This allows for much thinner windows with larger diameter
  - Thinner window allows less energy to be invested in disassembly AND less mass injected into the target
  - Bigger window diameter should reduce likelihood of laser interactions with the wall

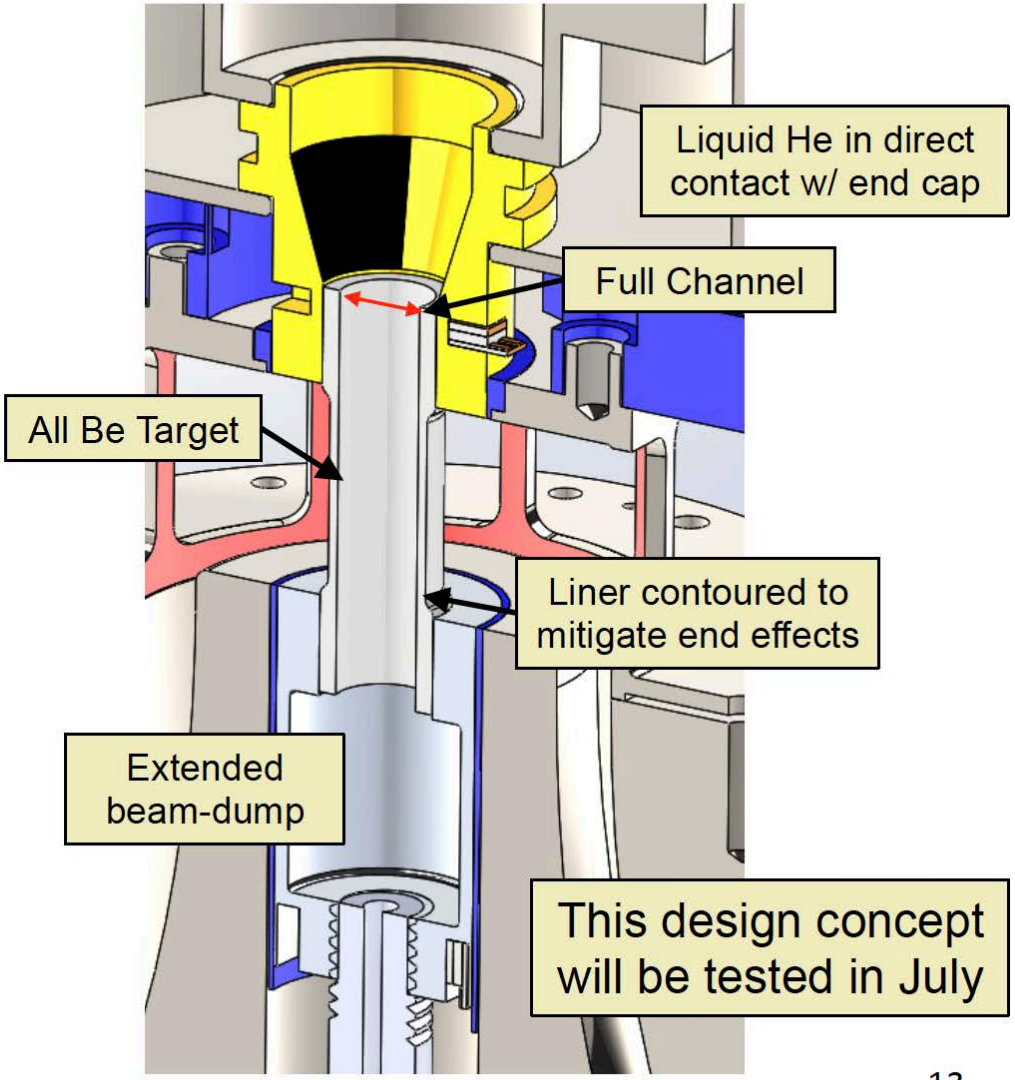

Design work done by Tom Awe, Adam Sefkow and Keegan Shelton

We are also planning numerous facility upgrades that will enable enhanced target performance

Sandia National Laboratories

- Z-Beamlet Laser
  - Increased energy
  - Improved beam profile
  - Co-injection of Z-Petawatt laser
- Improved Current Delivery
  - 31 cm convolute
  - Vacuum stack upgrade
- Coils capable of reaching 30 T
- Tritium operations on Z

Overview of semi-analytic MagLIF model (SAMM):

Sandia National Laboratories

$z,\ \rho_g,\ p_g,\ T_g$

$$T_g(r) = T_c \left\{ 1 - \left(\frac{r}{r_g} \right)^{\gamma} \left[1 - \left(\frac{T_B}{T_c} \right) \right] \right\}$$

$$\rho_g(r) = \rho_c \left\{ 1 - \left(\frac{r}{r_g} \right)^{\gamma} \left[1 - \left(\frac{T_B}{T_c} \right) \right] \right\}^{-1}$$

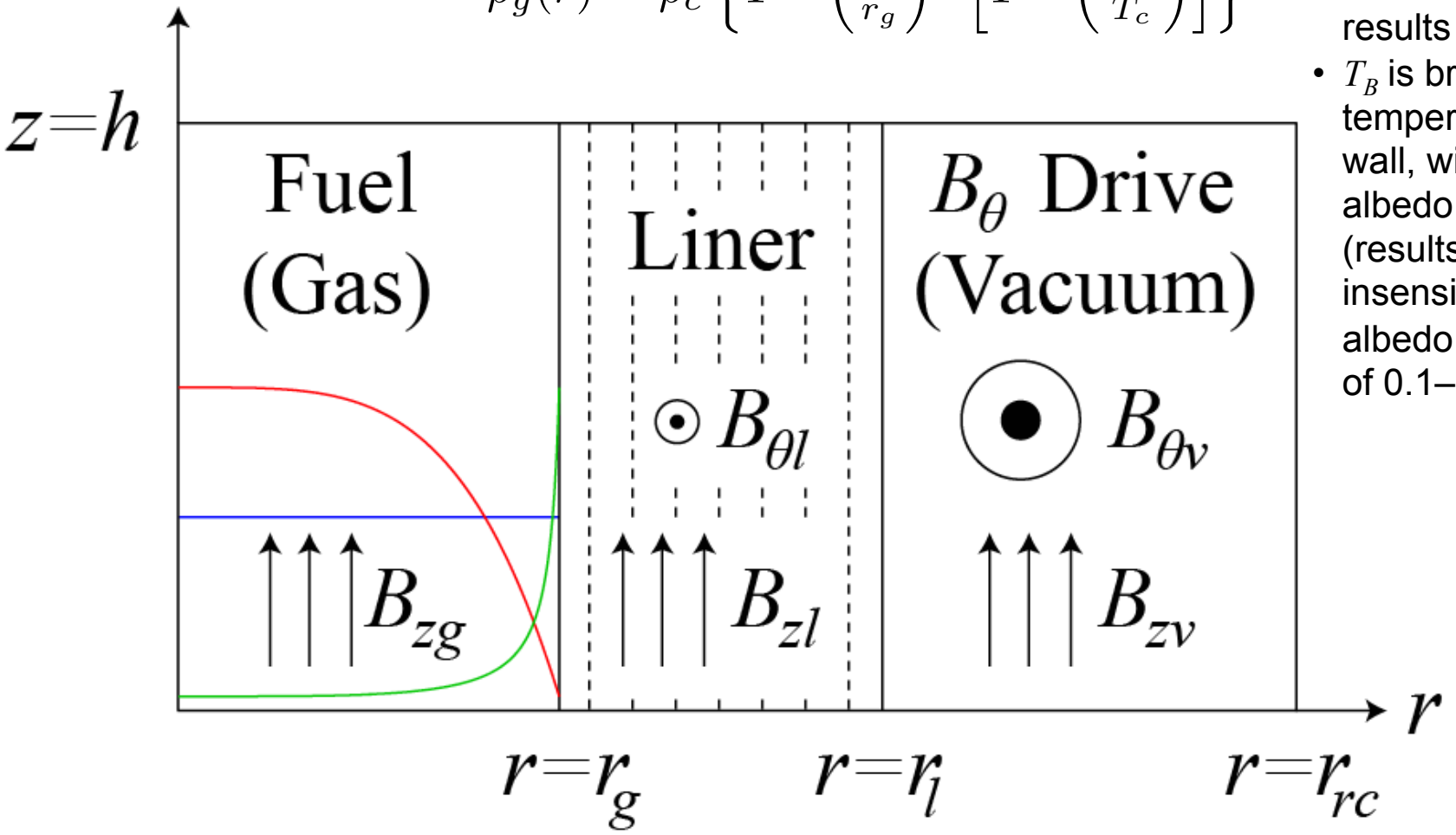

- γ~4 from least-squares fits to full MHD simulation results
- T_B is brightness temperature at wall, with albedo of ~0.5 (results are insensitive to albedo in range of 0.1–0.9)

Overview of semi-analytic MagLIF model (SAMM):

Sandia National Laboratories

- System of ordinary differential equations that are straight forward to solve with MATLAB, IDL, Mathematica, etc.
- ~20 seconds/simulation on my laptop
- Parameter scans of ~3000 simulations in ~5 minutes using Sandia cluster

$$\dot{I}_s = \frac{\varphi_{oc} - Z_0 I_s - \varphi_c}{L}$$

$$\dot{\varphi}_c = \frac{I_s - I_l - \varphi_c / R_{loss}}{C}$$

$$\dot{I}_l = \frac{\varphi_c - \dot{L}_l I_l}{L_0 + L_l}$$

$$\ddot{r}_g = \frac{p_g + p_{B_{zg}} - p_l - q_l - p_{B_l}}{m_l/2} \cdot 2\pi r_g \cdot h$$

$$\ddot{r}_l = \frac{p_l + q_l + p_{B_l} - p_{B_{\theta v}}}{m_l/2} \cdot 2\pi r_l \cdot h$$

$$\dot{E}_g = P_{pdV} + P_{ph} + P_\alpha - P_r - P_{ce} - P_{ci}$$

$$\dot{E}_l = -\left(\frac{2}{3}\frac{E_l}{V_l} + q_l\right)\dot{V}_l + P_r + P_{ce} + P_{ci} + I_l^2 R_l$$

$$\dot{\Phi}_{B_z} = -2\pi r_g f(\omega\tau) \left.\frac{dT_g}{dr}\right|_{r=r_g,\, T_g=T_B}$$

$$\dot{N}_{dj} = n_d n_j \langle\sigma v\rangle_{dj} \cdot (1 - \delta_{dj}/2) \cdot V_g \quad (j = d, t)$$

Overview of semi-analytic MagLIF model (SAMM):

Sandia National Laboratories

Drive (circuit model driven by open-circuit voltage φ_{oc})

$$\dot{I}_s = \frac{\varphi_{oc} - Z_0 I_s - \varphi_c}{L}$$

$$\dot{\varphi}_c = \frac{I_s - I_l - \varphi_c / R_{loss}}{C}$$

$$\dot{I}_l = \frac{\varphi_c - \dot{L}_l I_l}{L_0 + L_l}$$

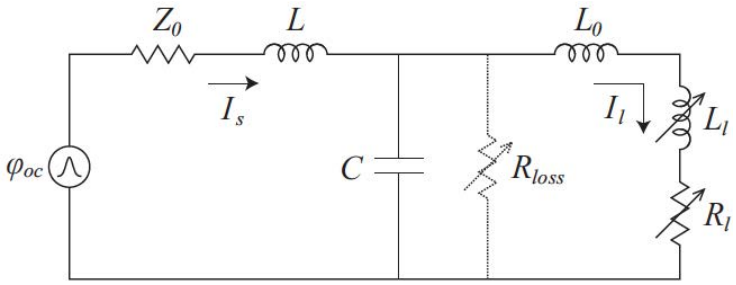

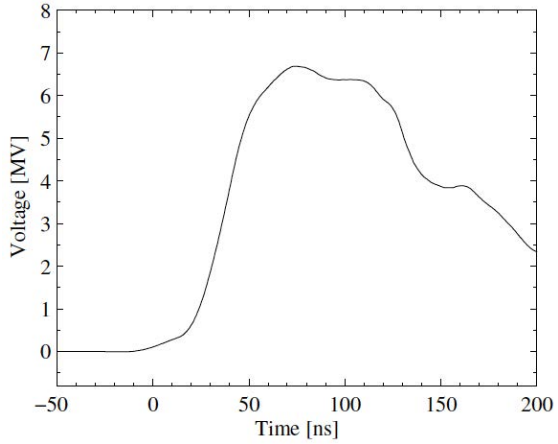

$$\ddot{r}_g = \frac{p_g + p_{B_{zg}} - p_l - q_l - p_{B_l}}{m_l/2} \cdot 2\pi r_g \cdot h$$

$$\ddot{r}_l = \frac{p_l + q_l + p_{B_l} - p_{B_{\theta v}}}{m_l/2} \cdot 2\pi r_l \cdot h$$

$$\dot{E}_g = P_{pdV} + P_{ph} + P_\alpha - P_r - P_{ce} - P_{ci}$$

$$\dot{E}_l = -\left(\frac{2}{3}\frac{E_l}{V_l} + q_l\right)\dot{V}_l + P_r + P_{ce} + P_{ci} + I_l^2 R_l$$

$$\dot{\Phi}_{B_z} = -2\pi r_g f(\omega\tau) \left.\frac{dT_g}{dr}\right|_{r=r_g,\, T_g=T_B}$$

$$\dot{N}_{dj} = n_d n_j \langle\sigma v\rangle_{dj} \cdot (1 - \delta_{dj}/2) \cdot V_g \quad (j = d, t)$$

Overview of semi-analytic MagLIF model (SAMM):

Sandia National Laboratories

$$\dot{I}_s = \frac{\varphi_{oc} - Z_0 I_s - \varphi_c}{L}$$

$$\dot{\varphi}_c = \frac{I_s - I_l - \varphi_c / R_{loss}}{C}$$

$$\dot{I}_l = \frac{\varphi_c - \dot{L}_l I_l}{L_0 + L_l}$$

Dynamics (fuel and liner) →

- p_l = ideal gas + Birch-Murnaghan cold curve (used for analytic fits to SESAME tables)
- q_l ~ simple v^2 dependence

$$\ddot{r}_g = \frac{p_g + p_{B_{zg}} - p_l - q_l - p_{B_l}}{m_l/2} \cdot 2\pi r_g \cdot h$$

$$\ddot{r}_l = \frac{p_l + q_l + p_{B_l} - p_{B_{\theta v}}}{m_l/2} \cdot 2\pi r_l \cdot h$$

$$\dot{E}_g = P_{pdV} + P_{ph} + P_\alpha - P_r - P_{ce} - P_{ci}$$

$$\dot{E}_l = -\left(\frac{2}{3}\frac{E_l}{V_l} + q_l\right)\dot{V}_l + P_r + P_{ce} + P_{ci} + I_l^2 R_l$$

$$\dot{\Phi}_{B_z} = -2\pi r_g f(\omega\tau) \left.\frac{dT_g}{dr}\right|_{r=r_g,\, T_g=T_B}$$

$$\dot{N}_{dj} = n_d n_j \langle\sigma v\rangle_{dj} \cdot (1 - \delta_{dj}/2) \cdot V_g \quad (j = d, t)$$

Overview of semi-analytic MagLIF model (SAMM):

Sandia National Laboratories

$$\dot{I}_s = \frac{\varphi_{oc} - Z_0 I_s - \varphi_c}{L}$$

$$\dot{\varphi}_c = \frac{I_s - I_l - \varphi_c / R_{loss}}{C}$$

$$\dot{I}_l = \frac{\varphi_c - \dot{L}_l I_l}{L_0 + L_l}$$

$$\ddot{r}_g = \frac{p_g + p_{B_{zg}} - p_l - q_l - p_{B_l}}{m_l/2} \cdot 2\pi r_g \cdot h$$

$$\ddot{r}_l = \frac{p_l + q_l + p_{B_l} - p_{B_{\theta v}}}{m_l/2} \cdot 2\pi r_l \cdot h$$

Energetics (fuel and liner) →

- P_α = Basko
- P_r = Grey model with emissivity & opacity integral over T & ρ profiles
- P_{ce} = Epperlein-Haines
- P_{ci} = Braginskii
- $I_l^2 R_l$ = From assumed distribution: $B_\theta(r) \sim r^{\beta(\delta skin)}$ and Maxwell's equations (results somewhat sensitive to β)

$$\dot{E}_g = P_{pdV} + P_{ph} + P_\alpha - P_r - P_{ce} - P_{ci}$$

$$\dot{E}_l = -\left(\frac{2}{3}\frac{E_l}{V_l} + q_l\right)\dot{V}_l + P_r + P_{ce} + P_{ci} + I_l^2 R_l$$

$$\dot{\Phi}_{B_z} = -2\pi r_g f(\omega\tau) \left.\frac{dT_g}{dr}\right|_{r=r_g,\, T_g=T_B}$$

$$\dot{N}_{dj} = n_d n_j \langle\sigma v\rangle_{dj} \cdot (1 - \delta_{dj}/2) \cdot V_g \quad (j = d, t)$$

Overview of semi-analytic MagLIF model (SAMM):

Sandia National Laboratories

$$\dot{I}_s = \frac{\varphi_{oc} - Z_0 I_s - \varphi_c}{L}$$

$$\dot{\varphi}_c = \frac{I_s - I_l - \varphi_c / R_{loss}}{C}$$

$$\dot{I}_l = \frac{\varphi_c - \dot{L}_l I_l}{L_0 + L_l}$$

$$\ddot{r}_g = \frac{p_g + p_{B_{zg}} - p_l - q_l - p_{B_l}}{m_l/2} \cdot 2\pi r_g \cdot h$$

$$\ddot{r}_l = \frac{p_l + q_l + p_{B_l} - p_{B_{\theta v}}}{m_l/2} \cdot 2\pi r_l \cdot h$$

$$\dot{E}_g = P_{pdV} + P_{ph} + P_\alpha - P_r - P_{ce} - P_{ci}$$

$$\dot{E}_l = -\left(\frac{2}{3}\frac{E_l}{V_l} + q_l\right)\dot{V}_l + P_r + P_{ce} + P_{ci} + I_l^2 R_l$$

B_z flux loss due to the Nernst thermoelectric effect (Braginskii) →

$$\dot{\Phi}_{B_z} = -2\pi r_g f(\omega\tau) \left.\frac{dT_g}{dr}\right|_{r=r_g,\, T_g = T_B}$$

$$\dot{N}_{dj} = n_d n_j \langle \sigma v \rangle_{dj} \cdot (1 - \delta_{dj}/2) \cdot V_g \quad (j = d, t)$$

Overview of semi-analytic MagLIF model (SAMM):

Sandia National Laboratories

$$\dot{I}_s = \frac{\varphi_{oc} - Z_0 I_s - \varphi_c}{L}$$

$$\dot{\varphi}_c = \frac{I_s - I_l - \varphi_c / R_{loss}}{C}$$

$$\dot{I}_l = \frac{\varphi_c - \dot{L}_l I_l}{L_0 + L_l}$$

$$\ddot{r}_g = \frac{p_g + p_{B_{zg}} - p_l - q_l - p_{B_l}}{m_l/2} \cdot 2\pi r_g \cdot h$$

$$\ddot{r}_l = \frac{p_l + q_l + p_{B_l} - p_{B_{\theta v}}}{m_l/2} \cdot 2\pi r_l \cdot h$$

$$\dot{E}_g = P_{pdV} + P_{ph} + P_\alpha - P_r - P_{ce} - P_{ci}$$

$$\dot{E}_l = -\left(\frac{2}{3}\frac{E_l}{V_l} + q_l\right)\dot{V}_l + P_r + P_{ce} + P_{ci} + I_l^2 R_l$$

$$\dot{\Phi}_{B_z} = -2\pi r_g f(\omega\tau) \left.\frac{dT_g}{dr}\right|_{r=r_g,\, T_g=T_B}$$

DD & DT Fusion Burn →

- Analytic $\langle\sigma v\rangle$ (Bosch & Hale)

$$\dot{N}_{dj} = n_d n_j \langle\sigma v\rangle_{dj} \cdot (1 - \delta_{dj}/2) \cdot V_g \quad (j = d, t)$$

Overview of semi-analytic MagLIF model (SAMM):

Sandia National Laboratories

$$\dot{I}_s = \frac{\varphi_{oc} - Z_0 I_s - \varphi_c}{L}$$

$$\dot{\varphi}_c = \frac{I_s - I_l - \varphi_c / R_{loss}}{C}$$

$$\dot{I}_l = \frac{\varphi_c - \dot{L}_l I_l}{L_0 + L_l}$$

$$\ddot{r}_g = \frac{p_g + p_{B_{zg}} - p_l - q_l - p_{B_l}}{m_l/2} \cdot 2\pi r_g \cdot h$$

$$\ddot{r}_l = \frac{p_l + q_l + p_{B_l} - p_{B_{\theta v}}}{m_l/2} \cdot 2\pi r_l \cdot h$$

$$\ddot{r}_{l,i} = \frac{p_{in,i} + q_{in,i} - p_{out,i} - q_{out,i}}{m_l/n} \cdot 2\pi r_{l,i} \cdot h \qquad (i = 2, 3, \ldots, n)$$

$$\dot{E}_g = P_{pdV} + P_{ph} + P_\alpha - P_r - P_{ce} - P_{ci}$$

$$\dot{E}_l = -\left(\frac{2}{3}\frac{E_l}{V_l} + q_l\right)\dot{V}_l + P_r + P_{ce} + P_{ci} + I_l^2 R_l$$

$$\dot{E}_{l,i} = -\left(\frac{2}{3}\frac{E_{l,i}}{V_{l,i}} + q_{l,i}\right)\dot{V}_{l,i} + \left(P_r + P_{ce} + P_{ci} + I_l^2 R_l\right)/n \qquad (i = 1, 2, \ldots, n)$$

$$\dot{\Phi}_{B_z} = -2\pi r_g f(\omega\tau)\left.\frac{dT_g}{dr}\right|_{r=r_g,\, T_g = T_B}$$

$$\dot{N}_{dj} = n_d n_j \langle\sigma v\rangle_{dj} \cdot (1 - \delta_{dj}/2) \cdot V_g \qquad (j = d, t)$$

We found that we needed to discretize the liner to obtain more reasonable convergence ratios

- This is particularly important for near term, low preheat energy solutions

“Blast wave” solution implemented to handle radial fractions of fuel preheated

- Fuel split into two parts that evolve:
  - The preheated fuel becomes the hot spot region
  - The rest becomes a cold, dense shelf region
- Entire fuel is still at constant pressure radially
- Shelf temperature set to brightness/radiation temperature, T_B
- Shelf reduces brems losses since radiation model is given by:

$$P_{rad} = A_{br} \int_0^{r_g} n_i(r) n_e(r) \bar{Z}^2 \sqrt{T_g(r)} \left[1 - \left(\frac{T_B}{T_g(r)}\right)^4\right] r dr$$

$$P_{rad} = (1-\alpha)\sigma T_B^4 \cdot A_w$$

- Shelf provides a buffer region between the hotspot and the liner wall
- Shelf erosion model given by:

$$E = \frac{3}{2} N k T$$

$$\rightarrow \dot{m} = \frac{2}{3} \frac{\bar{m}_i}{(\bar{T}_{hot} - \bar{T}_{shelf})} \cdot P_{therm}$$

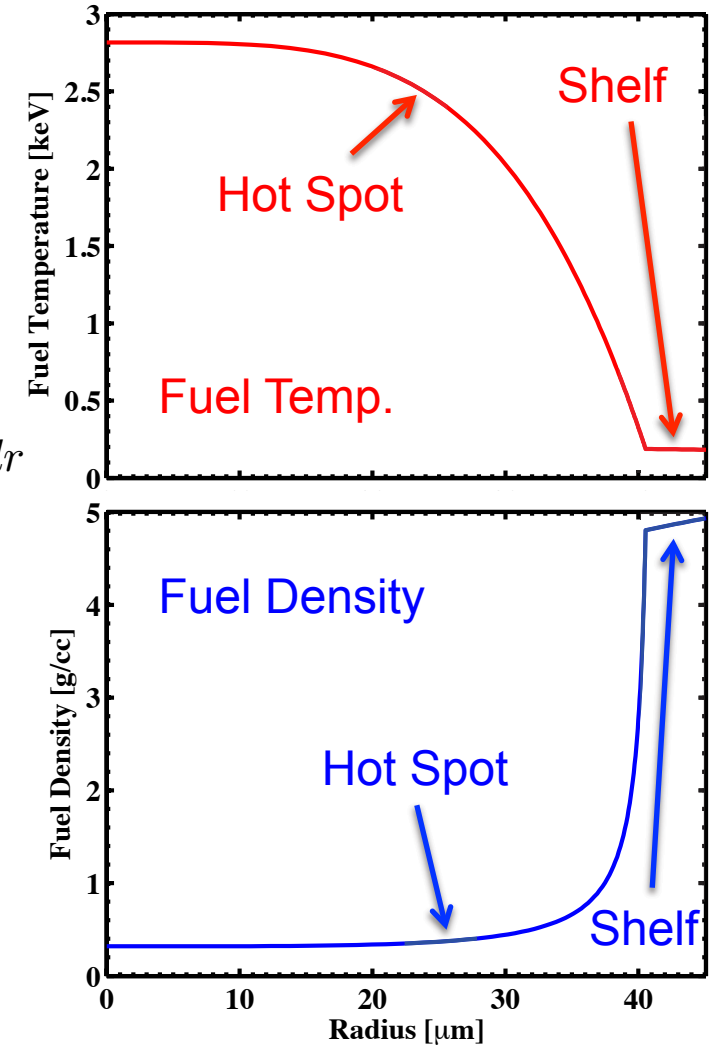

SAMM with new fuel shelf erosion model, brems, and only a fraction of the fuel uniformly preheated:

Sandia National Laboratories

Semi-analytic model with uniformly preheated fuel from $r = 0$ to $r = 0.5\ r_g$

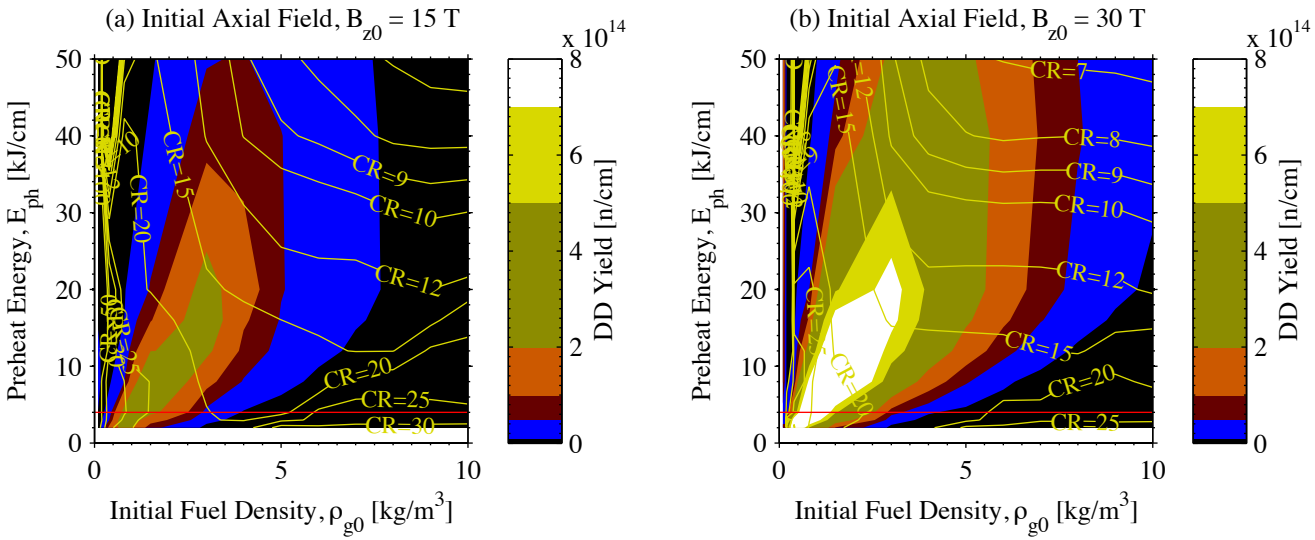

LASNEX simulations with uniformly preheated fuel from $r = 0$ to $r = 0.5\ r_g$

(LASNEX contour plots courtesy of R. A. Vesey)

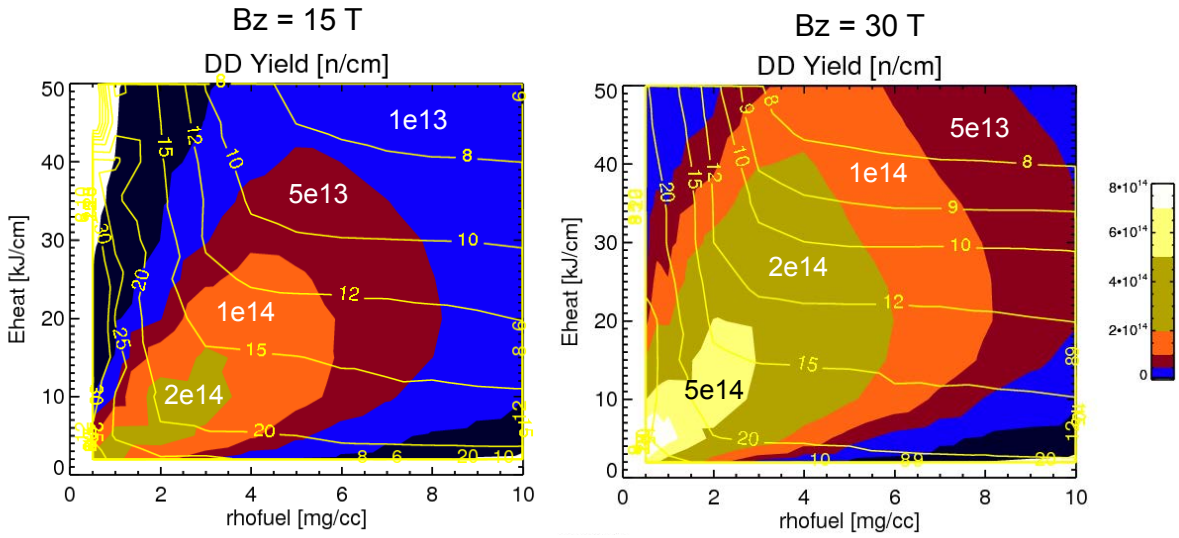

SAMM with all fuel uniformly preheated and brems:

Sandia National Laboratories

Semi-analytic model where all fuel is uniformly preheated

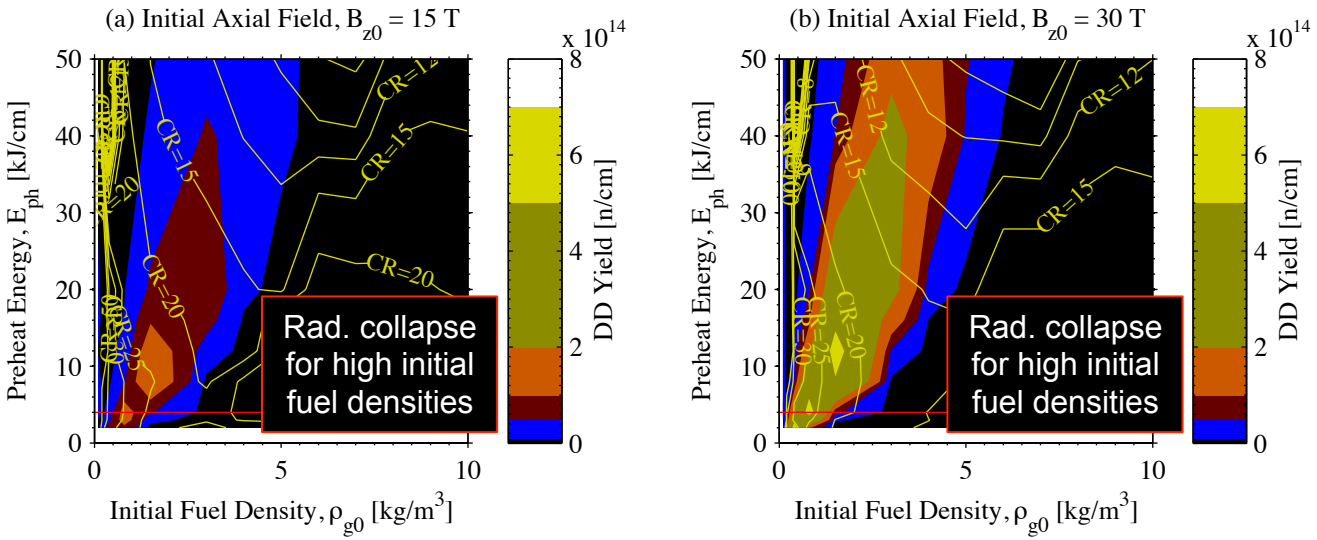

LASNEX simulations with uniformly preheated fuel from r = 0 to r = 0.5 r_g

(LASNEX contour plots courtesy of R. A. Vesey)

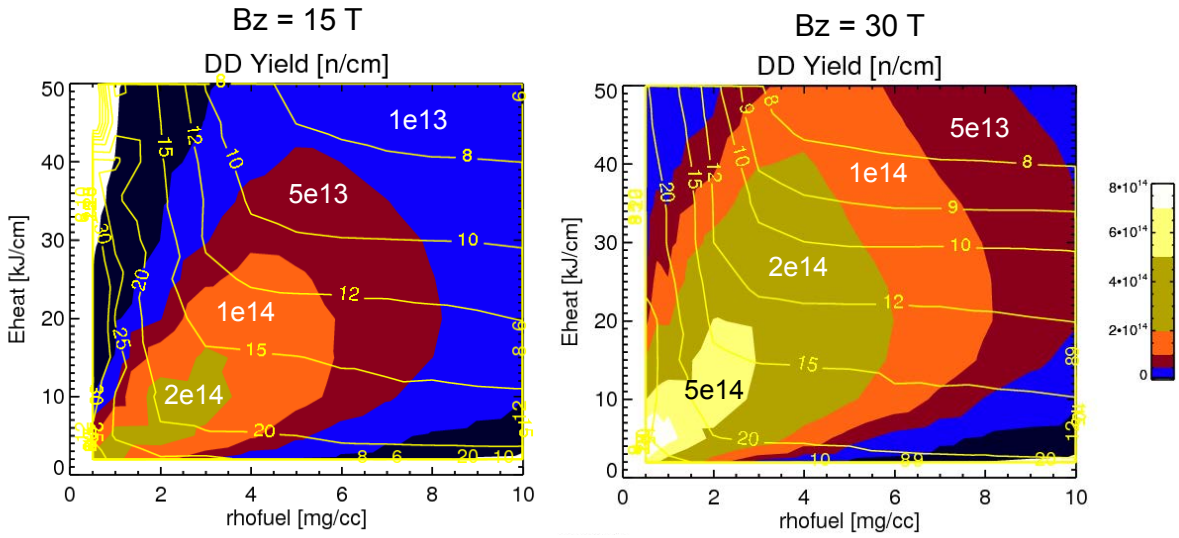

2D LASNEX simulations of MagLIF suggest an optimum at an aspect ratio (AR) of 6*

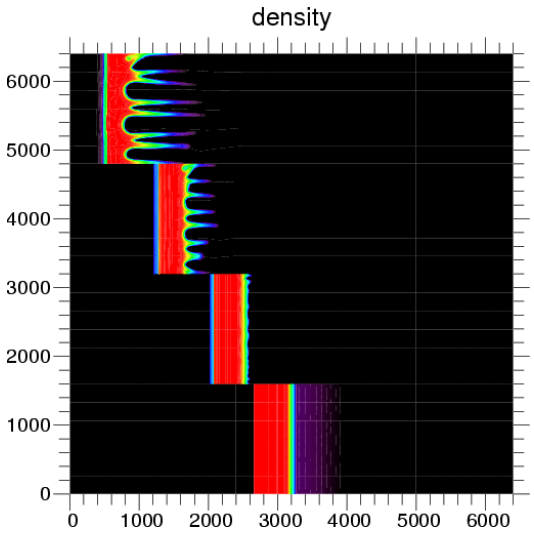

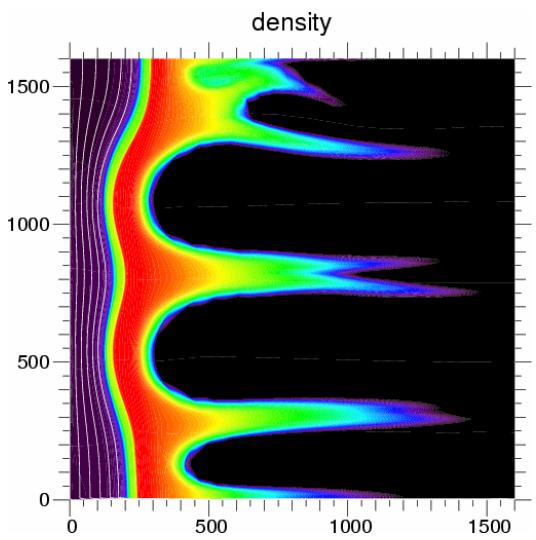

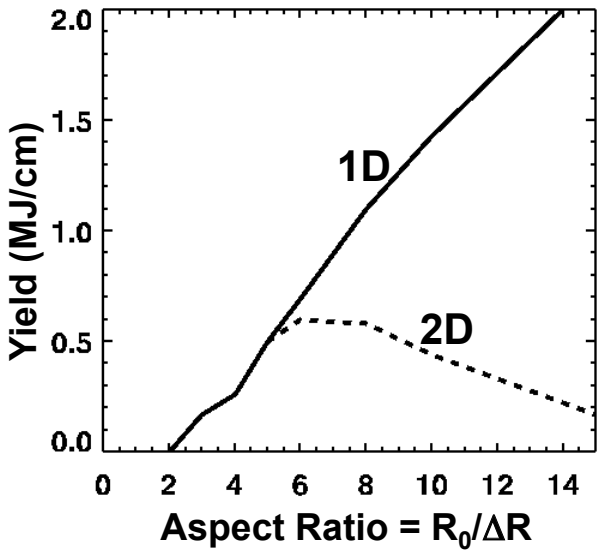

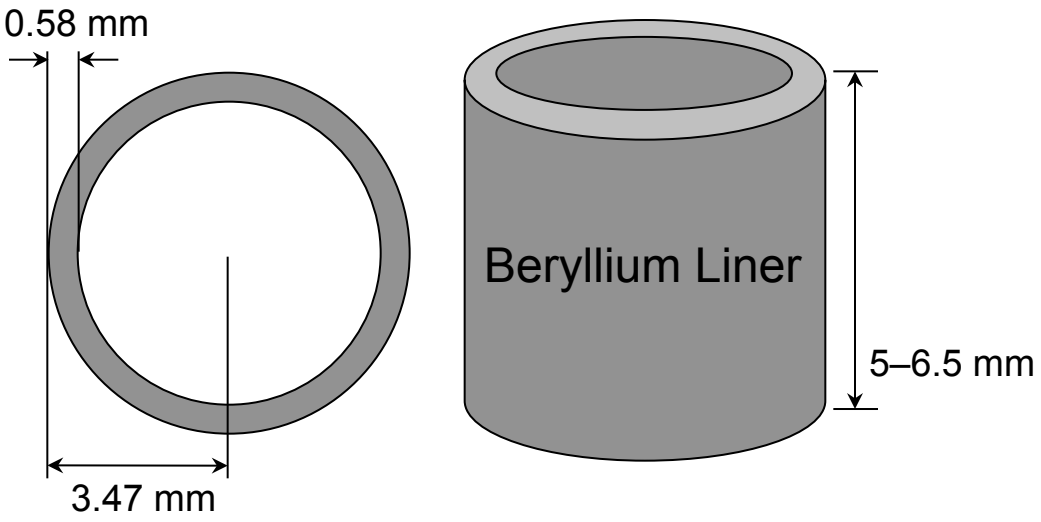

$$\mathrm{AR} \equiv \frac{R_{outer,0}}{\Delta R_0}$$

* S. A. Slutz *et al.*, Phys. Plasmas **17**, 056303 (2010).

Beryllium experiments showed surprisingly correlated instability growth

- This led to the competing hypotheses that the observed azimuthal correlation is the result of:
  a. The azimuthal correlation in the initial surface finish of the liner (i.e., from the diamond-turned machining/lathe marks)
  b. The "overheat"/striation form of the electro-thermal instability (ETI)
  c. A combination of both

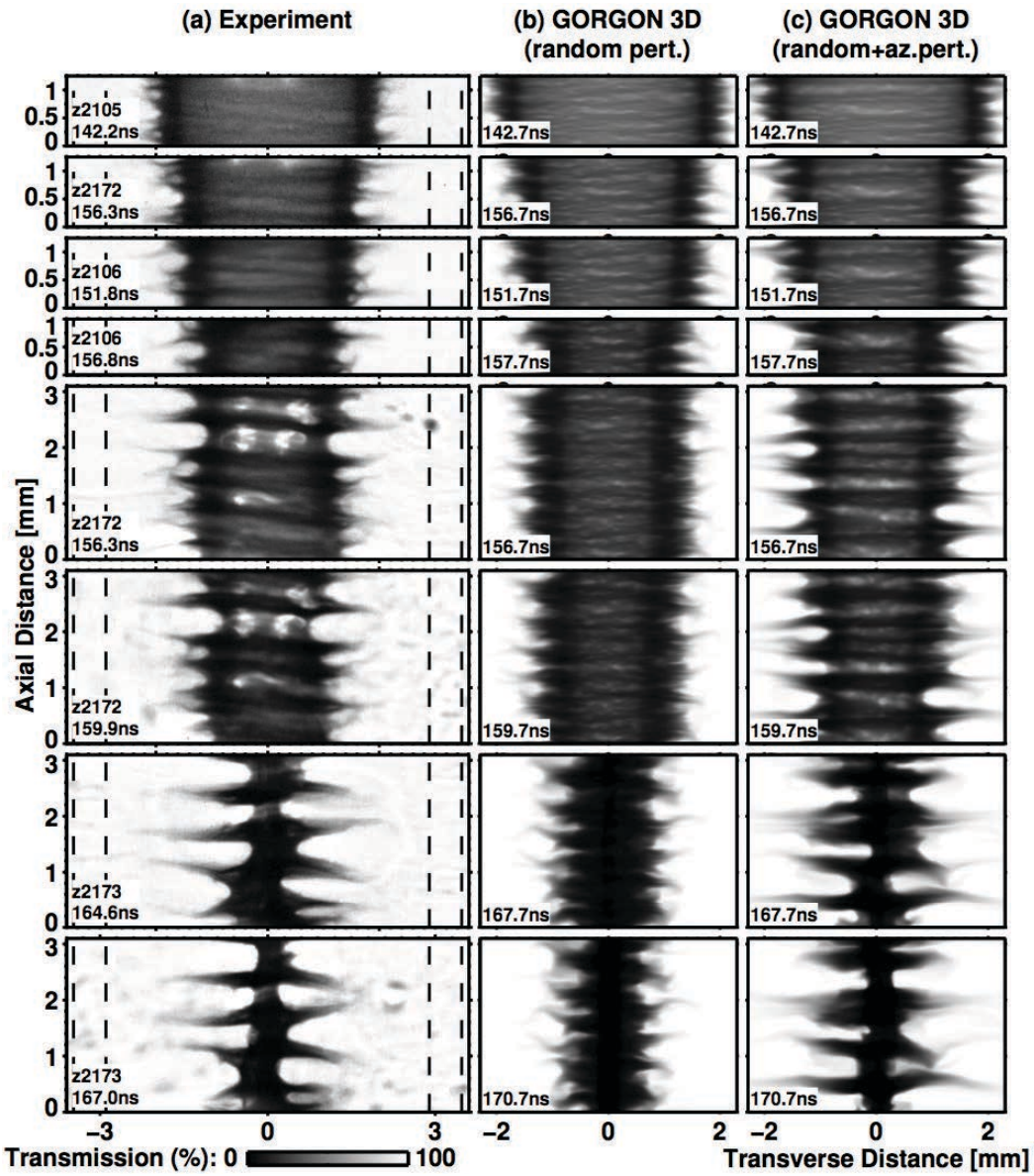

Our liners are diamond-turned on a lathe to provide smooth surfaces, but this process leaves azimuthally-correlated tool marks

Sandia National Laboratories

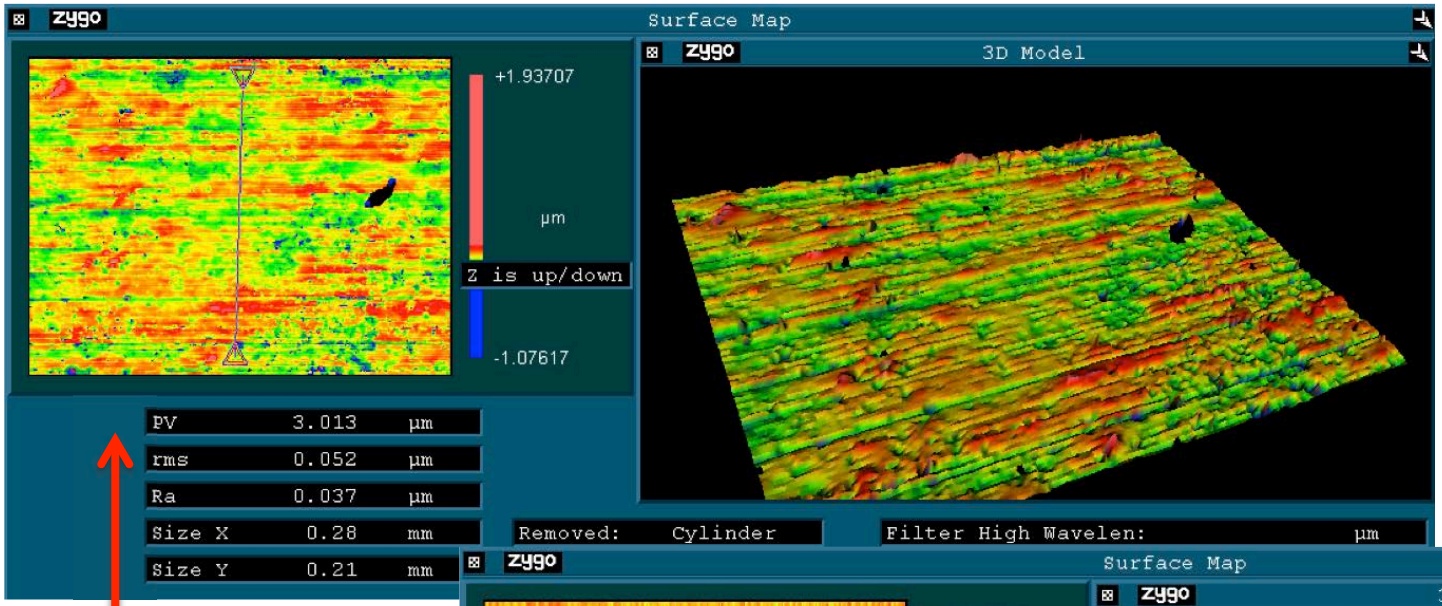

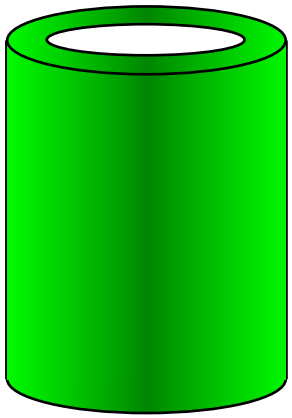

Standard process
(50 nm RMS)

After axial polishing
process applied
(50 nm RMS)

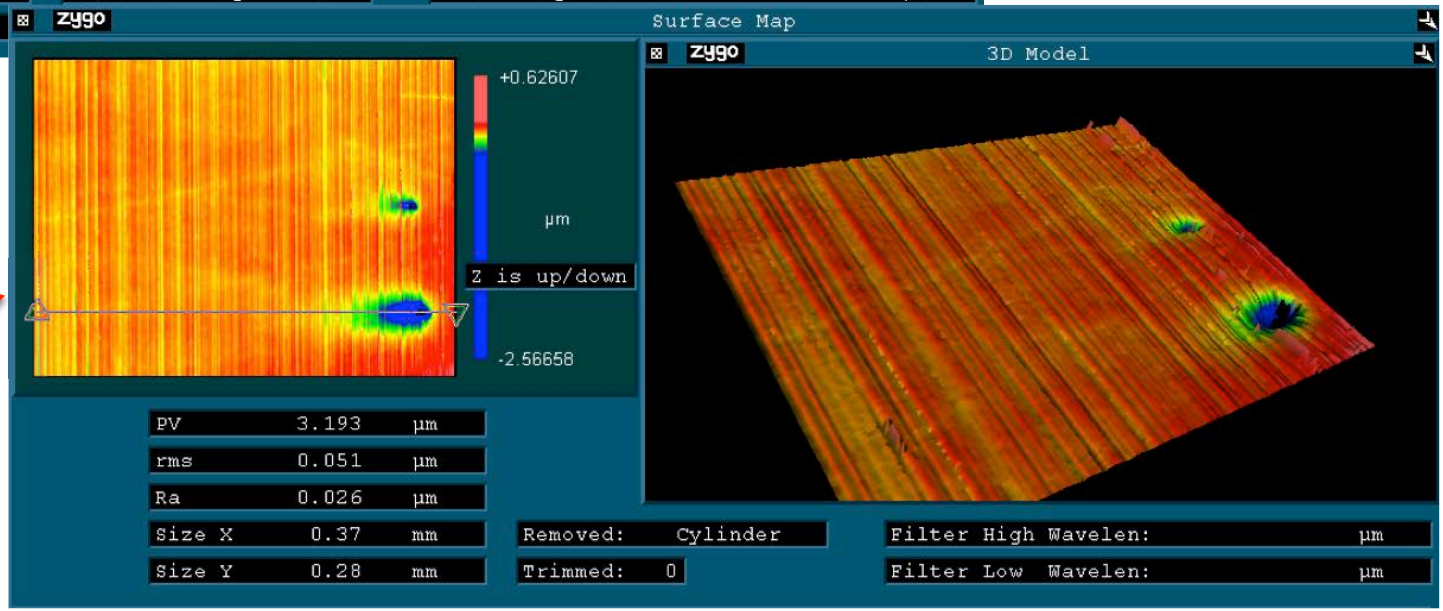

Changing the character of the surface did not change the observation:

Sandia National Laboratories

Axially-polished liner growth

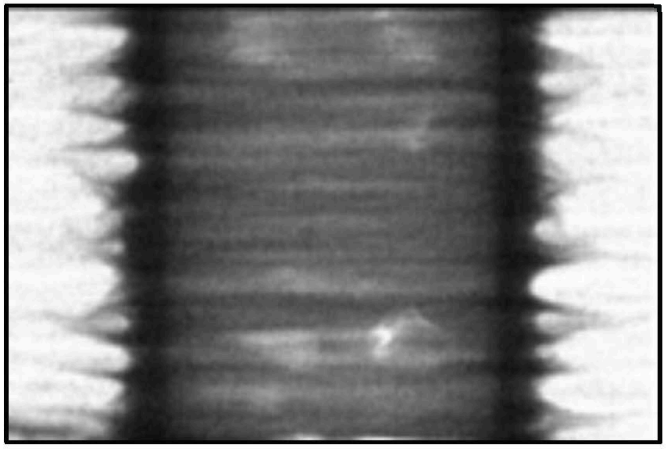

D. B. Sinars *et al.*, manuscript in preparation.

Non-polished data

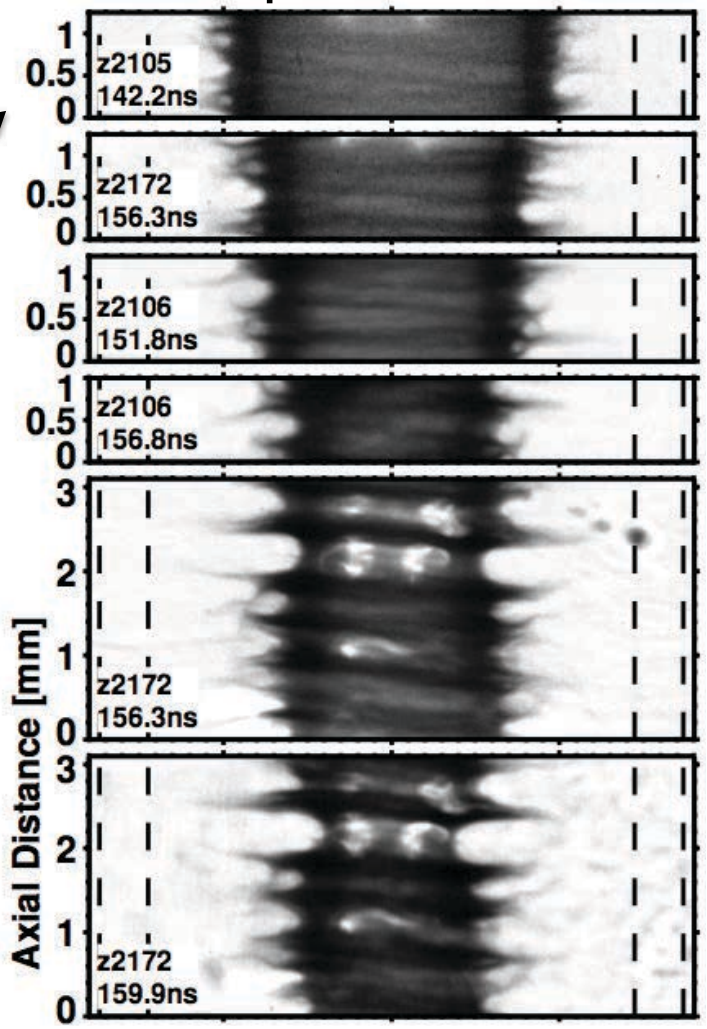

R. D. McBride *et al.*, PRL **109**, 135004 (2012).

Electrothermal instabilities occur when material conductivity is dependent on temperature

Sandia National Laboratories

Theory

Filamentations

$$\frac{d\eta(T)}{dT} < 0$$

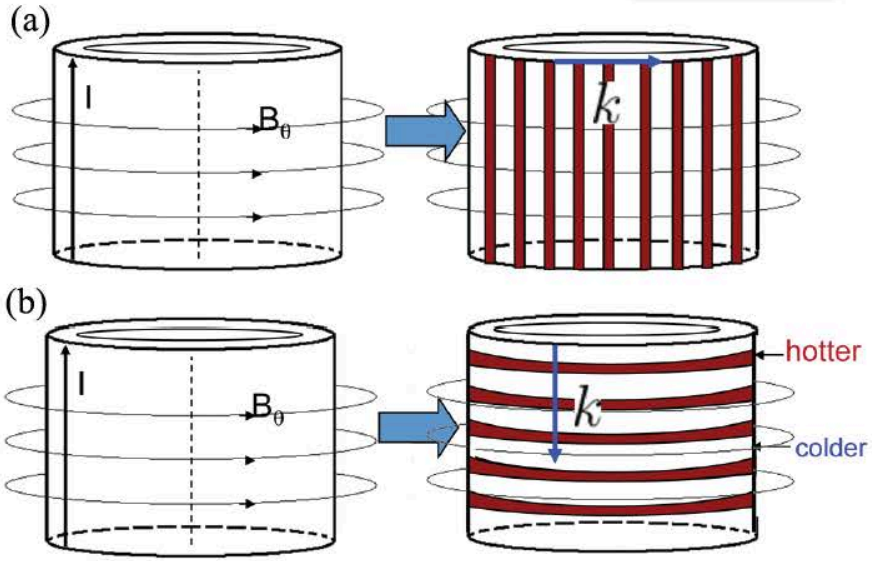

- High temperature (>10 eV) plasmas
- This is commonly the situation that occurs when the term *"electrothermal instabilities"* is referred to in the literature

Striations

$$\frac{d\eta(T)}{dT} > 0$$

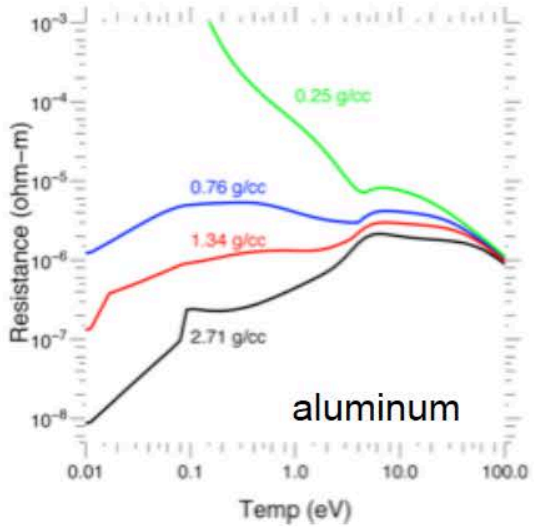

- Also sometimes referred to as thermal *"overheat"* instabilities
- Occurs in condensed states of metals
- Focus of remainder of talk

K. J. Peterson *et al*., PoP **19**, 092701 (2012); K. J. Peterson *et al*., PoP **20**, 056305 (2013).

Based on hypothesis that the electro-thermal instability seeds the MRT instability, a mitigation strategy has been developed

Sandia National Laboratories

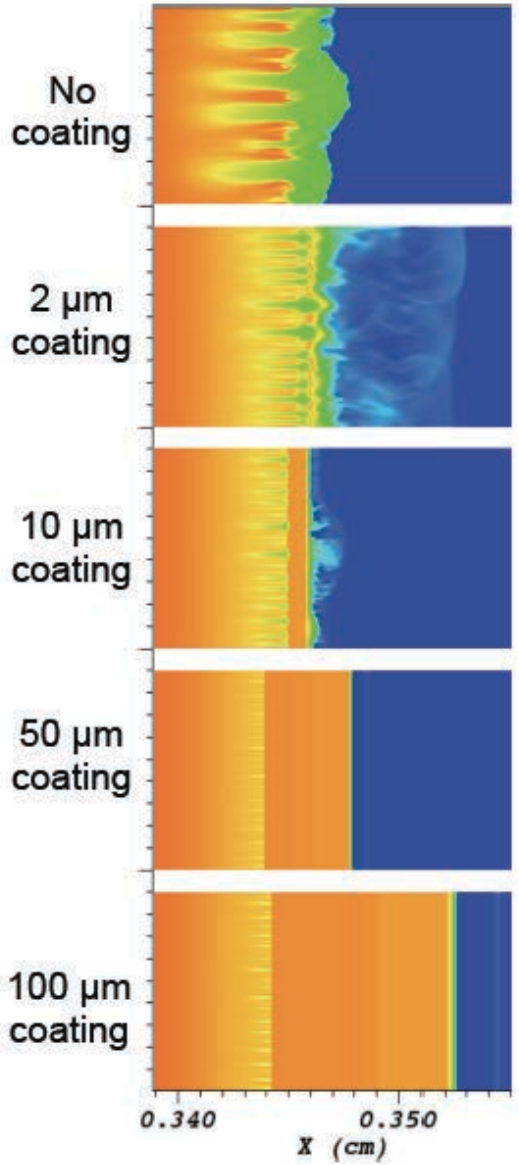

Thick insulating coatings suppress liner instabilities that are seeded by the electro-thermal instability

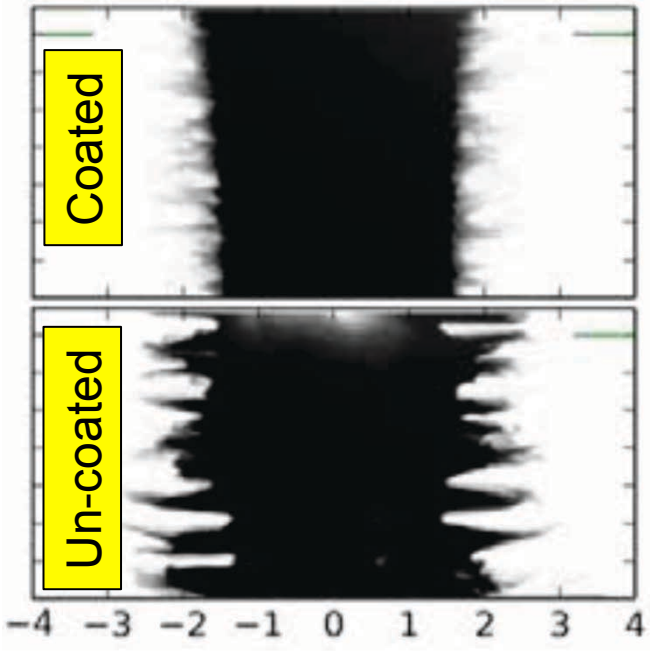

Data collected during past year appears to support the mitigation idea

K. J. Peterson *et al*., Phys. Plasmas **19**, 092701 (2012);
K. J. Peterson *et al*., Phys. Plasmas **20**, 056305 (2013);
K. J. Peterson *et al*., Phys. Rev. Lett. **112**, 135002 (2014).

The addition of a 7-10 T axial magnetic field produces a dramatic change in the structure of the liner instabilities

Sandia National Laboratories

CR =2.7

CR =6.4

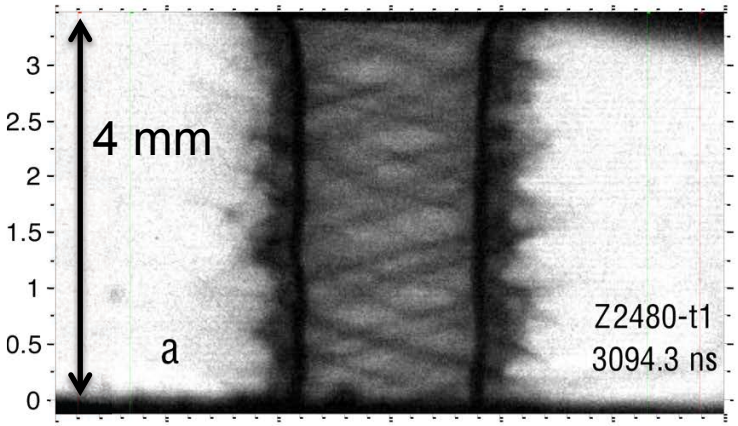

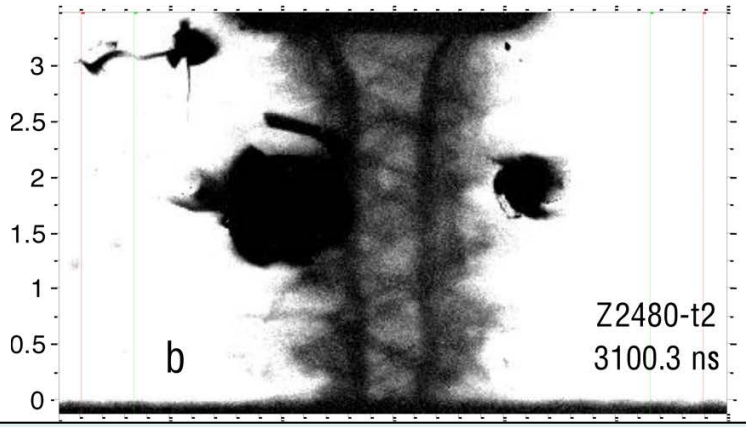

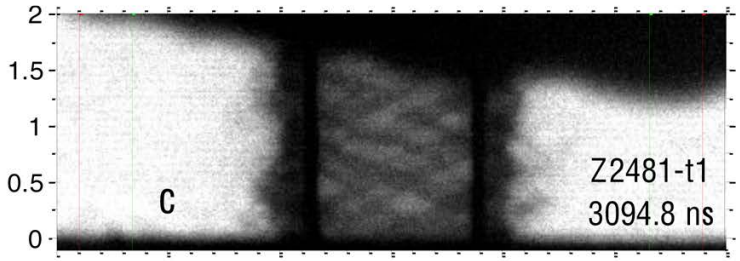

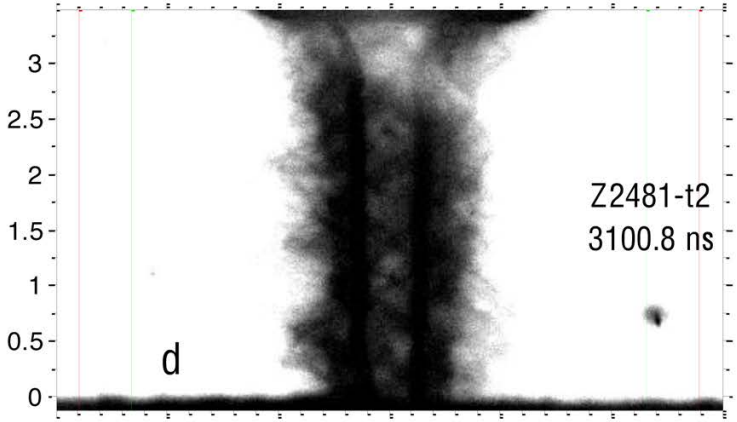

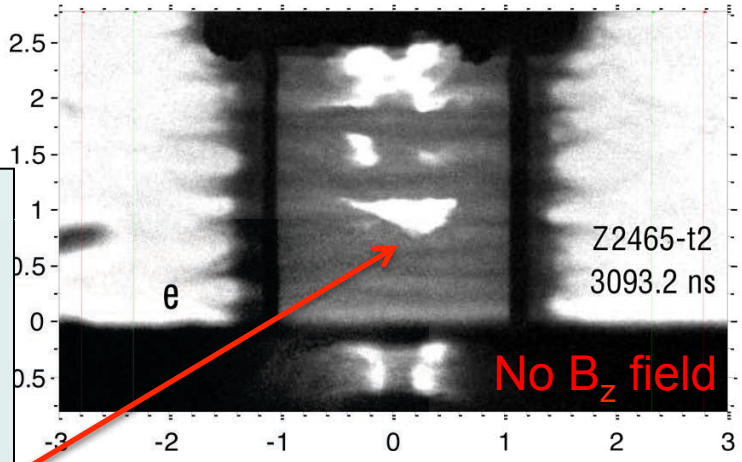

CR =2.9

CR =6.9

CR =2.0

- Rather than cylindrically symmetric structures, we see helical structures
- Use of compressible electrodes mitigates edge instabilities
- Magnetic field reduced multi-keV x rays associated with late-time instabilities

T. J. Awe *et al.*, Phys. Rev. Lett. **111**, 235005 (2013).

The addition of a 7-10 T axial magnetic field produces a dramatic change in the structure of the liner instabilities

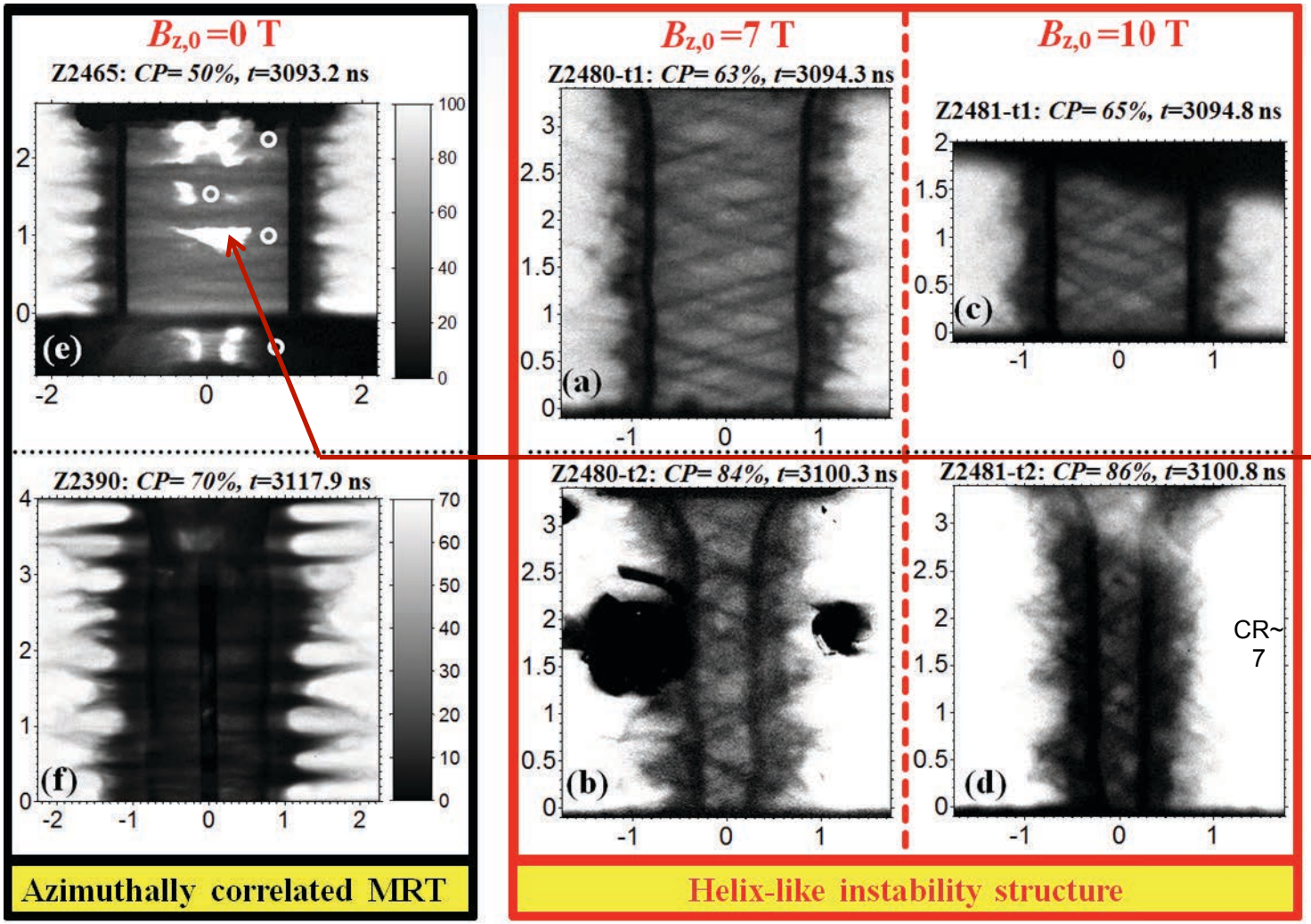

- Rather than cylindrically symmetric structures, we see helical structures
- Magnetic field reduced multi-keV x-rays associated with late-time instabilities

B_z + dielectric coated liners for most stable implosions yet:

Sandia National Laboratories

Magnetized & CH-coated Be implosion (CR is 13-21)

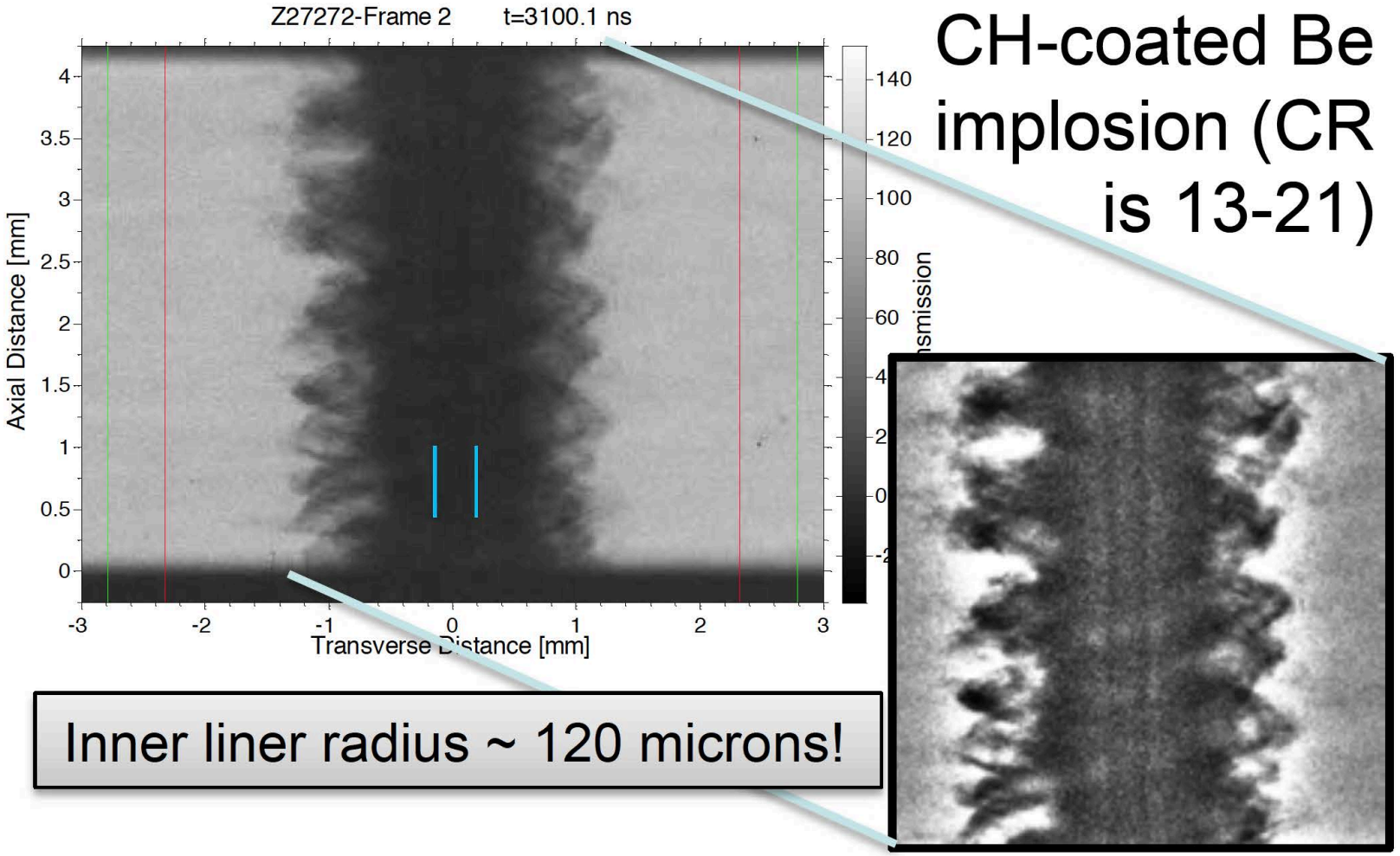

Helical structure still present in outer parts, but very stable inner surface at CR ~ 13–21!

Platform development for high pressure deceleration & stagnation dynamics

- Pulse-shaping on Z used to compress cryogenic/liquid D2 to extreme pressures & densities
- High-density, low temperature surrogate platform for studying ignition relevant deceleration & stagnation dynamics
- ~2 Gbar stagnation pressures
- $P\tau$ ~ 5 Gbar-ns (ignition relevant for MagLIF)

$$\langle \rho \rangle = 60 \text{ g/cm}^3$$
$$\langle \rho R \rangle = 0.5 \text{ g/cm}^2$$
$$r_{stag} = 110 - 170 \ \mu\text{m}$$
$$CR \approx 19$$

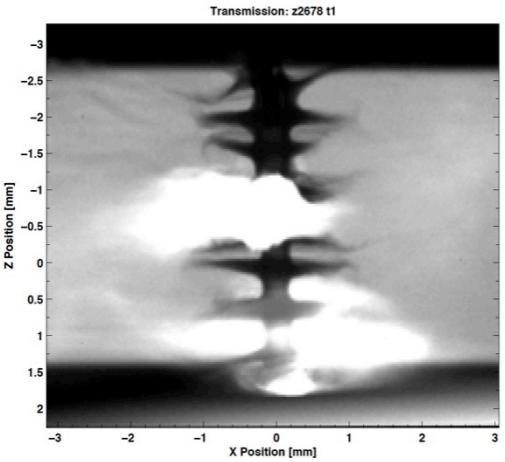

- Successfully measured the liner velocity and the D2 shock velocity with new radial PDV diagnostic

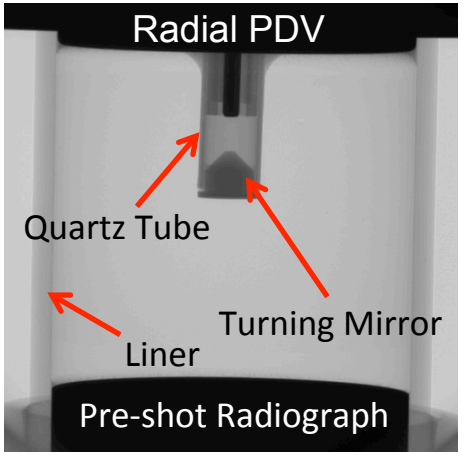

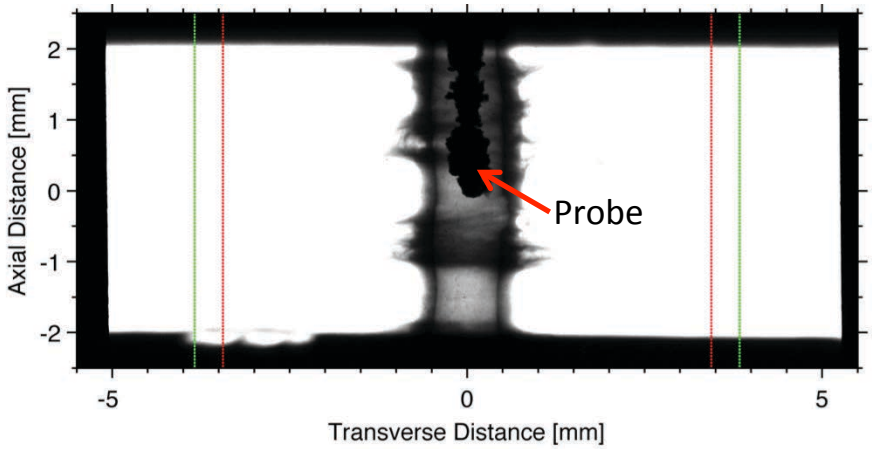

Summary & Conclusions

- Liner implosion studies using penetrating radiography have provided valuable data for benchmarking codes and characterizing MagLIF-relevant liner implosions through to stagnation
- Dielectric coatings + B_z have led to the most stable implosions yet
- Neutron diagnostics and various new B-field diagnostics indicate that flux compression is working well on Z

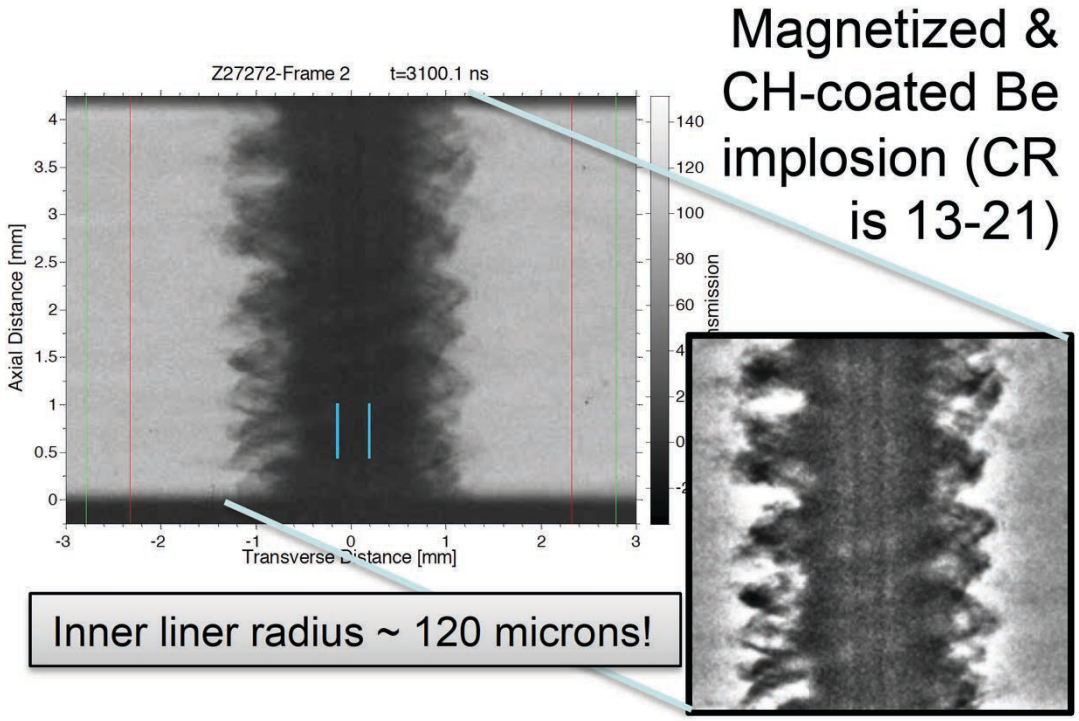

Sandia National Laboratories

Backups…

We have done significant work to date on liner implosion dynamics that is relevant to MagLIF

Sandia National Laboratories

- D.B. Sinars *et al.*, Phys. Rev. Lett. **105**, 185001 (2010).
- D.B. Sinars *et al.*, Phys. Plasmas **18**, 056301 (2011).
- M.R. Martin *et al.*, Phys. Plasmas **19**, 056310 (2012).
- R.D. McBride *et al.*, Phys. Rev. Lett. **109**, 135004 (2012).
- R.D. McBride *et al.*, Phys. Plasmas **20**, 056309 (2013).
- K.J. Peterson *et al.*, Phys. Rev. Lett. **112**, 135002 (2014).
- K.J. Peterson *et al.*, Phys. Plasmas **19**, 092701 (2012).
- K.J. Peterson *et al.*, Phys. Plasmas **20**, 056305 (2013).
- T.J. Awe *et al*. Phys. Rev. Lett. **111**, 235005 (2013).
- T.J. Awe *et al*. Phys. Plasmas **21**, 056303 (2014).
- M.R. Gomez *et al.*, Phys. Rev. Lett. **113**, 155003 (2014).
- M.R. Gomez *et al.*, Phys. Plasmas **22**, 056306 (2015).
- P.F. Schmit *et al.*, Phys. Rev. Lett. **113**, 155004 (2014).
- P.F. Knapp *et al*. Phys. Plasmas **22**, 056312 (2015).
- P.F. Knapp *et al.*, manuscript in preparation (2015).

Thank you for your attention

Sandia National Laboratories

- For additional information please see the following publications
  - S. A. Slutz et al., Phys. Plasmas, **17** 056303 (2010).
  - S. A. Slutz and R. A. Vesey, Phys. Rev. Lett., **108** 025003 (2012).
  - M. E. Cuneo et al., IEEE Trans. Plasma Sci. **40**, 3222 (2012).
  - A. B. Sefkow et al., Phys. Plasmas **21**, 072711 (2014).
  - M. R. Gomez et al., Phys. Rev. Lett. **113**, 155003 (2014).
  - P. F. Schmit et al., Phys. Rev. Lett. **113**, 155004 (2014).
  - M. R. Gomez et al., Phys. Plasmas **22**, 056306 (2015).
  - P. F. Knapp et al., Phys. Plasmas **22** 056312 (2015).
  - S. B. Hansen et al., Phys. Plasmas **22** 056313 (2015).
  - R. D. McBride and S. A. Slutz, Phys. Plasmas **22** 052708 (2015).

The Z-Beamlet Laser (ZBL) at Sandia* can be used to heat fusion fuel and to radiograph liner targets

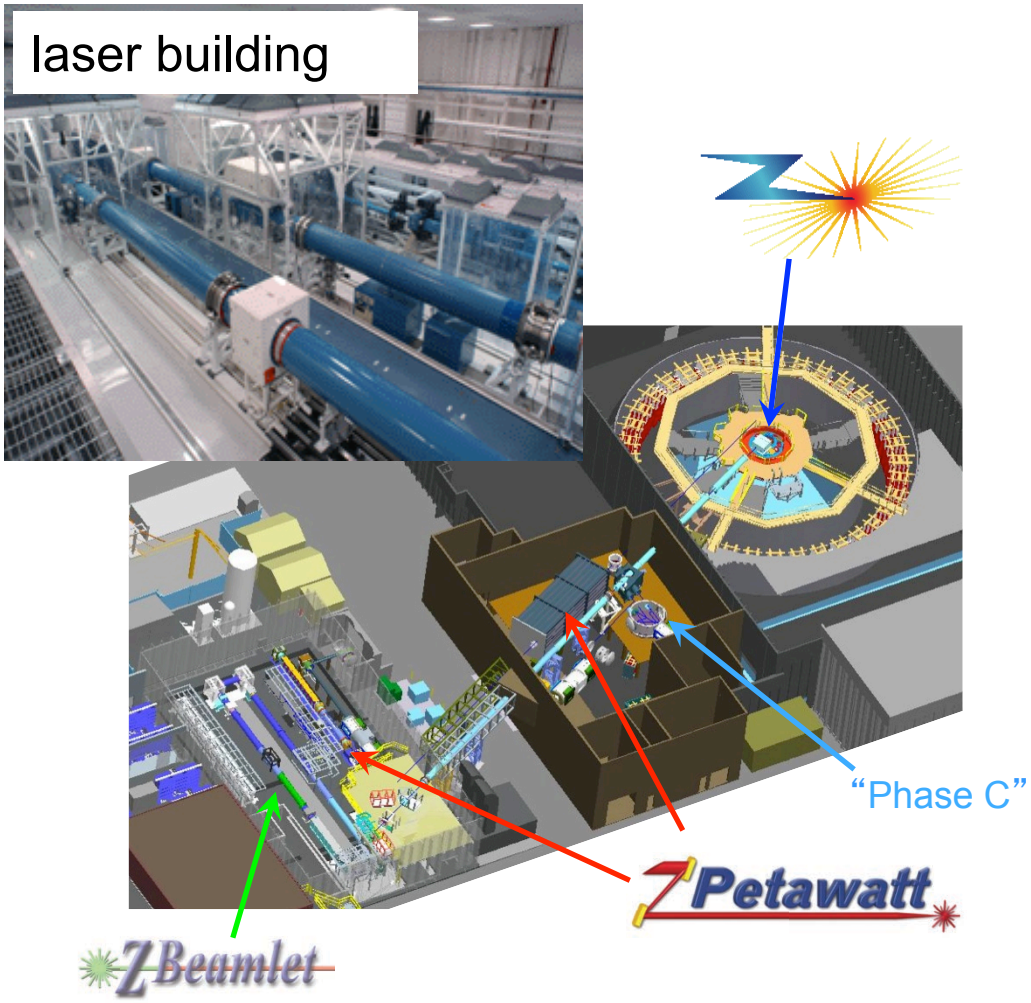

ZBL was originally a prototype laser for the National Ignition Facility (NIF)

Today ZBL is located at Sandia and is routinely used to deliver ~2.4 kJ of 2ω light in 2 pulses for radiographing Z experiments

Recently upgraded to deliver 4 kJ of 2ω in 4 ns

* P. K. Rambo *et al.*, Applied Optics **44**, 2421 (2005).

Prototype coils have been demonstrated that generate 10 T axial fields over a several cm^3 volume for MagLIF with full diagnostic access

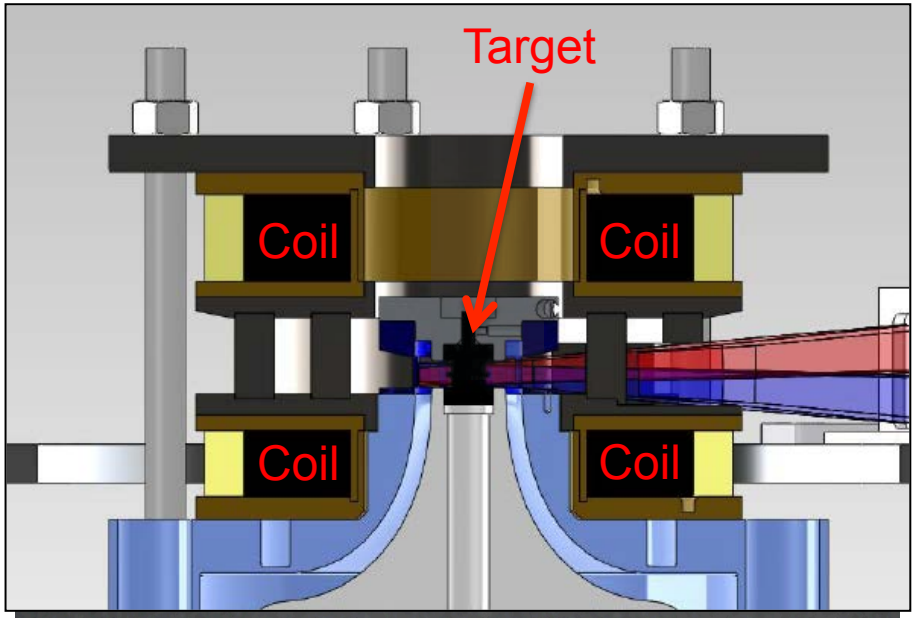

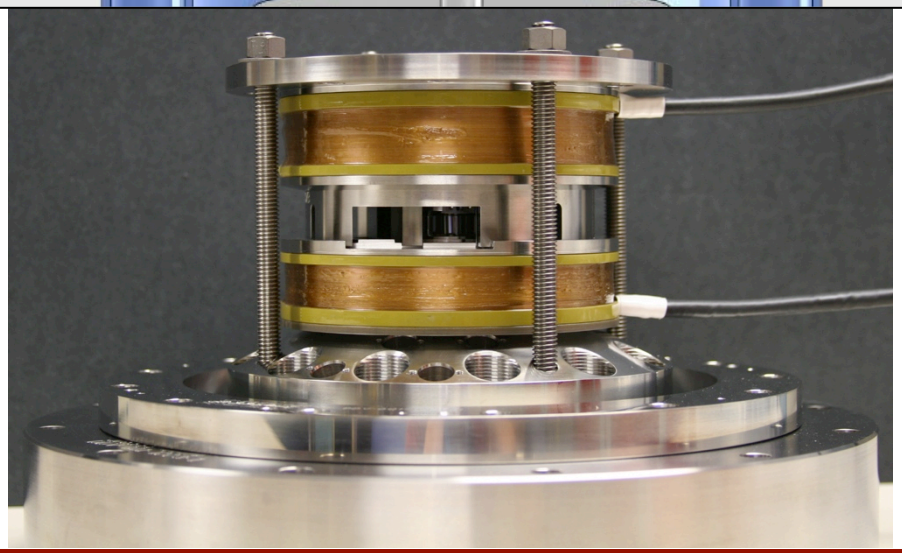

10 Tesla point design

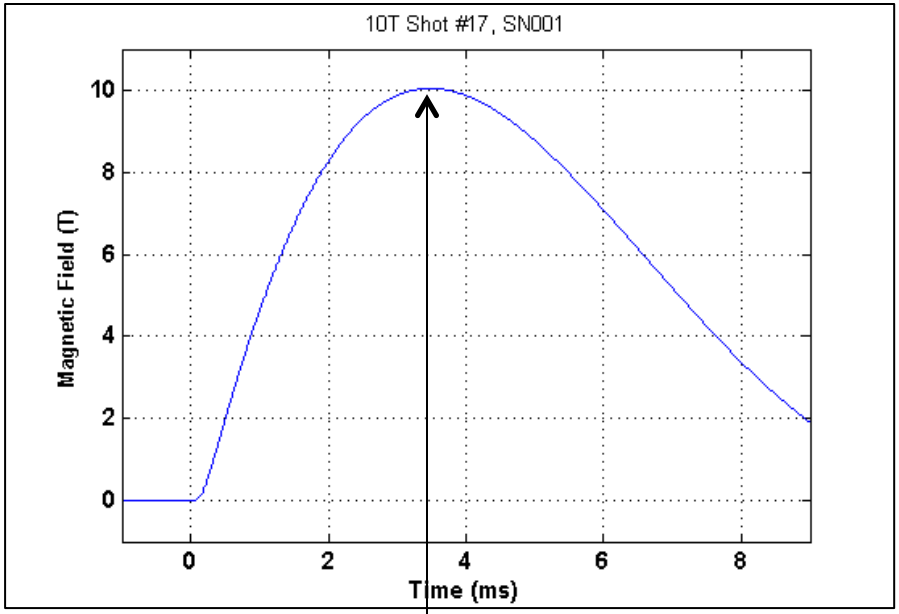

Time to peak field = 3.49 ms

Long time scale needed to allow field to diffuse through the liner without deformation

An 8 mF, 15 kV, 900 kJ capacitor bank has been installed on Z to drive the coils

Sandia National Laboratories

- Two identical units (repurposed from ion beam facilities) allows for high-fidelity surrogacy testing in separate test facility
- We believe 900 kJ is enough to meet our short and long term goals (30 T)

The SITF Testbed in Bldg. 970

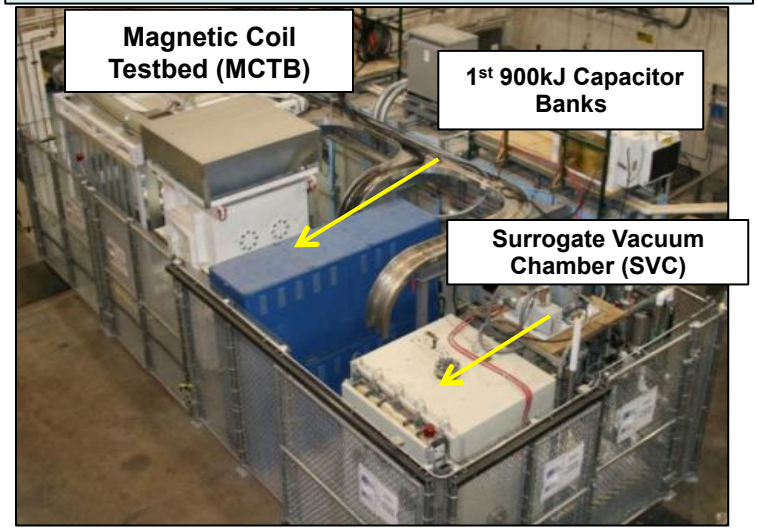

Commissioning of coils in the Z chamber completed in Feb. 2013

Photo of capacitor bank w/o covers; with covers

D.C. Rovang *et al.*, see http://www.sandia.gov/pulsedpower/maglifpres/Agenda.html

Debris from MagLIF experiments must be carefully managed (several MJ energy release equivalent to few sticks of dynamite)

Sandia National Laboratories

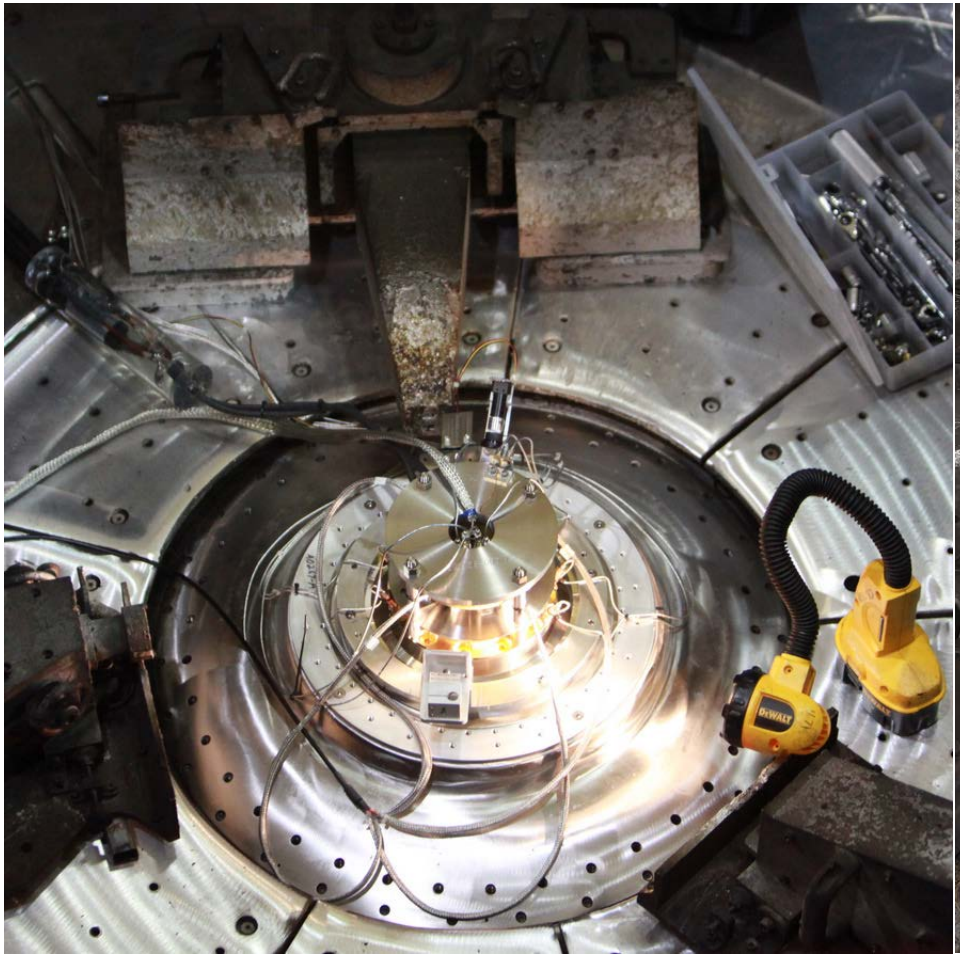

Pre-shot photo of coils & target hardware

Post-shot photo

z2592 micro-Bdot Results

- One single-ended probe, BMIC05 (black curve), gave a good signal that agrees well with a simple simulation (its differential-pair partner, BMIC08, did not survive however)

- The red vertical dashed line indicates the time when the liner hits the outer radius of the on-axis Faraday probe housing, and thus marks the end of the flux compression experiment

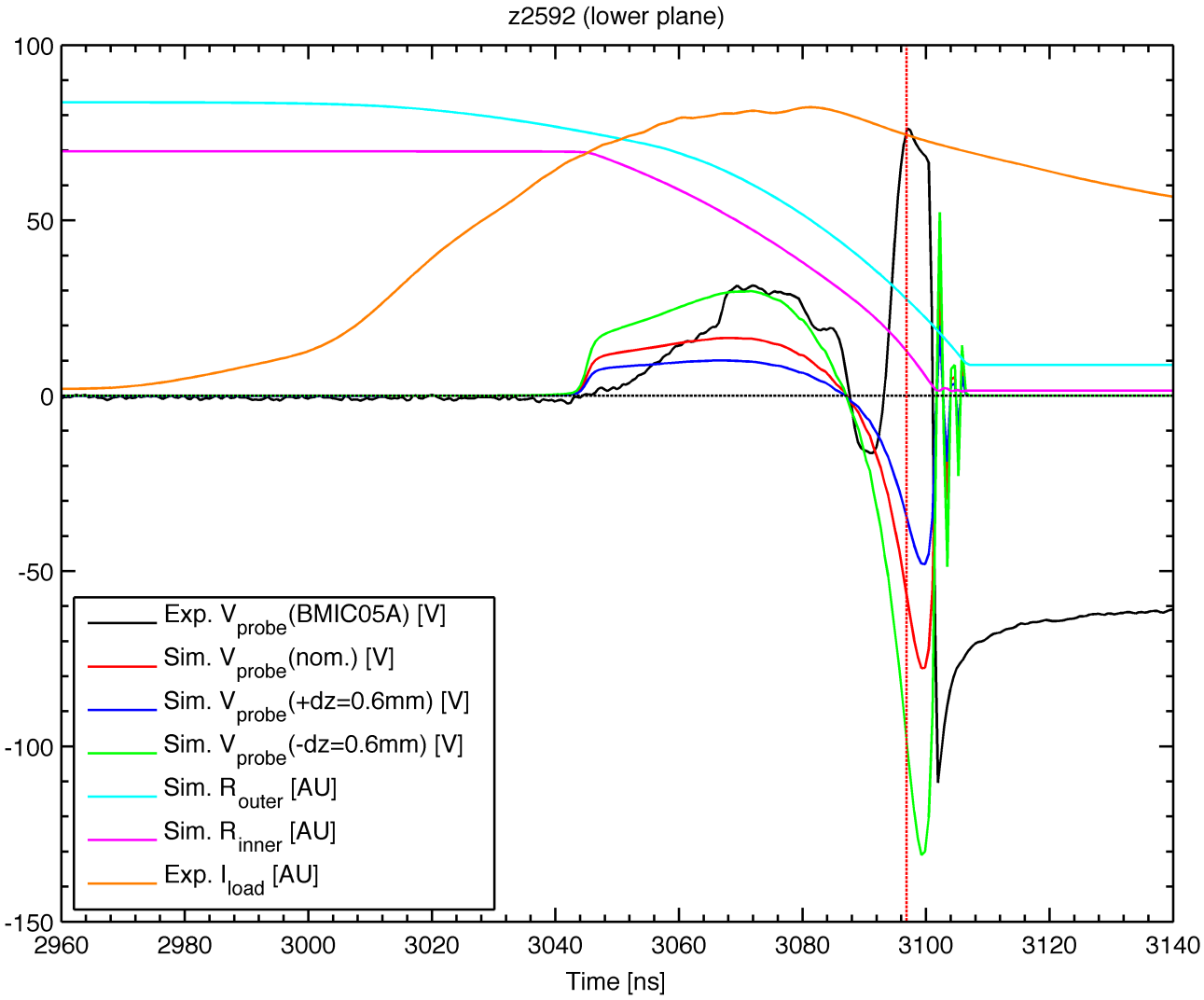

Recent experiments used 2 μm Al just inside the Be liner to enhance the contrast of the liner's inner surface*

Sandia National Laboratories

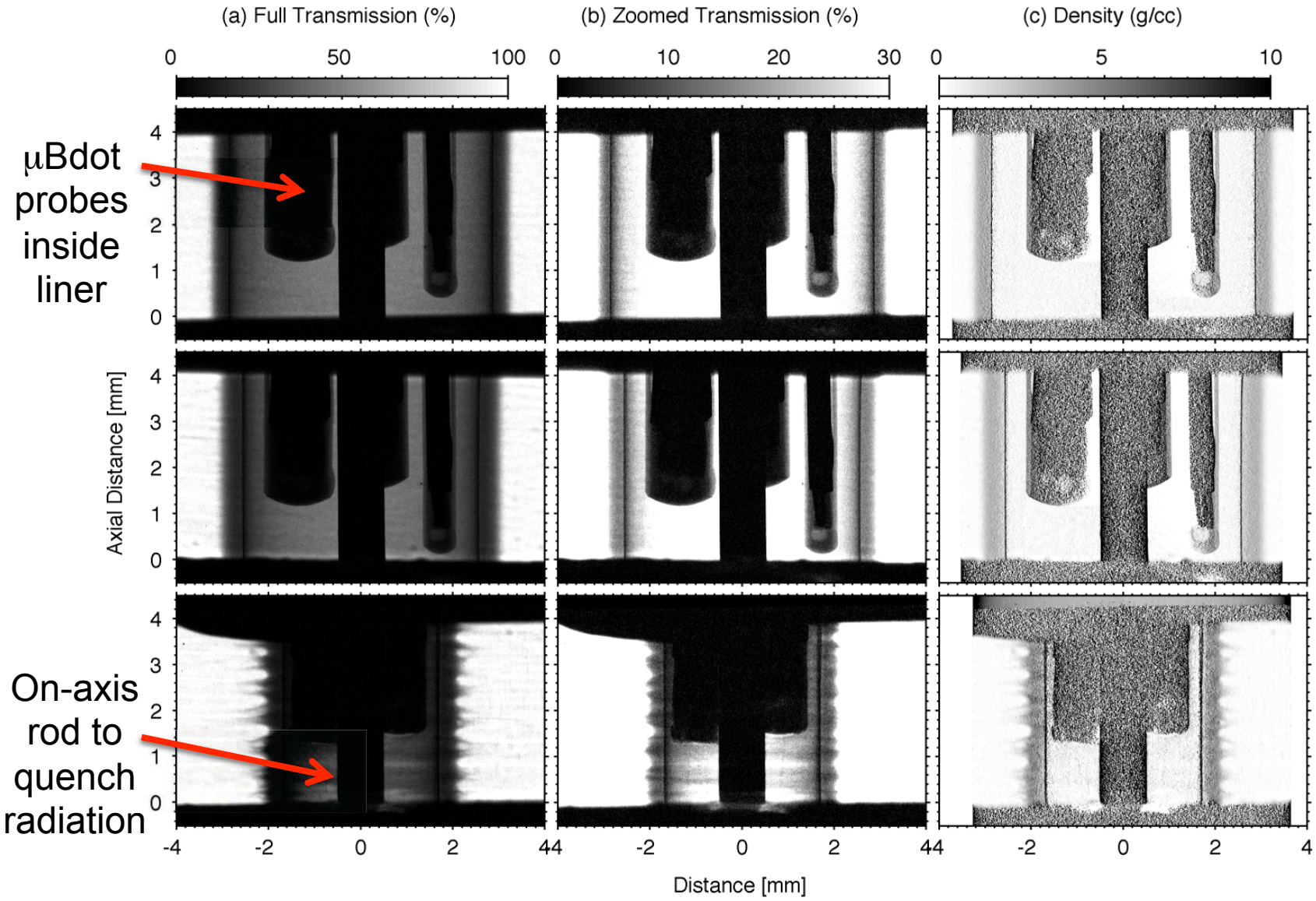

*Thin Al layer to enhance contrast suggested by D.D. Ryutov

R. D. McBride *et al.*, invited manuscript in preparation for Phys. Plasmas (2013).

Radiographs at a convergence ratio of ~5 show remarkably good stability for inner liner surface

Sandia National Laboratories

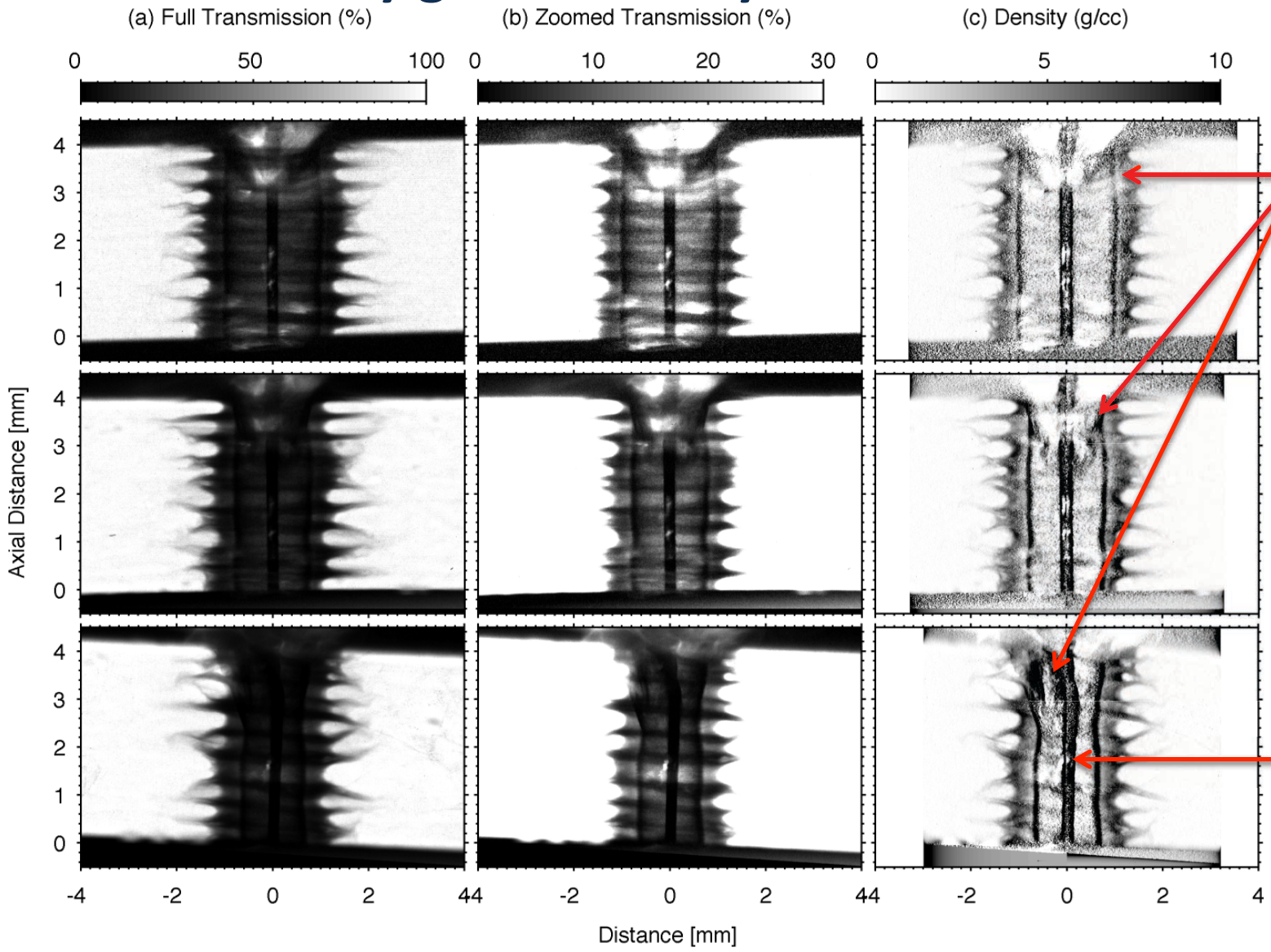

Note: Most disruption to liner stability caused by electrode end-effects and jetting material

Note: MagLIF requires final compression to about diameter of on-axis rod

R. D. McBride *et al.*, invited manuscript in preparation for Phys. Plasmas (2013).

Radiographs at a convergence ratio of ~5 show remarkably good stability for inner liner surface

Note: MagLIF requires final compression to on-axis rod

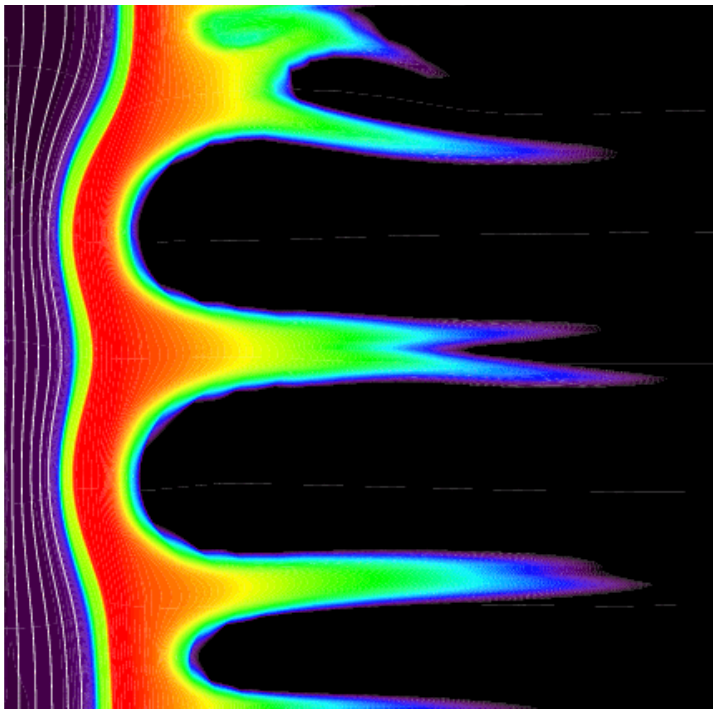

LASNEX 2D from
S. A. Slutz, *et al.*, PoP (2010)

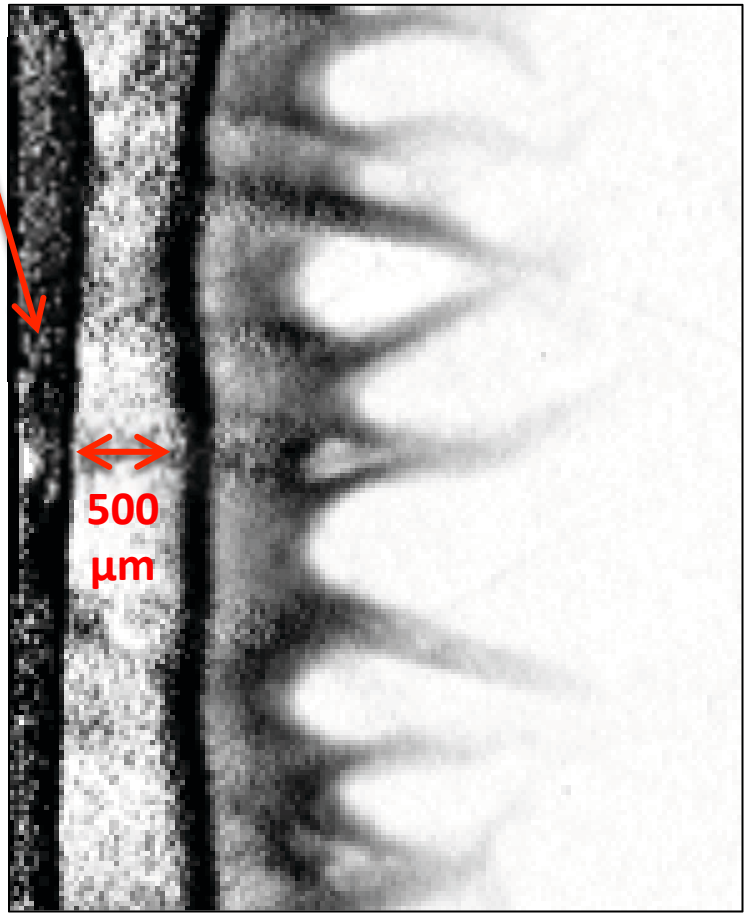

Experiment

R. D. McBride et al., Phys. Plasmas **20**, 056309 (2013).

Cylindrical Be ICE to >5 Mbar

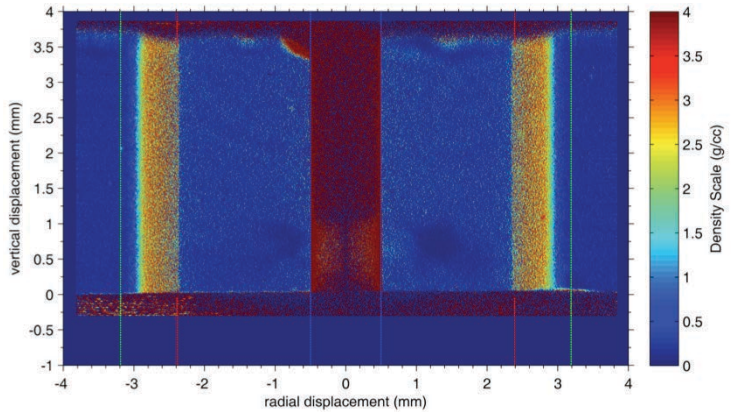

$$\frac{\partial(rv)}{\partial m} = \frac{1}{2\pi}\frac{D}{Dt}\left(\frac{1}{\rho}\right),$$

$$\frac{\partial P_T}{\partial m} = -\frac{1}{2\pi r}\frac{Dv}{Dt}.$$

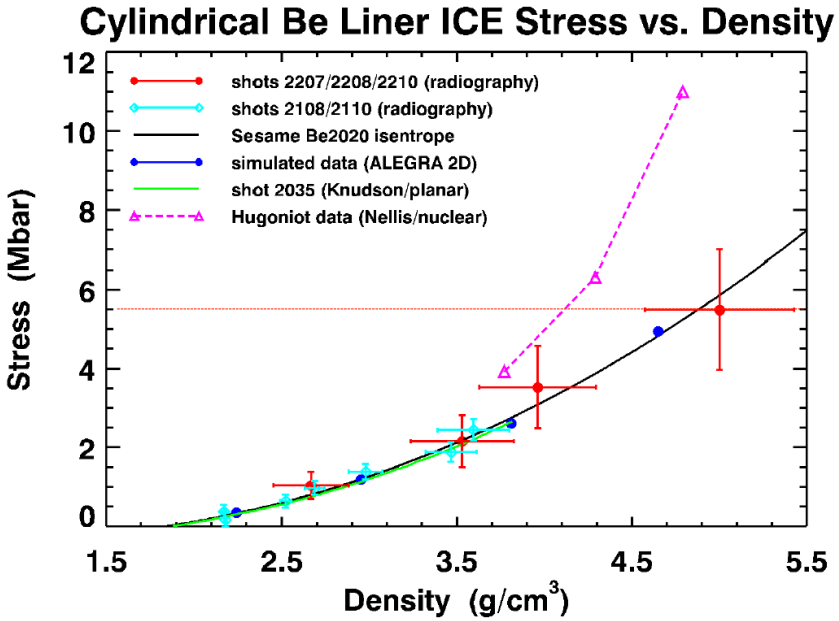

EOS unfolds by
M. R. Martin

M. R. Martin, R. W. Lemke, R. D. McBride *et al.*, Phys. Plasmas 19, 056310 (2012).

Vacuum Magnetic Flux Compression:

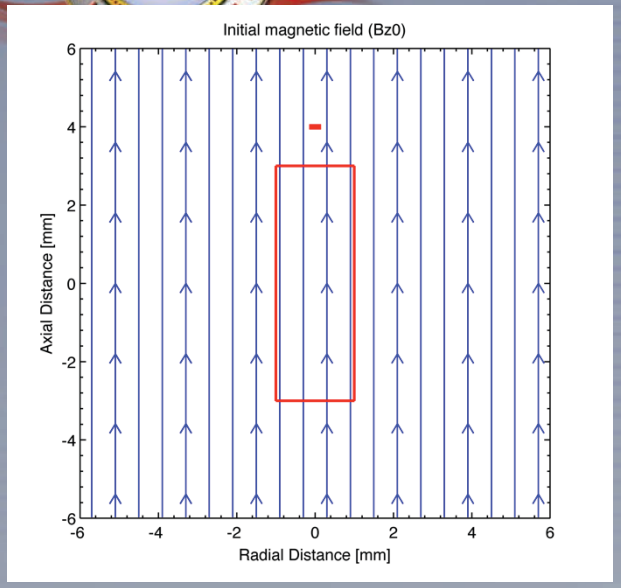

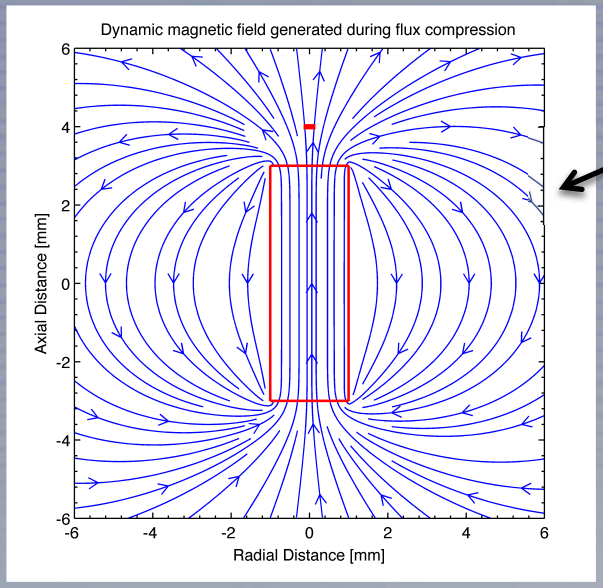

Bdot probes detect dynamic field

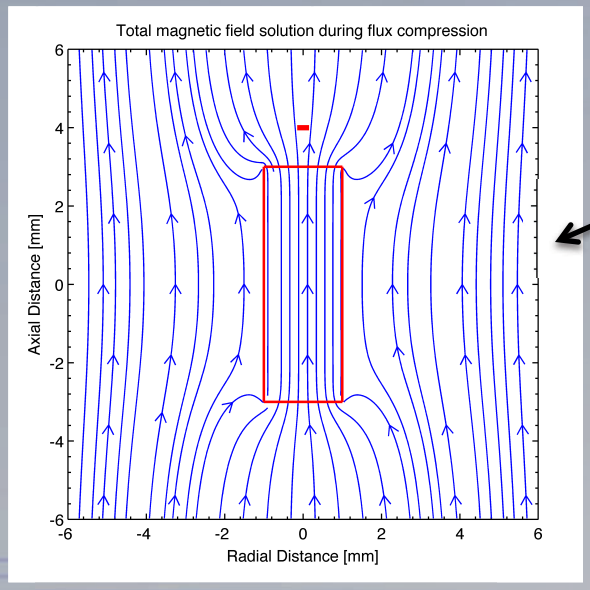

Faraday rotation and Zeeman spectroscopy measure total field

LDRD LABORATORY DIRECTED RESEARCH & DEVELOPMENT

Sandia National Laboratories

Platform development for diagnosing magnetic flux compression on Z

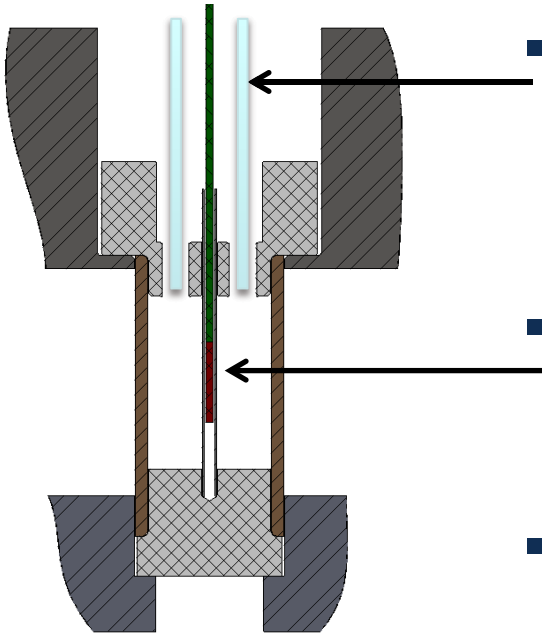

Side view B

- 2 fibers in top end cap for streaked visible Zeeman spectroscopy
- Faraday rotation fiber on axis
- 4 micro B-dots in top end cap

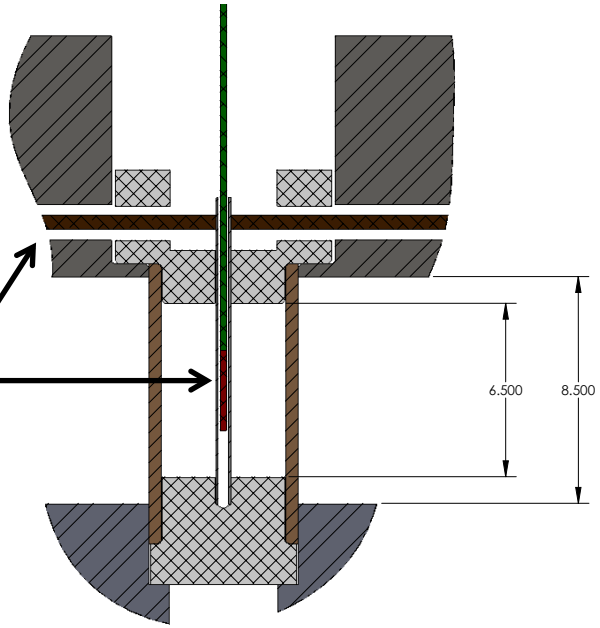

Side view A

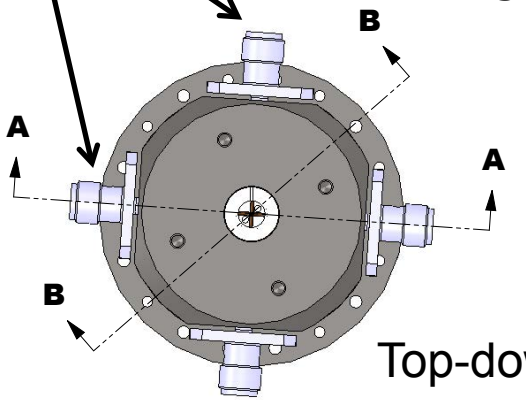

Top-down view

Faraday rotation system developed with Tom Intrator at Los Alamos

Streaked visible absorption spectroscopy recorded Zeeman splitting / early stages of flux compression

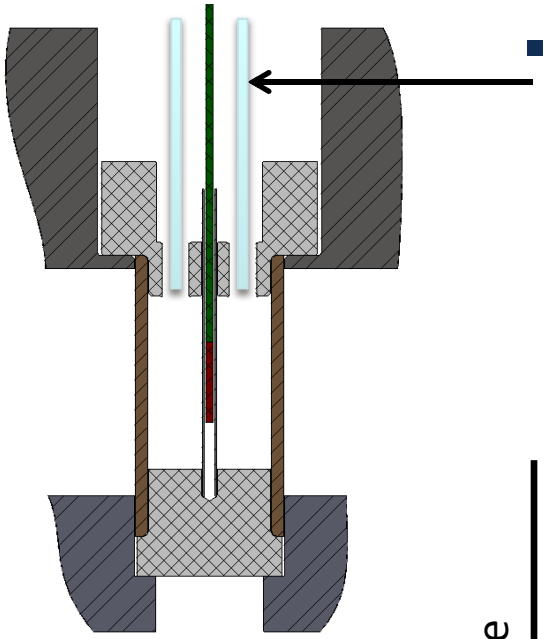

Side view B

- 2 fibers in top end cap for streaked visible Zeeman spectroscopy

The width of the absorption line can be used to infer magnetic field strength

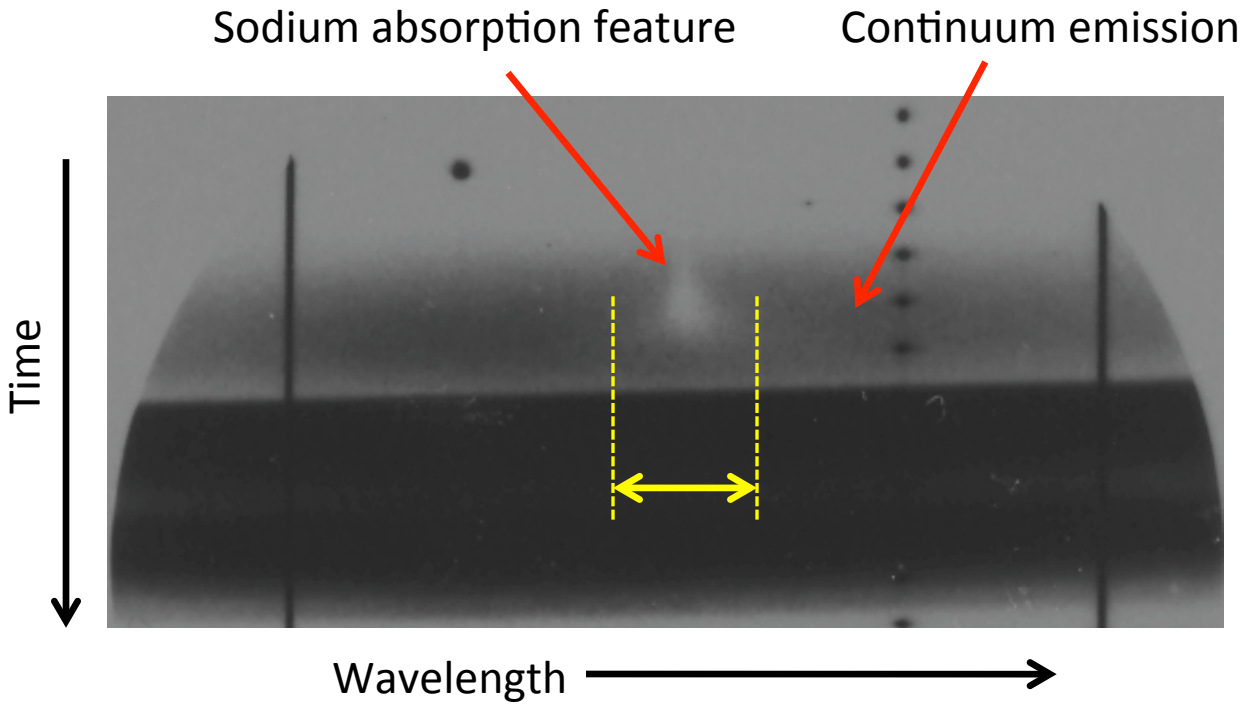

Data courtesy of M. R. Gomez & S. B. Hansen

Streaked visible absorption spectroscopy recorded Zeeman splitting / early stages of flux compression

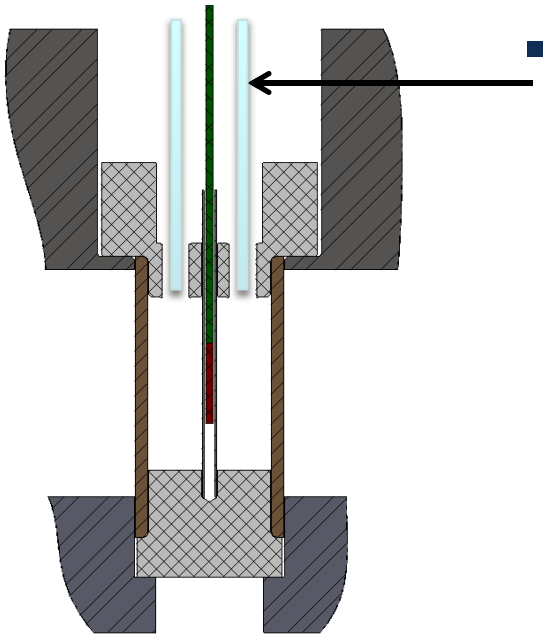

Side view B

- 2 fibers in top end cap for streaked visible Zeeman spectroscopy

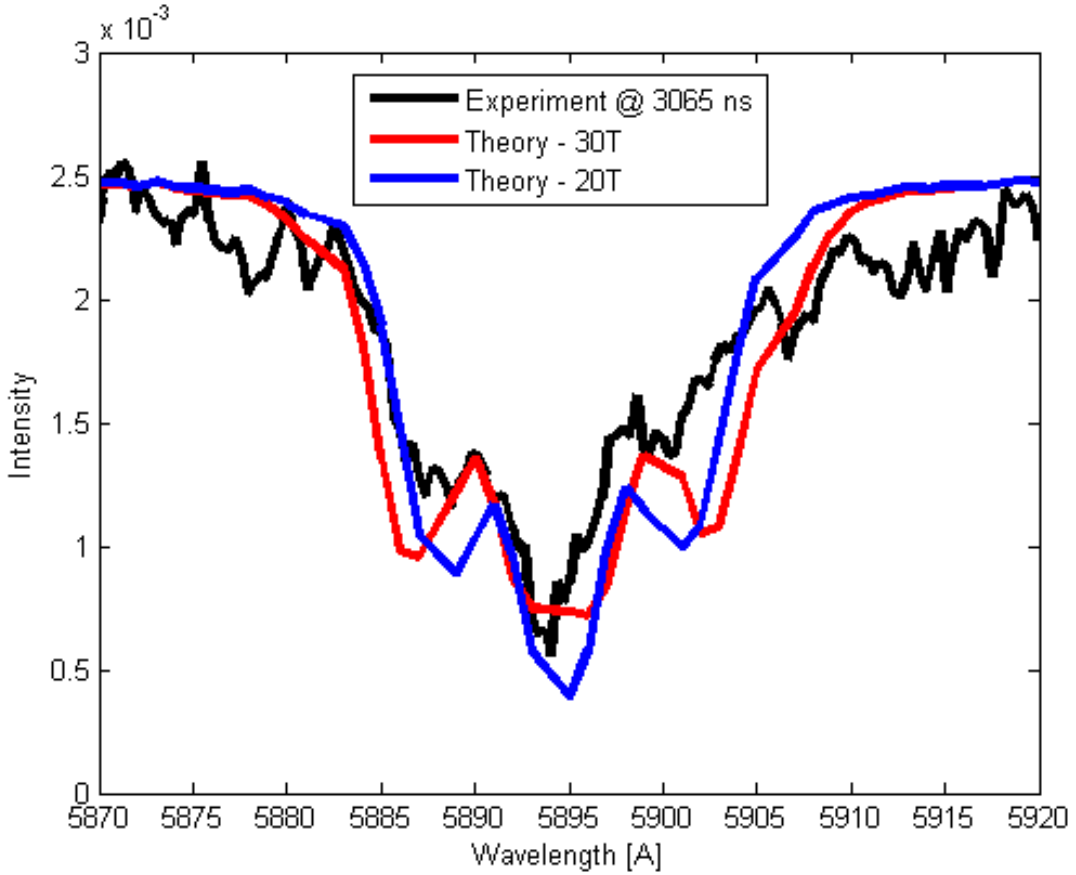

Data courtesy of M. R. Gomez & S. B. Hansen

Fringe field micro B-dots working well, but failed early

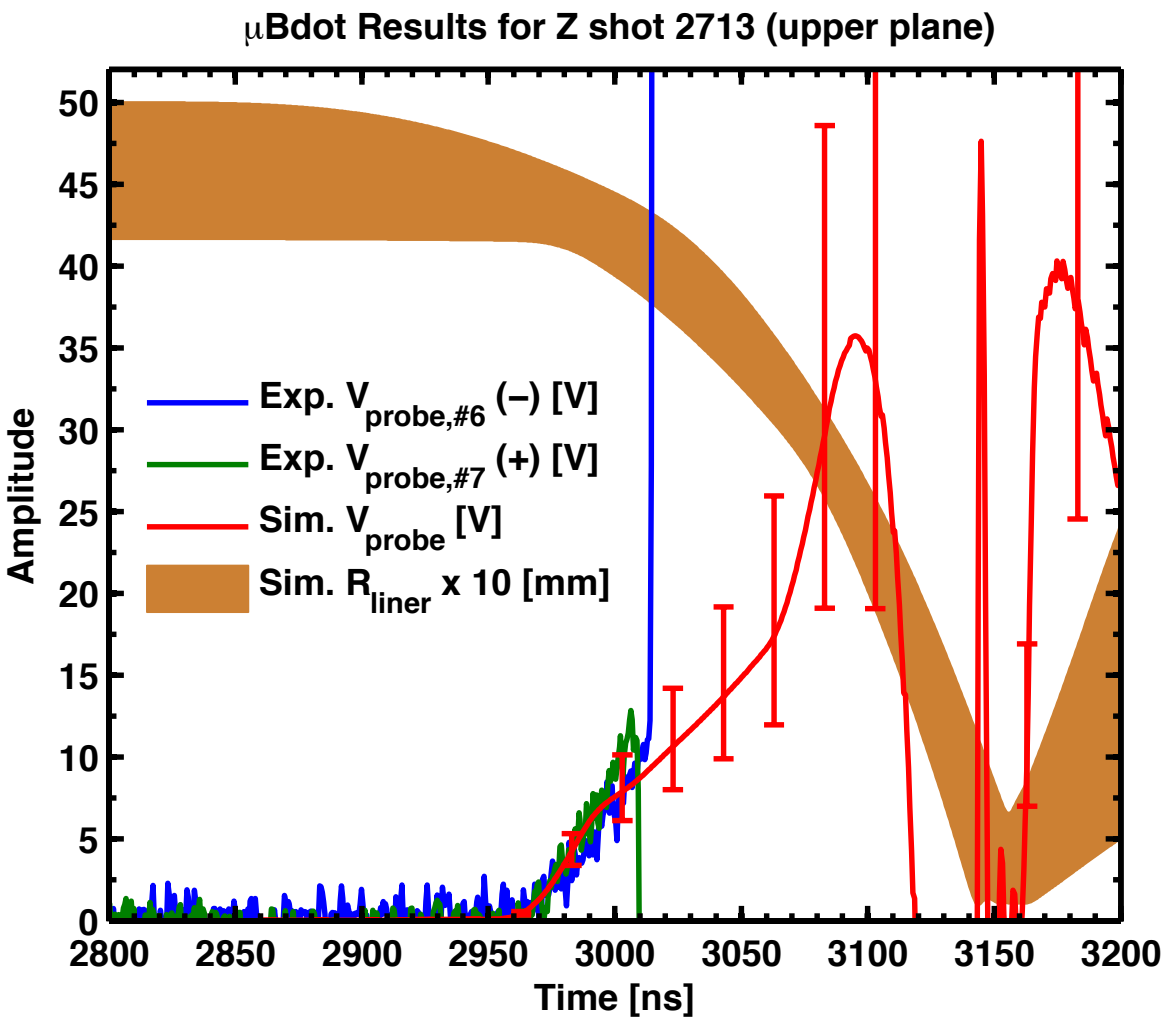

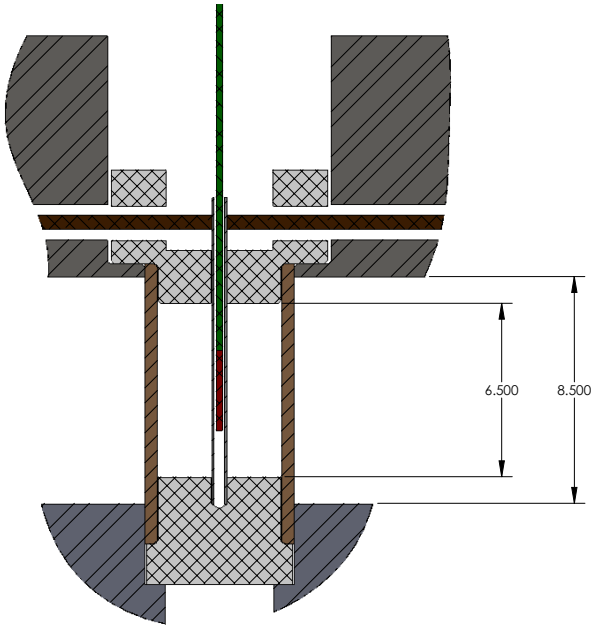

Side view A

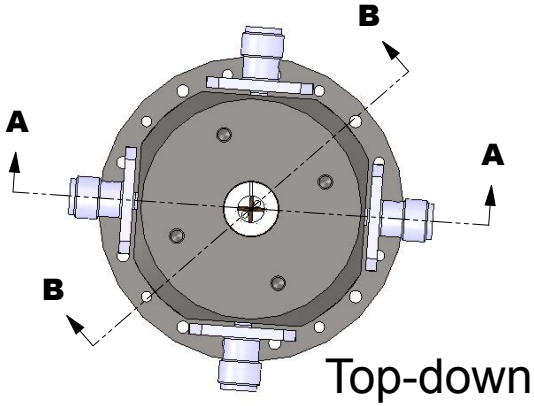

Top-down view

Faraday rotation working well, but failed early

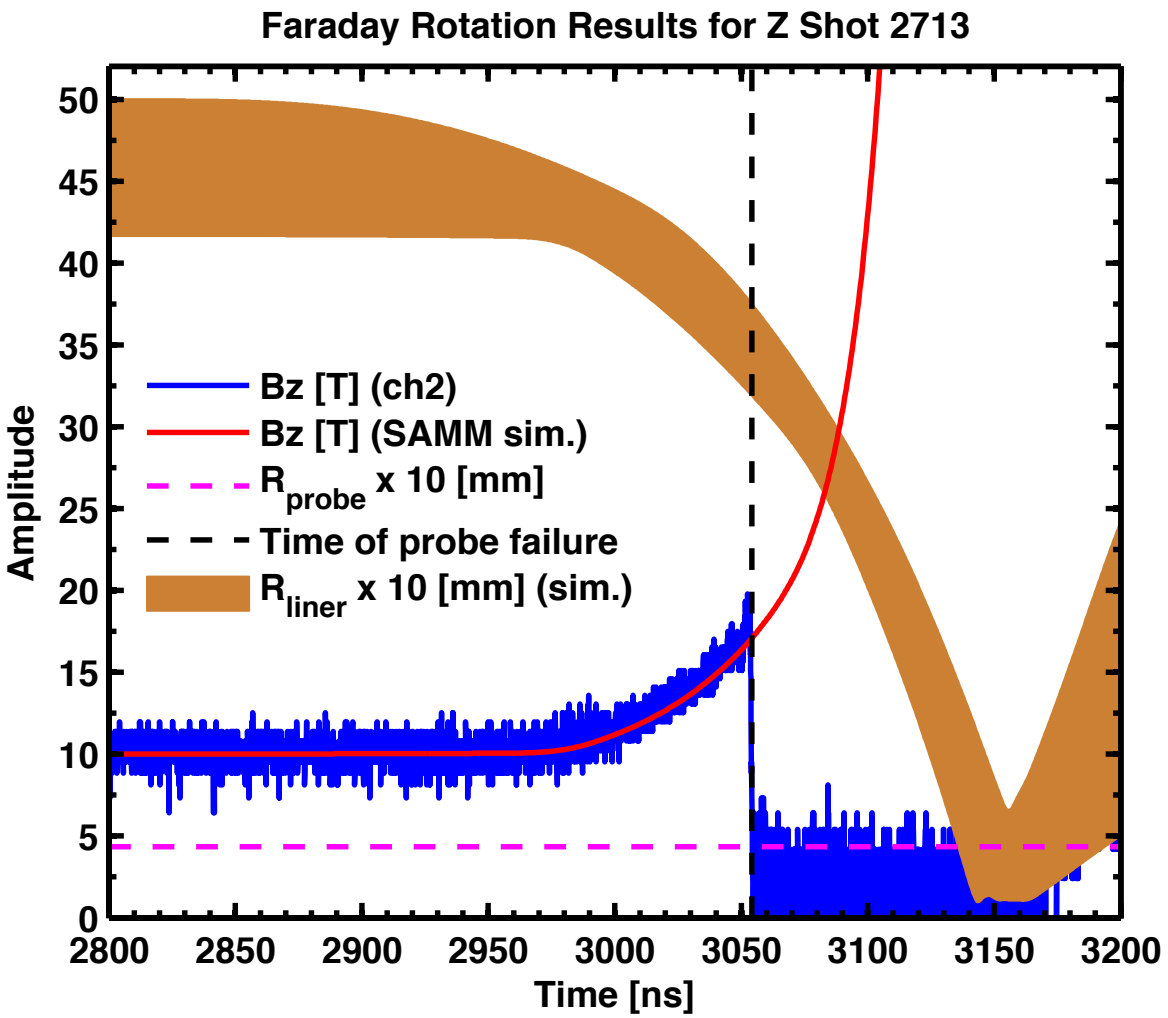

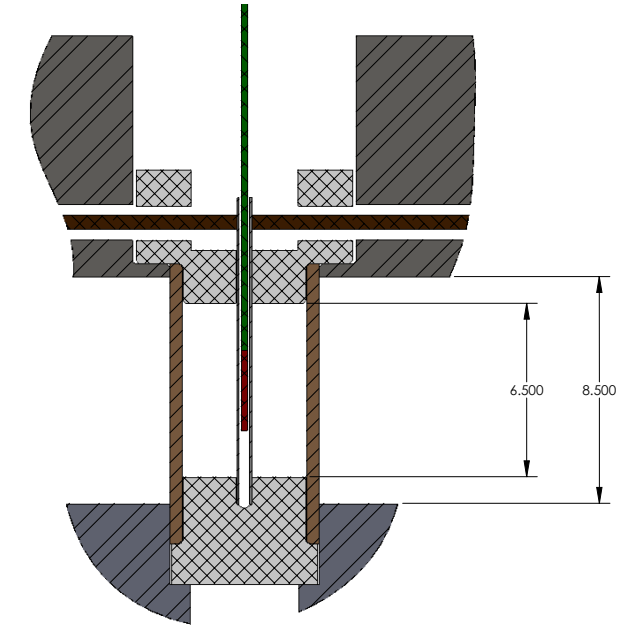

Side view A

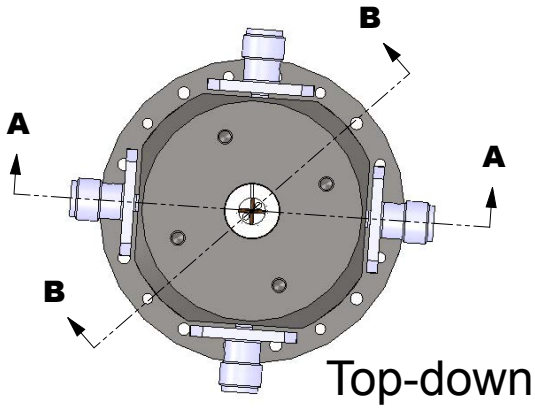

Top-down view

Premature failure of Faraday probe and micro B-dots likely due to target design

Sandia National Laboratories

- The 100-micron tolerance gap between liner body and upper electrode likely allowed a magnetic bubble to propagate up into the dielectric end-cap material, first crushing the micro B-dot cable, and then propagating down the micro B-dot feed-through channel and crushing the Faraday fiber at a slightly later time

- Will make future liners monolithic with upper electrode material to mitigate this failure mode

- New design will be tested in December 2015

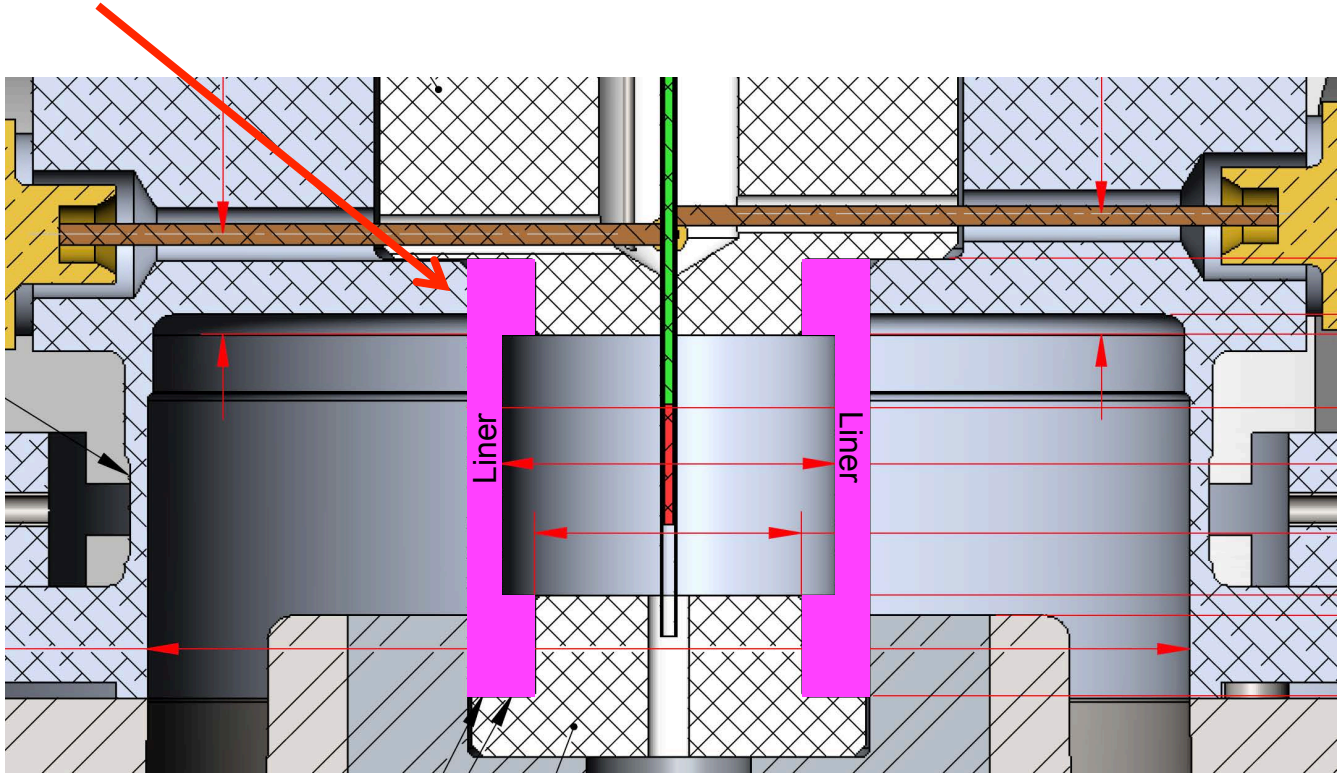

As the triton's Larmor radius becomes comparable to the plasma radius there is a significant enhancement in the DT/DD yield ratio as the effective path length increases

Sandia National Laboratories

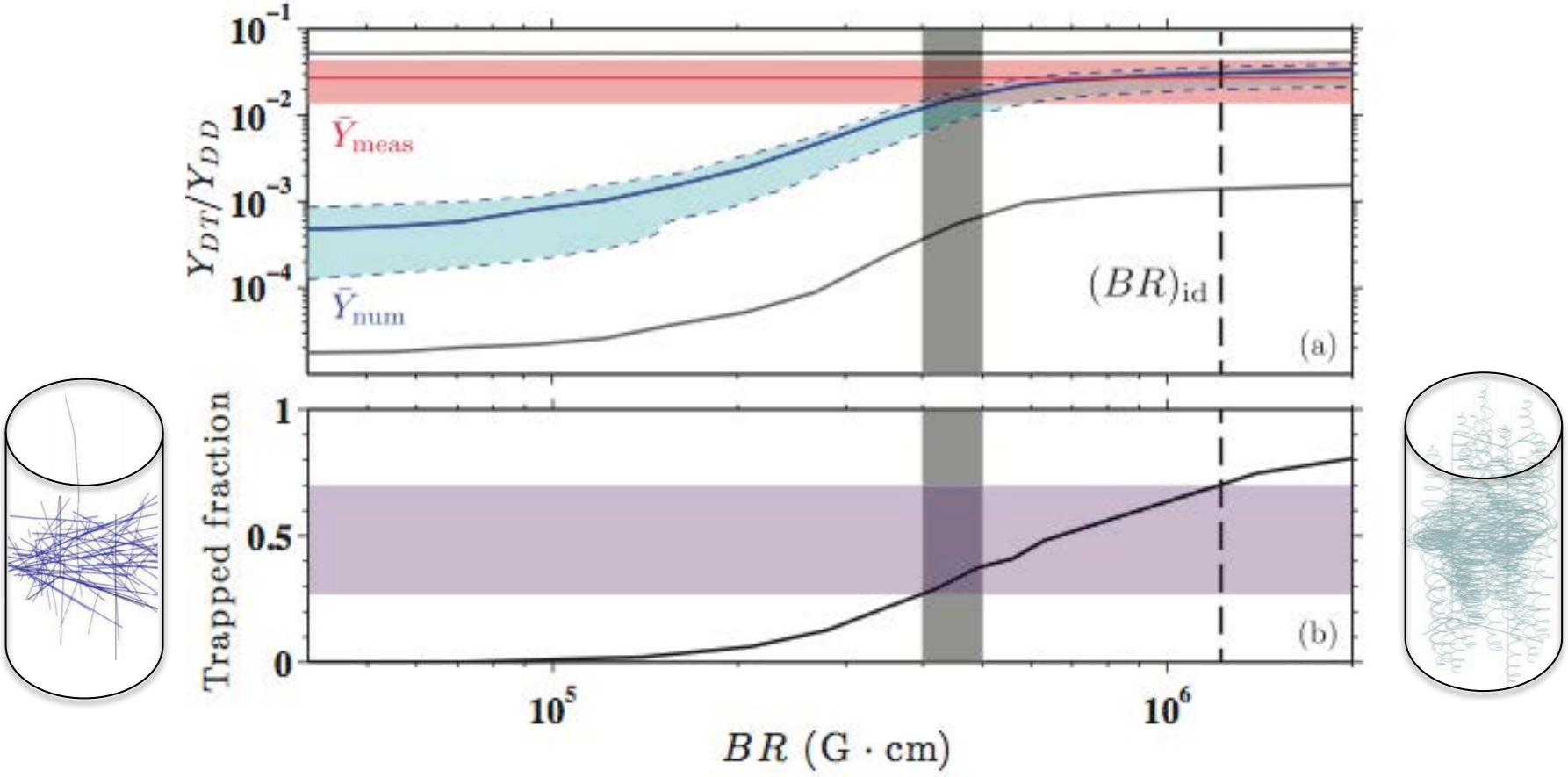

Magnetized tritons implies magnetized electrons:

$$\omega_{ci}\tau_{ie} \approx \omega_{ce}\tau_{ee}$$

Magnetized tritons implies magnetized alpha particles:

$$r_t \approx 1.1 r_\alpha$$

P.F. Schmit *et al.,* PRL **113**, 155004 (2014); P.F. Knapp *et al*. PoP **22**, 056312 (2015).

Relative to the primary ICF approach, MagLIF uses a very different (conservative?) fuel compression method and largely untested magneto-inertial fusion principles

Sandia National Laboratories

Metric	X-ray Drive on NIF	100 kJ MagLIF on Z
P	~140-160 Mbar	26 MA at 1 mm is 100 Mbar
P vs. R	Goes as R^2	Goes as 1/R^2
Drive nature	Surface-like	Can be significant redistribution from diffusion & low-density plasma
Peak velocity	350-380 km/s	70-100 km/s
IFAR	17 (high foot) to 20 (low foot)	8.5
Hot spot CR	35 (high foot) to 45 (low foot)	25
Volume Change	42875x to 91125x (high & low foot)	625x
Fuel rho-R	>0.3 g/cm^2	~0.003 g/cm^2
Liner rho-R	n/a	>0.3 g/cm^2
BR	n/a	>0.5 MG-cm
Burn time	~0.02 ns	~2 ns
T_ion	>4 keV	>4 keV

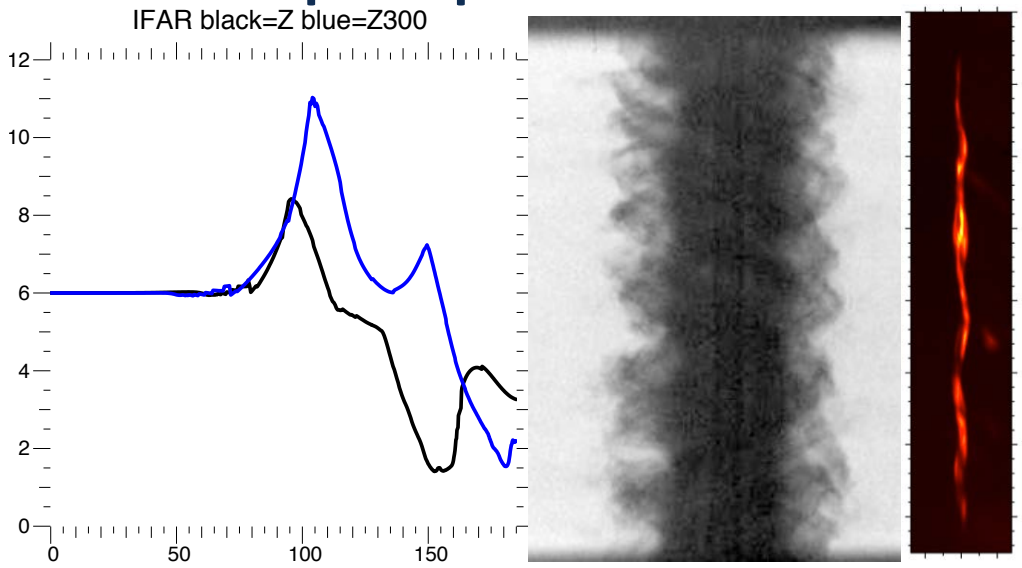

- By traditional ICF implosion metrics MagLIF is very conservative, though different P vs. R
- Reaching fusion conditions relies on largely untested MIF principles
  - Long stagnation time (2 ns) → more susceptible to high-Z contamination
  - Magnetic suppression of heat transport

Comparison of 1D and 2D HYDRA calculations of near-term Z experiments (19 MA, 10 T, 2 kJ)

Sandia National Laboratories

Parameter	1D ideal	2D integrated
• E_{gas}^{abs}	2.20 kJ	1.74 kJ
• m_{loss}	0%	43%
• Φ_{loss}	36%	38%
• CR_{2D}	28 (r_{stag} 84 μm)	37 (r_{stag} 63 μm)
• T_i^{peak}	5.0 keV	6.5 keV
• $\langle T_i \rangle^{DD}$	2.9 keV	3.2 keV
• ρ_{gas}^{stag}	0.6 g cm^{-3}	0.5 g cm^{-3}
• ρR_{liner}^{stag}	1.0 g cm^{-2}	0.9 g cm^{-2}
• P^{stag}	2.5 Gbar	2.2 Gbar (peak in bottle)
• $B_z^f r_{stag}$	4.1e5 G cm (r_{stag}/r_α 1.5)	5.3e5 G cm (r_{stag}/r_α 2.0)
• Y_n^{DD}	2.6e14 (in 7.5mm)	6.1e13 (24% of 1D)
• Y_n^{DD}/Y_n^{DT}	23	44
• t_{burn}^{FWHM}	3.2 ns	2.1 ns

Note: A unique property of magnetic drive is increasing pressure with decreasing radius. If less energy is coupled to fuel, target converges farther in simulations until plasma pressure is sufficient to stop the implosion.

A.B. Sefkow, S.A. Slutz *et al.*, Phys. Plasmas 21, 072711 (2014).

Two-frame monochromatic (6151±0.5 eV) crystal backlighting diagnostic to study liner dynamics on Z*

Sandia National Laboratories

- Spherically-bent quartz crystals (2243)
- Monochromatic (~0.5 eV bandpass)
- 15 micron resolution (edge-spread)
- Large field of view (10 mm x 4 mm)
- We can see through imploding beryllium (not so for aluminum and other higher-opacity materials)

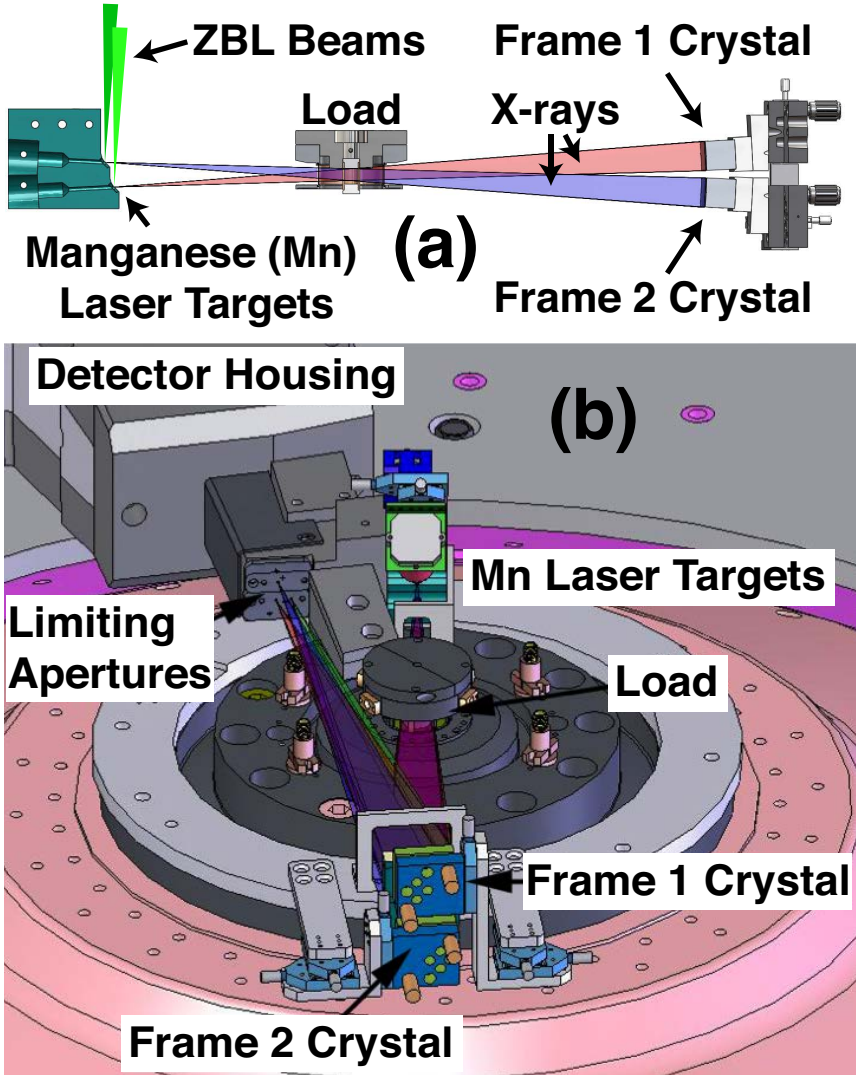

Code benchmarking MRT experiments with controlled sinusoidal perturbations in Al liners

Sandia National Laboratories

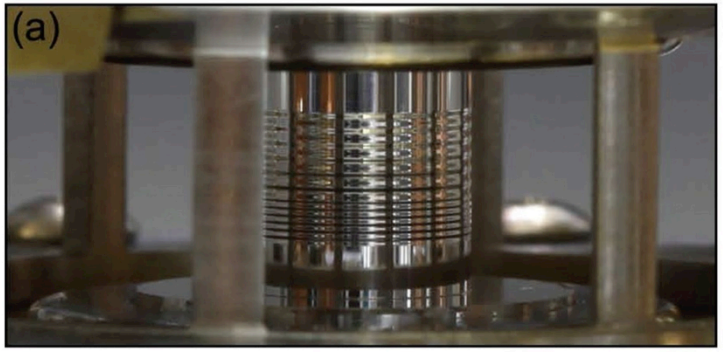

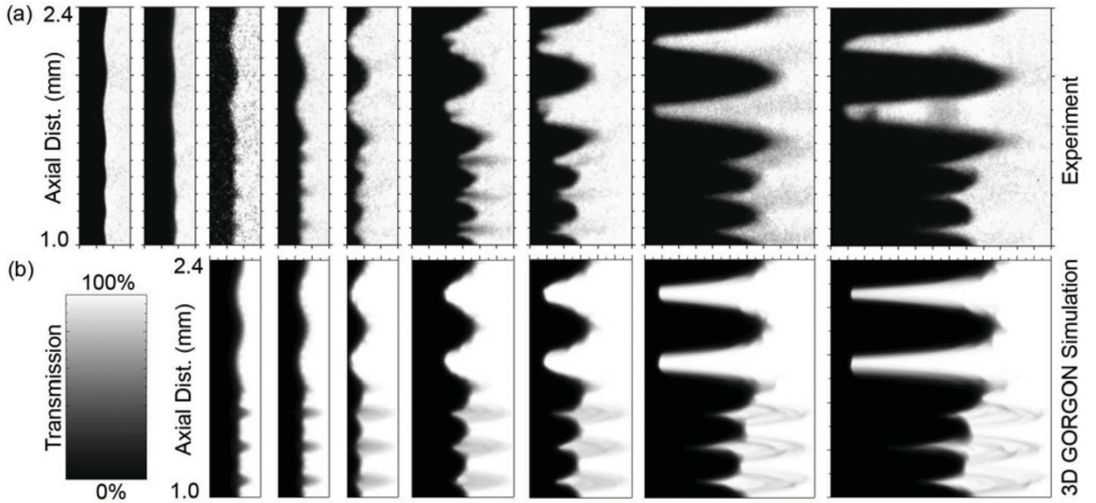

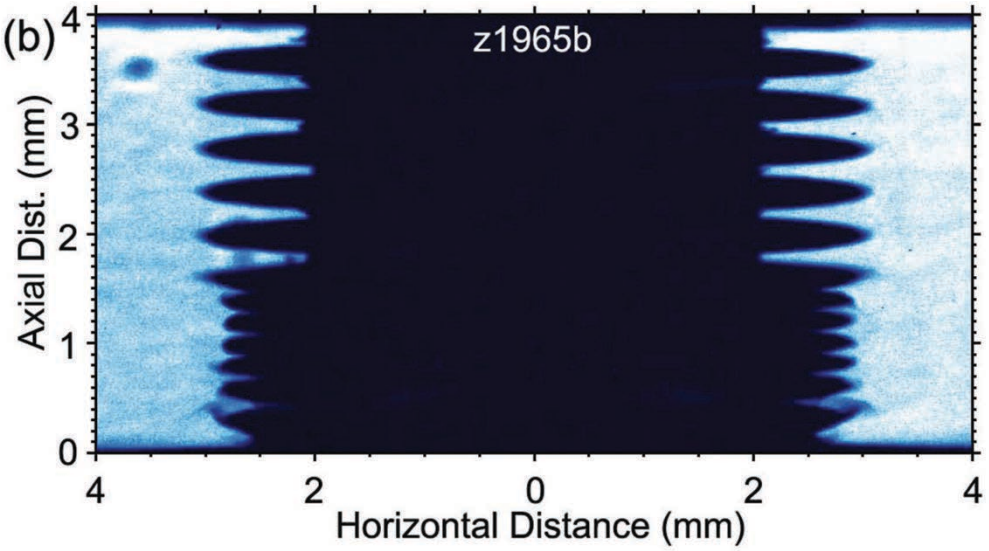

D. B. Sinars *et al.*, PRL **105**, 185001 (2010); D. B. Sinars *et al.*, PoP **18**, 056301 (2011).

Shock vs. Shockless (Quasi-Isentropic) compression for MagLIF[1]

- Shockless is more efficient hydrodynamically, though slower
- Shockless maintains solid metallic inner liner surface
- Shockless mitigates ejecta from liner's inner surface at shock breakout
- Shockless could enable better pulsed-power coupling

- Shockless cylindrical EOS platform extended principal isentrope of Be out to 5 g/cc and 5.5 Mbar[2]

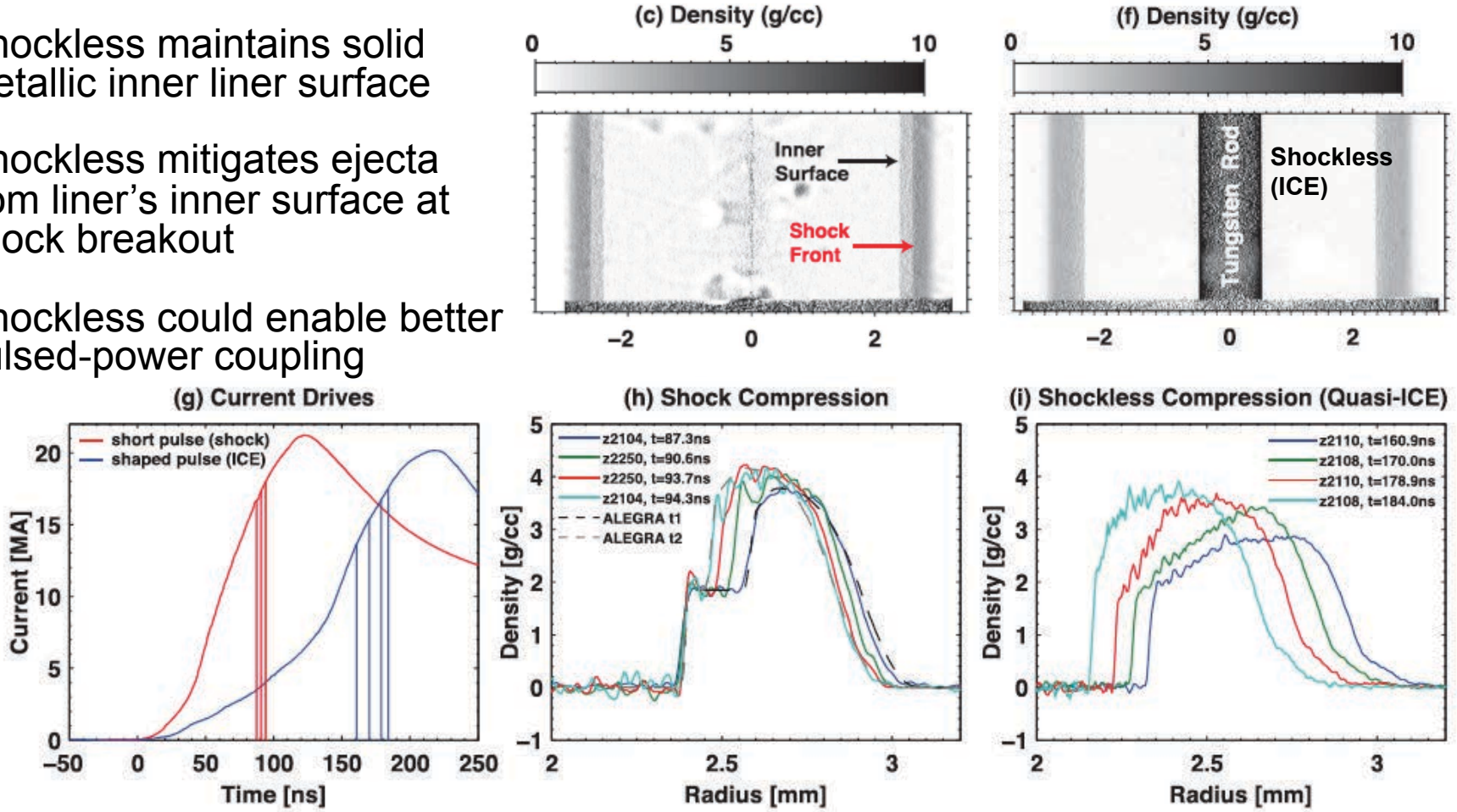

[1]R. D. McBride et al., PoP **20**, 056309 (2013). [2]M. R. Martin et al., PoP **19**, 056310 (2012).

SAMM provides some reasonable guidance for present MagLIF experiments:

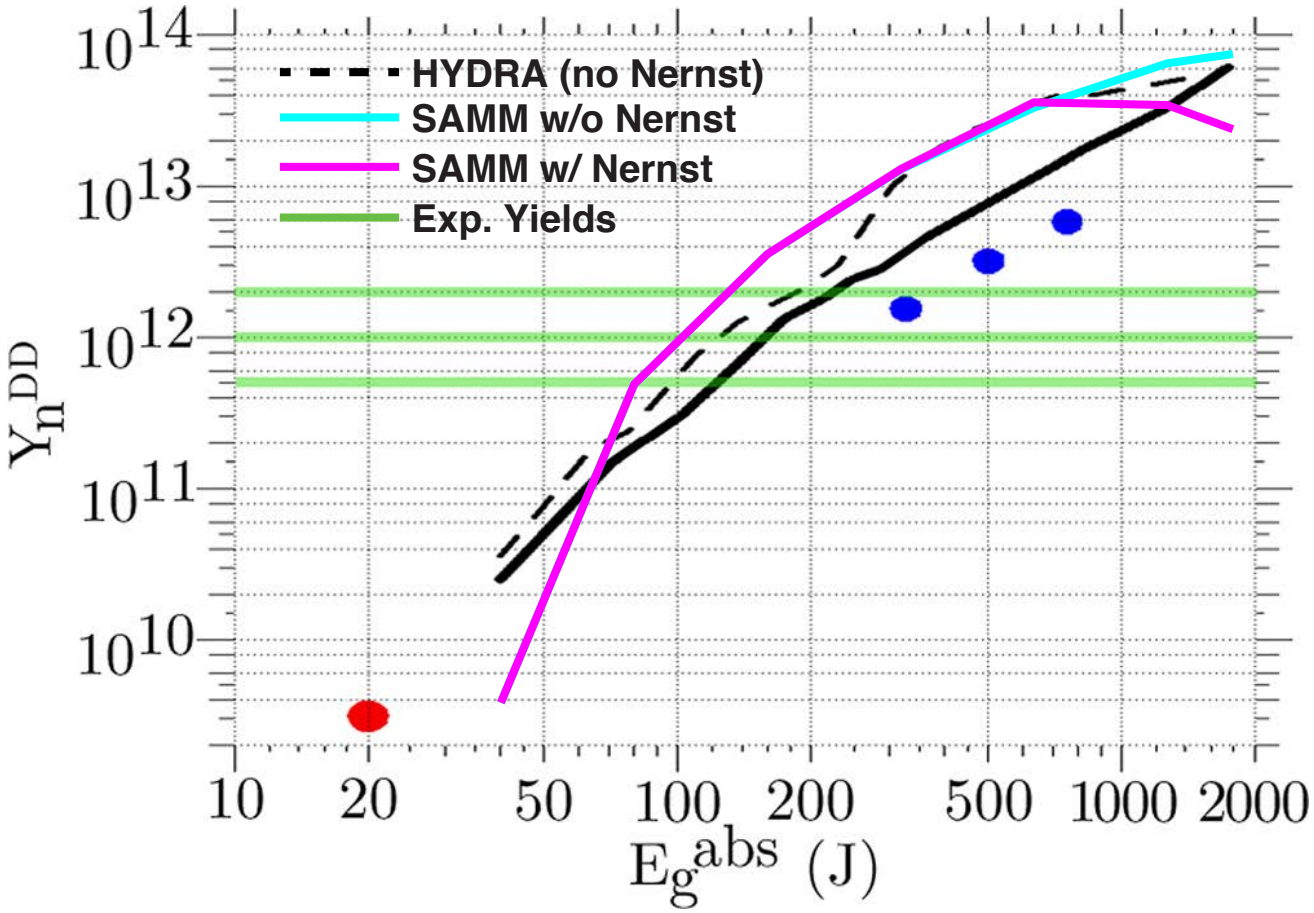

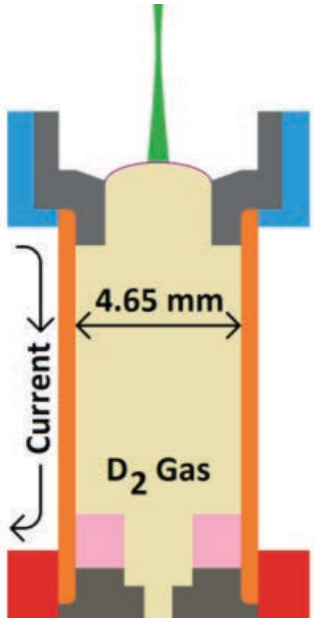

HYDRA Simulations by A. B. Sefkow – For more details, see:

- A. B. Sefkow *et al.*, Phys. Plasmas **21**, 072711 (2014).
- M. R. Gomez *et al.*, Phys. Rev. Lett. (submitted).
- Talk by M. R. Gomez, Session 4, at 8:30 AM

MagLIF Scans for Z300 & Z800:

Sandia National Laboratories

See talk by W. A. Stygar, Session 6, at 2:30 PM

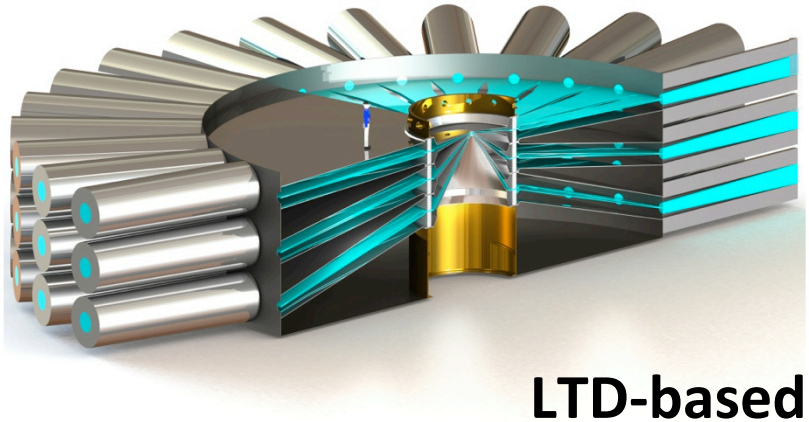

LTD-based architectures

Z300:

- 300 TW delivered
- 47 MJ stored
- 49 MA
- 130 ns rise
- 35 m in diameter (size of Z today)

Z800:

- 870 TW delivered
- 130 MJ stored
- 64 MA
- 120 ns rise
- 55 m in diameter

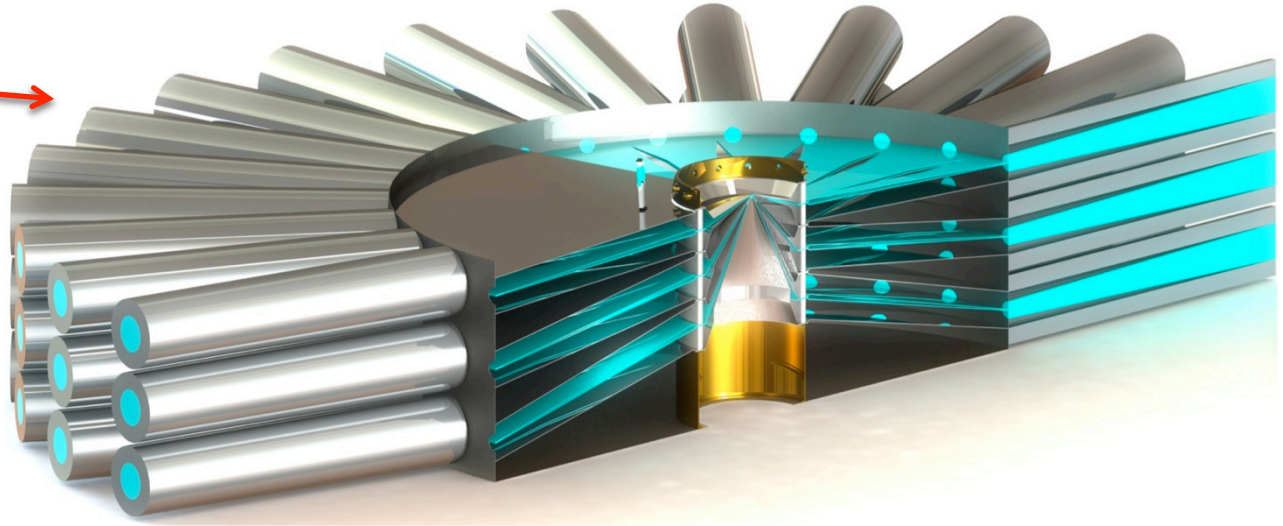

MagLIF Scans for Z300:

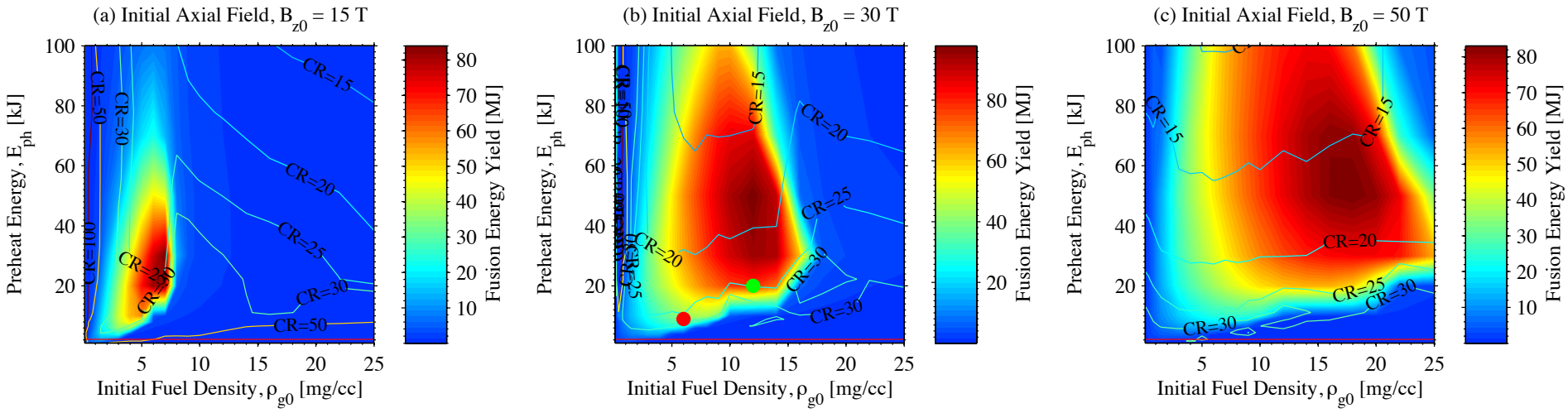

- 47 MJ stored in Z300
- 5.1 MJ absorbed by target
- 38.2 MJ fusion energy (w/ 9 kJ preheat)
- 77.7 MJ fusion energy (w/ 20 kJ preheat)
- CR~23–32
- B_{z0} = 30 T
- LTD-based architecture with footprint the size of Z today

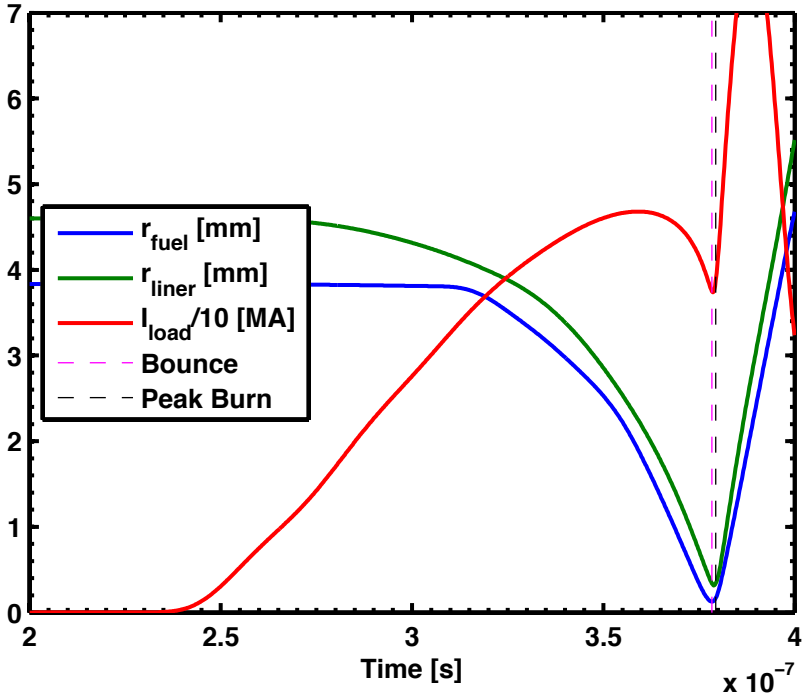

MagLIF Scans for Z800:

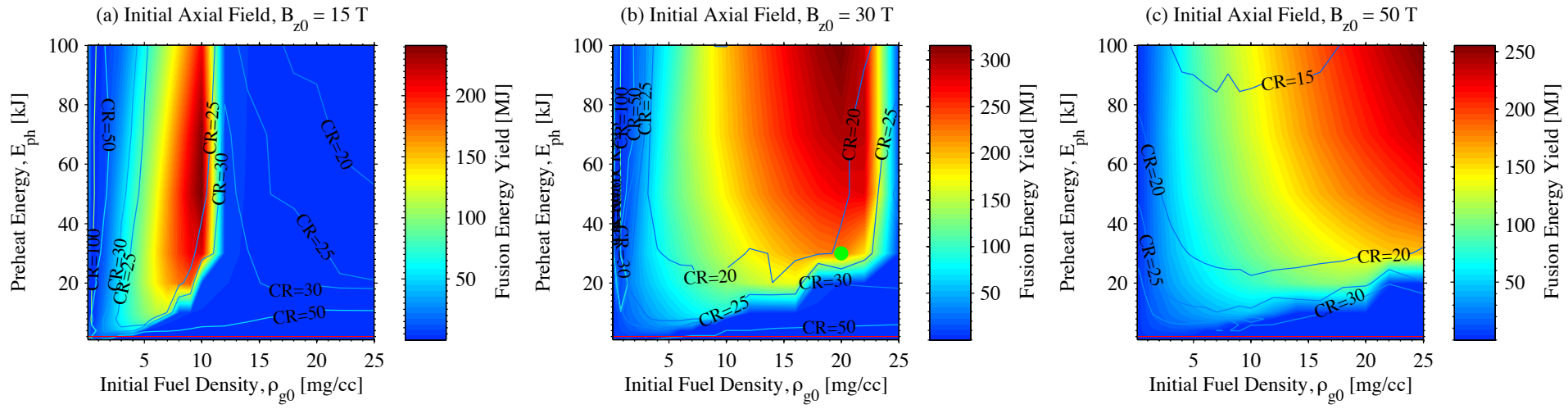

- 130 MJ stored in Z800
- 9.8 MJ absorbed by target
- 221.9 MJ fusion energy (w/ 30 kJ preheat)
- CR~20–31
- B_{z0} = 30 T